

University of Nevada, Reno

Understanding and Forecasting Tahoe Lake-Effect Snow

A thesis submitted in partial fulfillment of the requirements for the degree of
Master of Science in Atmospheric Sciences

By

Jeffrey P. Thompson

Dr. S. Jeffrey Underwood/ Thesis Advisor

May, 2010

Copyright by Jeffrey P. Thompson 2010
All Rights Reserved



University of Nevada, Reno
Statewide • Worldwide

THE GRADUATE SCHOOL

We recommend that the thesis
prepared under our supervision by

JEFFREY P. THOMPSON

entitled

Understanding And Forecasting Tahoe Lake-Effect Snow

be accepted in partial fulfillment of the
requirements for the degree of

MASTER OF SCIENCE

S. Jeffrey Underwood, Ph.D., Advisor

Arlen Huggins, Ph.D., Committee Member

Susan Donaldson, Ph.D., Graduate School Representative

Marsha H. Read, Ph. D., Associate Dean, Graduate School

May, 2010

Abstract

Lake-effect snowfall (LES) is common to the Great Lakes region and the Great Salt Lake, but research is limited on its occurrence on Lake Tahoe. Traditional definition and analysis of this process focus on a number of well-established parameters for lake effect development in other regions. These parameters have not been analyzed in detail during Tahoe lake-effect events.

This study of five well-defined LES cases on and downwind of Lake Tahoe analyzed parameters and their established thresholds currently in use by forecasters in the region for Lake Tahoe, along with those common to lake-effect snow events in other regions. Parameters discussed included the comparison of lake surface temperature to the 650-hPa temperature, comparison of lake surface temperature to land station temperature, presence of a capping inversion, maximum directional shear in the boundary layer, maximum wind speed in the boundary layer, mean relative humidity in the boundary layer, mean temperature of the boundary layer, thermodynamic instability, and upper level support. Findings confirmed that a number of established LES parameter thresholds do in fact occur in concert with Tahoe LES events. Implications for operational forecasting are discussed.

Acknowledgments

This thesis is the crowning achievement of a long and winding road through the wilds of academia for me, and many wonderful and supportive people have been part of my life during key points in that journey. Dr. Jeffrey Underwood must be first mentioned as a great mentor, teacher, employer, and friend, who gave many hours of support and guidance in this process. His inspiration was paramount in the selection of this research topic and plan, and his direction and enthusiasm proved to make the greatest difference in the final stages of preparation and presentation.

Dr. Susan Donaldson and Dr. Arlen Huggins were also instrumental as committee members and colleagues in shaping and completing the research. Sue has been a great partner for me on several outreach projects in the community through the years, and was a tremendous source of information on the shaping of the final thesis. Arlen provided great inspiration for this study through his radar analysis of the November 2000 event (Huggins et al., 2001), and took time away from his many projects and responsibilities at Desert Research Institute to take part in the committee. His added insight and supplemental information were integral in the early shaping of this study.

The National Weather Service includes some of our nation's finest minds and finest people. In response to my inquiries and requests for data and advice, everyone that I contacted did everything possible to assist this investigation and

me personally. From the Reno Forecast Office, Brian O'Hara was outstanding. He provided his own research materials, insight into office forecasting procedure, and data and data sources. Brian Brong and Chris Smallcomb are also owed a great deal of thanks for their assistance and insight. It was a tremendous honor to correspond with Stephen McLaughlin and Thomas Niziol with the Buffalo Forecast Office on Great Lakes research and forecasting methods. Their office has led the discussion and research and forecasting progress on this topic for half a century. Kevin Barjenbruch and Randy Graham were also very helpful with data, methods, and experience from their office in Salt Lake City, where western lake effect was first defined and researched.

Others in the scientific community were also very supportive. Dr. Simon J. Hook, with NASA's Jet Propulsion Laboratory, granted permission for use of Lake Tahoe surface temperature data from the four research buoys jointly operation by JPL and the University of California, Davis. Robert Radocinski prepared this data and passed it along for use in this thesis, and Todd Steissberg and Patty Arneson, with UC Davis, were both very helpful. Robert Coats, with Hydroikos Limited, deserves special thanks for providing this list of contacts. Jim Ashby and Kelly Redmond at the Western Regional Climate Center also readily gave observational data, along with other information and advice. Another great honor came to me through correspondence with Jim Steenburgh at the University of Utah. His research is a cornerstone of western lake-effect research, and his supplemental information concerning his work was invaluable.

I would also like to thank friends and contacts in the community for their support of this research. Snowfall accumulation data and other information was provided by Mark McLaughlin, the "Storm King" of Lake Tahoe, and my good friend and long time weather watcher Ken Wallace, at his home at 7000' above Carnelian Bay, California. My best friend Bob Brunson provided beautiful images through his professional camera lens, including one shot of the aftermath of the November 2000 snowfall. Norman Maher was kind enough to allow usage of his gorgeous poster image of the Tahoe Basin for use in this thesis free of charge, and KCRA-3 in Sacramento operated the camera that captured video of the October 2009 case study event, utilized in the research defense.

Most importantly, my family was the solid rock on which the structure of this project was able to take shape and ascend to completion. During the course of this program and research, I got married, bought a house, had two children, and changed jobs. In the midst of her busiest year, my wife Teresa gave her everlasting love and support to keep me working toward this goal. My children Lillian and Elijah also gave much of their time with me to this project. Special thanks go to my mom and dad, Sandra and Frank Thompson, for their lifelong love and support. They have been with me on this long journey from day one, and I owe so much of who I am today and this achievement to them. My mother Sandra Thompson wanted to provide a special addition to this paper. Figure 1 is her impression of a Tahoe lake-effect snow shower developing across the lake from Emerald Bay in acrylic, entitled "Emerald Isle."



Figure 1: "Emerald Isle" Sandra Thompson

Table of Contents

1. Introduction
 - 1.1 Importance of Tahoe Lake-Effect Snow Research
 - 1.1.1 Definition of LES
 - 1.2 LES Literature Review
 - 1.3 Study Area
 - 1.4 LES Forecasting Methods
 - 1.4.1 Great Lakes
 - 1.4.2 Great Salt Lake
 - 1.4.3 Lake Tahoe
 - 1.5 Hypothesis
2. Procedure
 - 2.1 Case Study Event Selection
 - 2.2 Identification of Tahoe LES Parameters
 - 2.3 Zero-Hour Definition and Time-Step Analysis
 - 2.4 Data
 - 2.5 Methods for LES Case Study Parameter Analysis
3. LES Case Studies
 - 3.1 Case I
 - 3.1.1 Event Summary
 - 3.1.2 Results of Time-Step Analysis
 - 3.1.3 Radar Analysis
 - 3.2 Case II
 - 3.2.1 Event Summary
 - 3.2.2 Results of Time-Step analysis
 - 3.2.3 Radar Analysis
 - 3.3 Case III
 - 3.3.1 Event Summary
 - 3.3.2 Results of Time-Step analysis
 - 3.3.3 Radar Analysis
 - 3.4 Case IV
 - 3.4.1 Event Summary
 - 3.4.2 Results of Time-Step analysis
 - 3.4.3 Radar Analysis
 - 3.5 Case V
 - 3.5.1 Event Summary
 - 3.5.2 Results of Time-Step analysis
 - 3.5.3 Radar Analysis

4. Summary and Conclusions
 - 4.1 Hypothesis Verification
 - 4.2 Parameter Analysis Summary
 - 4.3 Forecasting

References

List of Tables

1. Great Lakes Region LES Research
2. Great Salt Lake LES Research
3. Lake Tahoe LES Research
4. Lake Tahoe Region Communities and Landmarks
5. Tahoe City, CA: Monthly and annual temperatures ($^{\circ}\text{C}$), precipitation (cm), and snowfall (cm)
6. Lake Tahoe surface temperatures ($^{\circ}\text{C}$)
7. KTVL Temperatures ($^{\circ}\text{C}$)
8. Case I Parameter Analysis Results
9. Case II Parameter Analysis Results
10. Case III Parameter Analysis Results
11. Case IV Parameter Analysis Results
12. Case V Parameter Analysis Results

List of Figures

1. "Emerald Isle"
2. Clear Creek Canyon, November 2000
3. Douglas County, October 2009
4. Stages of LES Formation
5. Lake Tahoe Terrain and Major and Minor Axes
6. Maps of the Lake Tahoe Region, Communities and Landmarks
7. Emerald Bay Ice Cover, December 1999
8. Lake Tahoe Bathymetry
9. Great Lakes "Dockus Decision Tree"
10. Great Lakes "Dockus Decision Tree" (B and C)
11. Western New York "Forecasting Decision Tree"
12. Buffalo NWSFO "Forecasting Decision Tree"
13. Great Salt Lake (Forecasting Parameters)
14. Salt Lake City NWSFO (Forecasting Parameters)
15. Reno NWSFO "Forecasting Decision Tree"
16. Lake Tahoe Data Collection Buoys
17. 10 Mar 2006, 1200 UTC REV Upper Air Sounding
18. 10 Mar 2006, 1200 UTC 200, 500, 850, 1000-hPa Upper Air Analyses
19. 1 Nov 2003, 1200 UTC, 200, 500, 850, 1000-hPa Upper Air Analyses
20. 3 Nov 2003, 1200 UTC, 200, 500, 850, 1000-hPa Upper Air Analyses
21. Case I Reported Snowfall Totals (cm)

22. Case I ΔT_{650} , ΔT_{land}
23. Case I Maximum Directional Shear
24. Case I Maximum Wind Speed
25. Case I Mean Relative Humidity
26. Case I Mean Temperature
27. Case I Lifted Index
28. 1 Nov 2003, 0001 UTC Composite Reflectivity (KRGX)
29. 1 Nov 2003, 0504 UTC Composite Reflectivity (KRGX)
30. 1 Nov 2003, 0756 UTC Composite Reflectivity (KRGX)
31. 1 Nov 2003, 1230 UTC Composite Reflectivity (KRGX)
32. 3 Nov 2003, 1200 UTC Composite Reflectivity (KRGX)
33. 3 Nov 2003, 1452 UTC Composite Reflectivity (KRGX)
34. 3 Nov 2003, 1734 UTC Composite Reflectivity (KRGX)
35. 3 Nov 2003, 1829 UTC Composite Reflectivity (KRGX)
36. 10 Mar 2006, 1200 UTC 200, 500, 850, 1000-hPa Upper Air Analyses
37. Case II Reported Snowfall Totals
38. Case II ΔT_{650} , ΔT_{land}
39. Case II Maximum Directional Shear
40. Case II Maximum Wind Speed
41. Case II Mean Relative Humidity
42. Case II Mean Temperature

43. Case II Lifted Index
44. 10 Mar 2006, 0339 UTC Composite Reflectivity (KRGX)
45. 10 Mar 2006, 0658 UTC Composite Reflectivity (KRGX)
46. 10 Mar 2006, 0812 UTC Composite Reflectivity (KRGX)
47. 10 Mar 2006, 1201 UTC Composite Reflectivity (KRGX)
48. 10 Mar 2006, 1411 UTC Composite Reflectivity (KRGX)
49. 11 Mar 2006, 0215 UTC Composite Reflectivity (KRGX)
50. 11 Mar 2006, 0412 UTC Composite Reflectivity (KRGX)
51. 11 Mar 2006, 1200 UTC Composite Reflectivity (KRGX)
52. 11 Mar 2006, 1601 UTC Composite Reflectivity (KRGX)
53. 11 Mar 2006, 2303 UTC Composite Reflectivity (KRGX)
54. 21 Jan 2008, 1200 UTC 200, 500, 850, 1000-hPa Upper Air Analyses
55. Case III Reported Snowfall Totals
56. Case III ΔT_{650} , ΔT_{land}
57. Case III Maximum Directional Shear
58. Case III Maximum Wind Speed
59. Case III Mean Relative Humidity
60. Case III Mean Temperature
61. Case III Lifted Index
62. 21 January 2008, 0525 UTC Composite Reflectivity (KRGX)
63. 21 January 2008, 0903 UTC Composite Reflectivity (KRGX)
64. 21 January 2008, 1201 UTC Composite Reflectivity (KRGX)

65. 21 January 2008, 1629 UTC Composite Reflectivity (KRGX)
66. 21 January 2008, 1704 UTC Composite Reflectivity (KRGX)
67. 21 January 2008, 1856 UTC Composite Reflectivity (KRGX)
68. 21 January 2008, 2002 UTC Composite Reflectivity (KRGX)
69. 22 January 2008, 0000 UTC Composite Reflectivity (KRGX)
70. 22 January 2008, 0130 UTC Composite Reflectivity (KRGX)
71. 22 January 2008, 0331 UTC Composite Reflectivity (KRGX)
72. 11 October 2008, 0000 UTC 200, 500, 850, 1000-hPa Upper Air Analyses
73. Case IV Reported Snowfall Totals
74. Case IV ΔT_{650} , ΔT_{land}
75. Case IV Maximum Directional Shear
76. Case IV Maximum Wind Speed
77. Case IV Mean Relative Humidity
78. Case IV Mean Temperature
79. Case IV Lifted Index
80. 10 October 2008, 1615 UTC Composite Reflectivity (KRGX)
81. 10 October 2008, 1810 UTC Composite Reflectivity (KRGX)
82. 10 October 2008, 2103 UTC Composite Reflectivity (KRGX)
83. 11 October 2008, 0002 UTC Composite Reflectivity (KRGX)
84. 11 October 2008, 0036 UTC Composite Reflectivity (KRGX)
85. 11 October 2008, 0452 UTC Composite Reflectivity (KRGX)

86. 11 October 2008, 0527 UTC Composite Reflectivity (KRGX)
87. 11 October 2008, 1202 UTC Composite Reflectivity (KRGX)
88. 11 October 2008, 1329 UTC Composite Reflectivity (KRGX)
89. 11 October 2008, 1500 UTC Composite Reflectivity (KRGX)
90. 4 October 2009, 1200 UTC 200, 500, 850, 1000-hPa Upper Air Analyses
91. Case V Reported Snowfall Totals (cm)
92. Case V ΔT_{650} , ΔT_{land}
93. Case V Maximum Directional Shear
94. Case V Maximum Wind Speed
95. Case V Mean Relative Humidity
96. Case V Mean Temperature
97. Case V Lifted Index
98. 4 October 2009, 0700 UTC Composite Reflectivity (KRGX)
99. 4 October 2009, 0800 UTC Composite Reflectivity (KRGX)
100. 4 October 2009, 1102 UTC Composite Reflectivity (KRGX)
101. 4 October 2009, 1403 UTC Composite Reflectivity (KRGX)
102. 4 October 2009, 1546 UTC Composite Reflectivity (KRGX)
103. 4 October 2009, 1700 UTC Composite Reflectivity (KRGX)
104. 5 October 2009, 0230 UTC Composite Reflectivity (KRGX)
105. 5 October 2009, 0401 UTC Composite Reflectivity (KRGX)
106. Modified Lake Tahoe LES Forecast Procedure
107. Parameters for Heavy LES

1. Introduction

1.1 Importance of Tahoe Lake-Effect Snow Research

The state capital of Nevada, Carson City, was buried under 53 centimeters (cm) of snow in just three days in the early part of November 2000 (Cairns et al., 2001). From 9 November until 11 November, bands of heavy snow extended from Lake Tahoe downwind into the Carson City area. According to the Nevada Appeal, the local newspaper, plows worked nonstop for two days to keep roads passable for residents. This event marked the first time that senior forecasters at the National Weather Service Office (NWSFO) in Reno, Nevada, had ever observed a lake-effect snowfall (LES) in Nevada (Cairns et al., 2001). Figure 2 is a photograph taken following the event in Clear Creek Canyon, just northwest of Carson City.

In the following decade, improving technology and information learned from the 9-11 November 2000 event (Cairns et al., 2001; Huggins et al., 2001), made Tahoe LES part of the regional knowledge base and challenge for area forecasters. With the addition of the WSR-88D National Weather Service Radar (KRGX) in the 1990's, events that were missed in earlier decades were observed and defined as lake effect following the 2000 storm. For example, when the radar indicated snow banding that originated over the southern half of Lake Tahoe on 4-5 October 2009 the Reno NWSFO was prompted to issue a lake-effect snow advisory. This event produced 20 cm of snow in the Gardnerville area of Douglas County, Nevada (Figure 3).



Figure 2. Clear Creek Canyon, November 2000



**Figure 3. Douglas Co.
October 2009**

The purpose of this study was to expand the knowledge base on Lake Tahoe LES through the analysis of accepted LES forecasting parameters during five Lake Tahoe LES events. Parameter evolution was studied in each case to quantify conditions necessary for the development of Tahoe LES, and to analyze accepted forecasting methods. Modifications to forecasting procedures were recommended based on the findings from these specific events. It is hoped that this research will serve to advance knowledge of this phenomenon and provide forecasters in the region with additional insight into future Lake Tahoe LES events.

1.1.1 Definition of LES

The American Meteorological Society definitions for lake effect, lake-effect snow (LES), and lake-effect snowstorm are as follows (AMS Glossary, 2000):

Lake effect- Generally, the effect of any lake in modifying the weather about its shore and for some distance downwind.

Lake-effect snow- Localized, convective snow bands that occur in the lee of the lakes when relatively cold air flows over warm water.

Lake-effect snowstorm- Snowstorm occurring near or downwind from the shore of a lake resulting from the warming (destabilization) and moistening of relatively cold air during passage over a warm body of water.

Lake-effect snowstorms are manifestations of internal convective boundary layer growth as heat and moisture fluxes from relatively warm lake waters modify the lowest levels of cold air passing over the lake (Kristovich et al., 1998). This destabilization of arctic air can lead to convective bands that produce highly localized snowfalls; the convective nature of the bands can allow significant snow depth even with small liquid-equivalent precipitation (Juisto et al., 1970) (Lackmann, 2000). Because of the mesoscale nature of lake-effect events, sunny skies can prevail over one location, while a second location only 20 kilometers (km) away experiences a raging snowstorm that produces well over one meter (m) of snow (Niziol, 1987).

Figure 4 demonstrates the basic lake-effect process. The National Weather Service Office in Reno provided this six-stage process description for LES (Brong, personal communication, 2009).

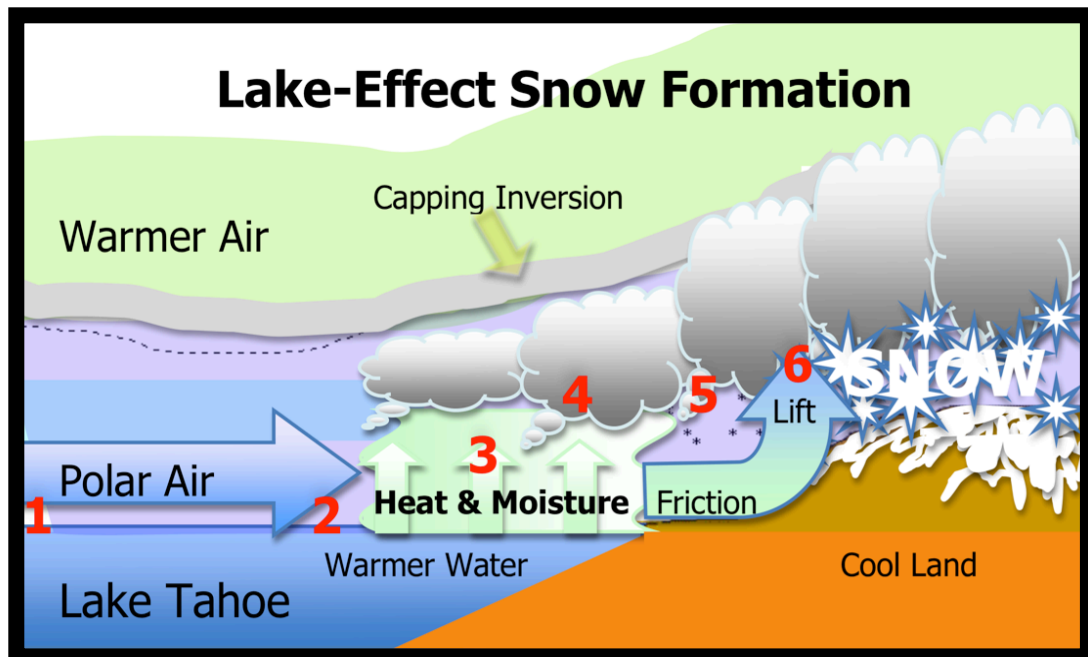


Figure 4. Stages of Lake-effect Snow (LES) Formation (1-6):

1. LES occurs when a cold air mass moves over a warm body of water, creating an unstable temperature profile.
2. Cold air advection over relatively warm water, is heated from below, making it more buoyant.
3. Evaporation occurs at the surface, saturating the air mass. Lake-warmed, moist air rises and cools, prompting condensation.
4. Condensation develops clouds as the air becomes increasingly unstable.
5. Latent heat is released, providing more fuel for lift.
6. Convergence (friction) and the upward sloping terrain along the shore increase the vertical motion and result in heavy snowfalls on the downwind shore of the lake.

1.2 LES Literature Review

The body of LES research has grown and advanced for nearly a century. It originated in the Great Lakes region and expanded to the Great Salt Lake and other smaller lakes including Lake Tahoe. Leading research in the Great Lakes region came out of Penn State University, the NWSFO Buffalo, the University of Chicago, Cornell, the University of Delaware, the Illinois State Water Project, and Hobart and William Smith Colleges. The NWSFO Salt Lake City and the University of Utah produced the Salt Lake LES research. Lake Tahoe LES papers were written by forecasters from the NWSFO Reno and researchers at Desert Research Institute in Reno, Nevada.

The body of knowledge on Lake Tahoe LES is currently based on one case study. Therefore, current detailed understanding of the process is limited. Parameters for forecasting LES in other regions have been established by a number of studies, but Tahoe LES parameters have received little research attention.

The following tables contain the citation information for a number of primary studies in the field, their years of publication, and important findings. Table 1 lists the Great Lakes region LES research chronologically. Table 2 lists important papers on LES on the Great Salt Lake, and Table 3 shows the two companion papers published to date on Lake Tahoe LES.

Table 1. Great Lakes Region LES Research

(Publication, Year)	Findings
(Dole, 1925)	<ul style="list-style-type: none"> • Large lake surface temperature to air temperature gradient important • LES similar to thunderstorms in appearance and can contain lightning
(Wiggin, 1950)	<ul style="list-style-type: none"> • Depth of polar air greater than 1,500 meters (m) important • Cyclonic curvature for heavy snow • Large temperature difference between lake surface and air • Long fetch over water important • Some shear beneficial to produce cells, stronger shear detrimental
(Pettersen, 1956)	<ul style="list-style-type: none"> • Arctic air mass often accompanied by low-level subsidence inversion • Topography enhanced precipitation • Snowfall increased greatly with longer length of over-water fetch
(Peace and Sykes, 1966)	<ul style="list-style-type: none"> • Winds aloft controlled snow band location and movement • A land breeze, shoreline frictional convergence, and orographic effects intensify LES
(Rothrock, 1969)	<ul style="list-style-type: none"> • Lake surface temperature to 850-hPa (hectopascal) level temperature difference (ΔT_{850}) of 13 °C or greater • Inversion height greater than (>) 900 m • Majority of events occurred under negative vorticity advection (NVA) at the 500-hPa level
(Holroyd, 1971)	<ul style="list-style-type: none"> • Friction induced convergence developed due to contrast in land and water surface roughness which enhanced LES • Thermally induced convergence occurred over the lake • LES cloud types defined as parallel bands resembling cloud streets • LES cloud types occurred when ΔT_{850} was 13 °C or greater

(Publication, Year)	Findings
(Hill, 1971)	<ul style="list-style-type: none"> • 25-50 centimeter (cm) increase in annual snowfall occurred with every 100 m of elevation gain in the lee of Lakes Ontario and Erie
(Lavoie, 1972)	<ul style="list-style-type: none"> • Lake surface temperature to boundary layer temperature difference was the critical factor in development of LES
(Jiusto and Kaplan, 1972)	<ul style="list-style-type: none"> • Wind direction and fetch were essential to downwind snowfall amounts on Great Lakes • Orographic influences less critical than lake-induced and synoptic influences • Strong correlation between time of year and amount of snowfall • Decline in ΔT_{850} reduced vertical fluxes of momentum, heat, and moisture
(Kelly, 1982)	<ul style="list-style-type: none"> • Horizontal-roll circulation in the boundary layer observed • Horizontal-roll convection discussed as important in development of heavier LES across shorter fetches
(Hjelmfelt and Braham, 1983)	<ul style="list-style-type: none"> • Verification of development of a mesoscale low-pressure center and land breeze front • Distribution of lake surface temperature had little effect on LES development
(Dockus, 1985)	<ul style="list-style-type: none"> • 850-hPa level temperature could be no warmer than -10 °C for LES to develop regardless of lake surface temperature • Lake effect and lake enhancement differentiated based on length of fetch • 160 kilometer (km) fetch defined for pure lake effect • 80 km fetch with upper level support defined for lake enhancement • Positive vorticity advection (PVA) was an enhancing factor for LES • Forecast decision tree developed for Great Lakes

(Publication, Year)	Findings
(Saulesleja, 1986)	<ul style="list-style-type: none"> • Deeper lakes did not develop appreciable ice cover • Ice cover detrimental to LES development
(Niziol, 1987)	<ul style="list-style-type: none"> • Defined ideal synoptic conditions for LES on Lakes Erie and Ontario • Surface to 700-hPa level wind direction best for determining LES orientation and movement on Great Lakes • Directional wind shear of $>30^\circ$ produced multiple banding and reduced snowfall rate • Shear $>60^\circ$ detrimental to development of LES • Higher inversion resulted in more intense convection • Forecast decision tree developed for western New York
(Hjelmfelt, 1990)	<ul style="list-style-type: none"> • LES morphologies identified in terms of banding type • Inversion in low levels shown to be detrimental to LES • Increase in surface roughness and land breeze corresponded with stronger LES events • Larger ΔT_{850} corresponded with stronger LES events
(Hjelmfelt, 1992)	<ul style="list-style-type: none"> • ΔT_{850} more critical to LES development than orographics • Orographics produced local enhancement
(Reinking et al., 1993)	<ul style="list-style-type: none"> • Higher inversions with greater depth of the unstable layer resulted in higher LES rates
(Niziol et al., 1995)	<ul style="list-style-type: none"> • Stable and unstable seasons for LES identified based on water to air temperature relationship • LES morphology expanded to five banding types
(Ellis and Leathers, 1996)	<ul style="list-style-type: none"> • Five synoptic patterns identified for LES development based on direction and strength of lower-tropospheric flow

(Publication, Year)	Findings
(Kristovich and Laird, 1998)	<ul style="list-style-type: none"> • Increases in total flux corresponded with an upwind shift of the LES cloud edge
(Kristovich et al., 2000)	<ul style="list-style-type: none"> • Data collection project describing utilization of new remote sensing equipment in information gathering during LES events
(Lackmann, 2001)	<ul style="list-style-type: none"> • LES events classified and analyzed utilizing parameter thresholds • Mobile upper trough identified as beneficial to LES enhancement
(Kristovich et al., 2003)	<ul style="list-style-type: none"> • Convective boundary layer growth was faster than horizontal scale growth
(Kristovich and Spinar, 2005)	<ul style="list-style-type: none"> • LES development had a distinct diurnal pattern • Maxima precipitation frequencies occurred between 0800 UTC and 1500 UTC.
(Laird et al., 2009)	<ul style="list-style-type: none"> • LES study on Lake Champlain, much smaller than Great Lakes • LES occurred during periods of southerly flow on a north-south meridionally oriented lake, not previously noted in LES research • Lake surface to land surface temperature difference averaged 14.4 °C • Surface inversion present, but lifted due to orographic forcing • ΔT_{850} exceeded 13 °C in 80% of cases • ΔT_{850} exceeded 18 °C in 50% of cases

Table 2. Great Salt Lake LES Research

(Publication, Year)	Findings
(Carpenter, 1993)	<ul style="list-style-type: none"> • The 700-hPa level to lake relationship was identified to investigate instability due to increased elevation • ΔT_{700} of 17 °C or greater critical to LES development • 700-hPa level wind direction between 270° and 360° necessary for LES • Upper level support shown to enhance LES
(Steenburgh et al., 2000)	<ul style="list-style-type: none"> • ΔT_{700} of at least 16 °C critical to LES development • Directional wind shear <60° except for weak flow • Low-level convergence over the lake enhanced LES • Greater land station air temperature to lake surface temperature differences produced stronger definition of lake-effect band structure • Organized banding structure over and downwind of the lake occurred when this difference was 8 °C or greater • Orographic forcing enhanced LES • Upstream low-level moisture enhanced LES
(Steenburgh and Onton, 2001)	<ul style="list-style-type: none"> • Individual convective cells over the lake transitioned into an organized snowband near the shoreline • Banding was parallel to the steering layer wind • Confluence due to a land-breeze front enhanced LES • Banding shifted to the mid-lake axis at maturity, aligned with the long axis of the lake

(Publication, Year)	Findings
(Onton and Steenburgh, 2001)	<ul style="list-style-type: none"> • Sensible and latent heating critical to LES development and snowband evolution • Moisture fluxes necessary to fully develop LES bands • Hypersaline water of the Great Salt Lake decreased moisture fluxes and reduced snowfall by 17% • Orographic effects not shown to generate LES bands, but affected distribution and intensity • Surface roughness contrast did not play a primary role in snowband formation
(Steenburgh, 2003)	<ul style="list-style-type: none"> • Mid-lake banding down the long axis of the lake produced highest LES accumulation rates • East shore land breeze enhanced by flow off the Wasatch Mountain front • LES and associated orographic enhancement of LES produced two-thirds of the measured snow during post frontal periods during a four day winter storm cycle

Table 3. Lake Tahoe LES Research	
(Publication, Year)	Findings
(Cairns et al., 2001)	<ul style="list-style-type: none"> • Case study of a three day Tahoe LES event that produced 53 cm of snow in Carson City • The 650-hPa level to lake relationship was identified to investigate instability due to increased elevation • ΔT_{650} exceeded 26 °C during case study • Convective available potential energy (CAPE) of 2000 Joules per kilogram (J/kg) was observed in soundings modified with enhanced warming and moisture from the lake • Directional wind shear did not exceed 40° • Fetch was perpendicular to long-axis of the lake and discussed as a minor factor • Moist layers in the soundings during the event fell into ideal temperature range for snow crystal development and growth
(Huggins et al., 2001)	<ul style="list-style-type: none"> • Pre-existing precipitation was enhanced over the lake • Radar returns originated near the eastern shore • Lifting over the steep terrain on the east side of the lake postulated as source for LES enhancement • Areas downwind of the lake showed much greater snowfall amounts than upwind • A broad shield pattern occurred when flow shifted northerly

1.3 Study Area

Lake Tahoe is a subalpine, freshwater lake, located in the Sierra Nevada Mountains on the California-Nevada border in the western United States. The lake surface is at an elevation of 1,897 m above sea level, and its volume sits in a roughly elliptical bowl surrounded entirely by mountains (Figure 5). The Carson Range defines the eastern side of the basin and the Sierra Nevada rises to the west. Terrain around the basin is rugged, averaging an elevation gain of more than 610 m in less than 3 km of distance from the water's edge.

Lake Tahoe is a longitudinal lake, with its long-axis oriented north-to-south. The longest over-water distance, or fetch, on Lake Tahoe is 35 km from near Incline Village, Nevada, to South Lake Tahoe, California. Maximum lateral fetch, or east-west distance, is 19 km from Homewood, California, to Glenbrook, Nevada (Figure 5). Lake Tahoe has a total surface area of 495 square km.

Figure 6 is a map of the Tahoe Basin and surrounding region, featuring communities and principle locations labeled in red, mountain peaks in green, and points of interest on the lake in blue. Table 4 is the legend for Figure 6, and includes peak mountain elevations. The location of Lake Tahoe Airport (KTVL) is also featured in black in Figure 6.

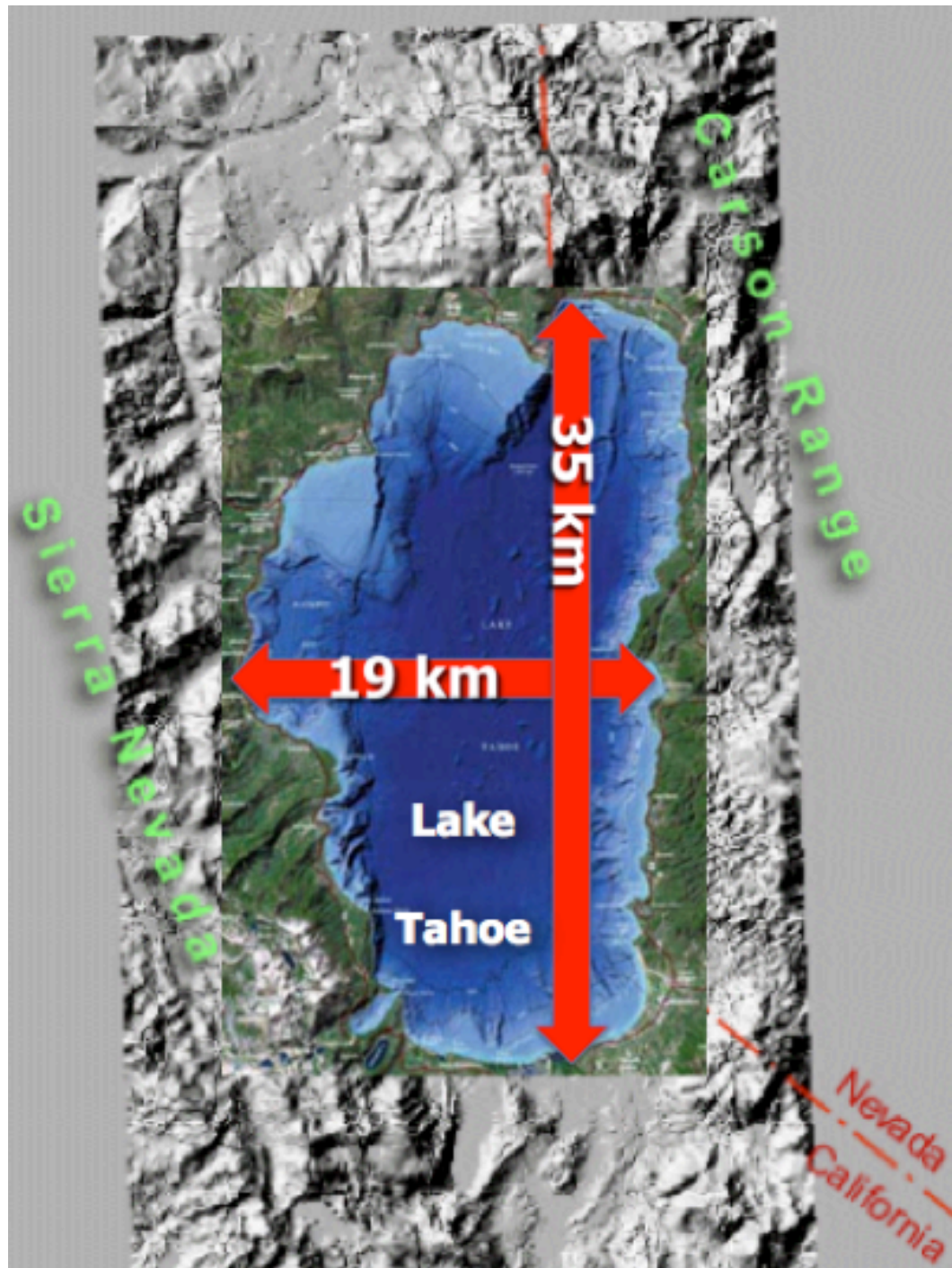


Figure 5. Map showing the terrain surrounding Lake Tahoe and the lengths of its major and minor axis (USGS)

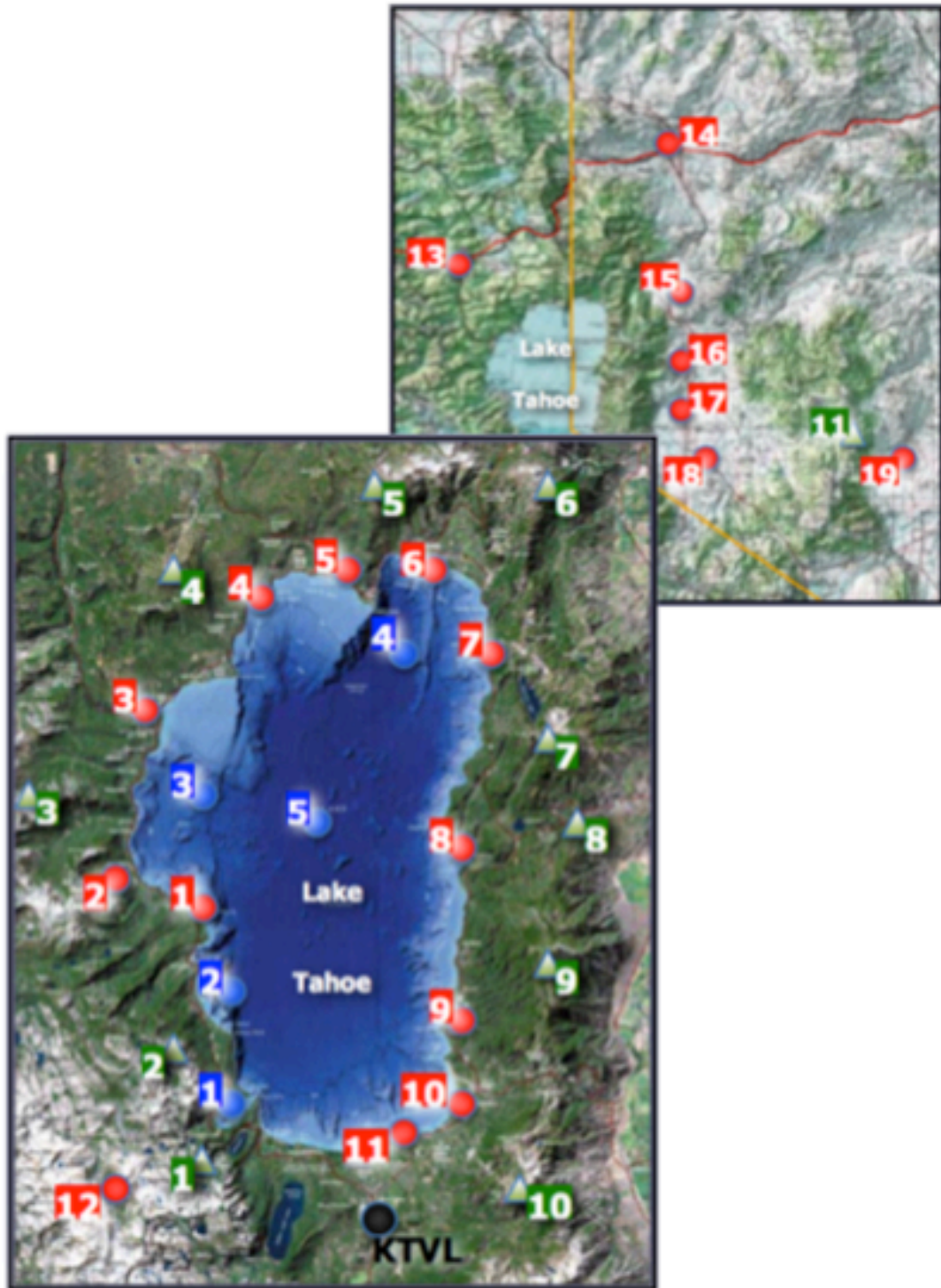


Figure 6. Maps of the Lake Tahoe region with communities and landmarks numbered and identified in Table 4

Communities/ Locations	
1. Tahoma	
2. Homewood Ski Area	
3. Tahoe City	
4. Carnelian Bay	
5. Kings Beach	
6. Incline Village	
7. Sand Harbor	
8. Glenbrook	
9. Zephyr Cove	
10. Stateline	
11. South Lake Tahoe	
12. Desolation Wilderness	
13. Truckee	
14. Reno-Sparks	
15. Washoe Valley	
16. Carson City	
17. Carson Valley	
18. Minden-Gardnerville	
19. Smith Valley	

Mountain Peaks	Elevation (m)
1. Mt. Tallac	2,967
2. Rubicon Peak	2,799
3. Stanford Rock	2,583
4. Mt. Pluto	2,626
5. Martis Peak	2,665
6. Mt. Rose	3,285
7. Marlette Peak	2,676
8. Spooner Summit	2,178
9. Genoa Peak	2,789
10. Freel Peak	3,317
11. Pine Nut Mtns.	2,745

Lake Tahoe Features
1. Emerald Bay
2. Rubicon Bay
3. McKinney Bay
4. Crystal Bay
5. Geographic Center

Table 4. Lake Tahoe Region Communities and Landforms

Given these substantial elevation gains in every direction at a relatively short distance from Lake Tahoe, lake-effect research suggests the likelihood of significant orographic enhancement of a lake effect around the Tahoe Basin. Observations during the LOWS project showed substantial enhancement of snow band radar echoes over the higher elevations of the Tug Hill Plateau east of Lake Ontario (Reinking et al., 1991). Hjelmfelt (1992) demonstrated through numerical simulations of lake-effect snowstorms over Lake Michigan that upwardly sloping topography enhanced mesoscale updrafts and precipitation rates. Muller (1966) noted a 12 to 20 cm increase in annual snowfall per 330 m increase in elevation in the lee of the Lakes Erie and Ontario. This value was substantially increased through (Hill, 1971), and established as a 25 to 50 cm increase in annual snowfall for every 100 m of elevation gain. Steenburgh et al. (2000) showed that interaction with downstream terrain did positively affect the distribution and intensity of snow bands in the lee of the Great Salt Lake, and (Huggins et al., 2001) postulated that convergence near the eastern shore of Lake Tahoe was enhanced by lifting over the steep terrain on the east side of the lake during the heavy snowfall event of 9-11 November 2000.

Lake Tahoe is the second deepest lake in the United States and the eleventh deepest in the world, and this depth keeps most of its surface from freezing during the Sierra winter. The only exception is in relatively shallow bays on the perimeter (Figure 7). The lake has a maximum depth of 501 m (USGS, 2010). This volume of water, 148 trillion liters, with its relatively small surface

area (Figure 8), stores enough heat during the summer months to resist freezing (Goldman and Court, 1968). As noted by (Saulesleja, 1986) and (Niziol, 1987) in comparing Lakes Erie and Ontario, deeper lakes did not develop appreciable ice cover. Without ice cover developing on the main body of the lake, latent and sensible heat modification of the boundary layer remains a possibility through the winter and into the spring (Jiusto and Kaplan, 1972). Tahoe surface water temperature cools to an average of 4.5 to 10 °C during February and March, and warms to 18 to 21 °C during August and September (Schladow, 2009). Lake surface temperature has not dropped below 5 °C in the last ten years (Schladow, 2009). Below a depth of 183 to 213 m, temperature averages a constant 4 °C (USGS, 2010).

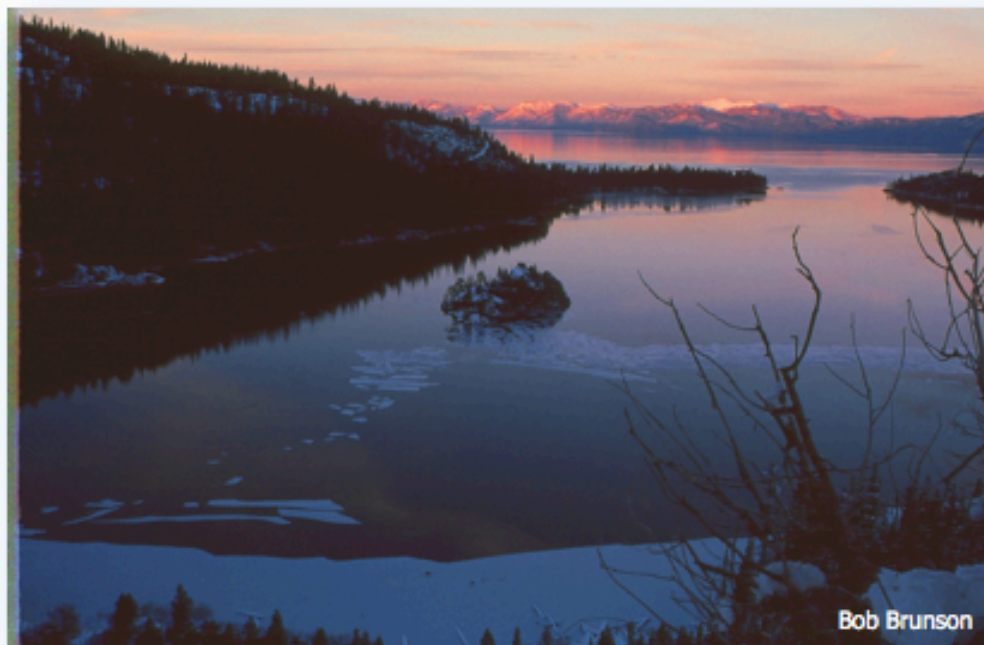
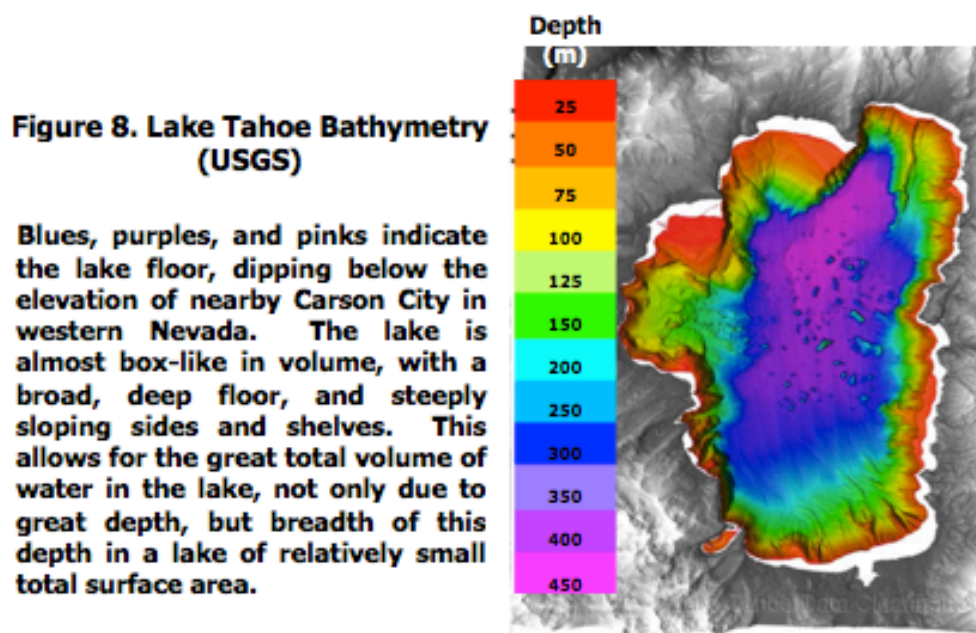


Figure 7. Emerald Bay Ice Cover, December 1999 (Note the lack of ice on the main body of the lake)



With the Sierra crest west of the Lake, the impact of topographic enhancement on annual precipitation is evident on the west shore of Lake Tahoe. The Sierra Nevada provides a good example of the rain shadow effect (a minimum in precipitation downwind of a mountain range), with topographic lift and adiabatic cooling of moist Pacific air resulting in some of the highest annual rainfall and snowfall totals in the United States (O'Hara, 2007). Storms deposit 497.8 cm of snow on average annually at Tahoe City, on the northwestern shore of the lake, with a precipitation total of 83 cm (Table 5). Other locations on the western side of the lake at higher elevations average as much as 140 to 203 cm of precipitation (USGS, 2010). With a prevailing west-to-east wind flow, there is an unequal distribution of moisture annually, with the eastern shore receiving 66 to 76 cm of total moisture a year (USGS, 2010). Downwind of the Carson Range, Carson City, Nevada, has an annual precipitation total of 30 cm.

Tahoe City, CA	Ave. High **	Record High (year)*	Ave. Low **	Record Low (Year)*	Ave. Precip. **	Ave. Snowfall **
Jan	4.7	15 (1990)	-6.6	-26 (1916)	15.3	108.5
Feb	5.6	16 (1985)	-5.9	-26 (1989)	14.5	95.5
Mar	7.3	19 (1996)	-4.3	-21 (1935)	11.6	88.1
Apr	10.8	23 (1981)	-2.4	-15 (1999)	4.6	40.6
May	15.6	27 (1986)	0.8	-13 (1974)	3.1	9.4
June	20.7	32 (1961)	4.2	-4 (2005)	2.0	0.5
July	25.3	34 (1934)	7.1	-6 (1975)	0.8	0.0
Aug	25.0	34 (1933)	7.1	-2 (1957)	1.2	0.0
Sep	21.2	31 (1955)	4.2	-6 (1965)	2.3	0.8
Oct	15.6	27 (1933)	0.2	-13 (1971)	5.0	5.8
Nov	8.8	21 (1988)	-3.6	-17 (1931)	10.8	41.1
Dec	5.2	16 (1990)	-6.3	-27 (1972)	11.9	89.7
Ann.	13.8	34 (1933)	-1.2	-27 (1972)	83.0	479.8

Table 5. Tahoe City, CA: Monthly and Annual Temperature (°C), Precipitation (cm), and Snowfall (cm)
(O'Hara et al., 2007)

*Since 1914
**1971-2000

1.4 LES Forecasting Methods

1.4.1 Great Lakes

As detailed in the literature review, research on this topic dates back to the early 20th century, and this sizable amount of research has yielded a number of forecasting parameters common to significant lake-effect events:

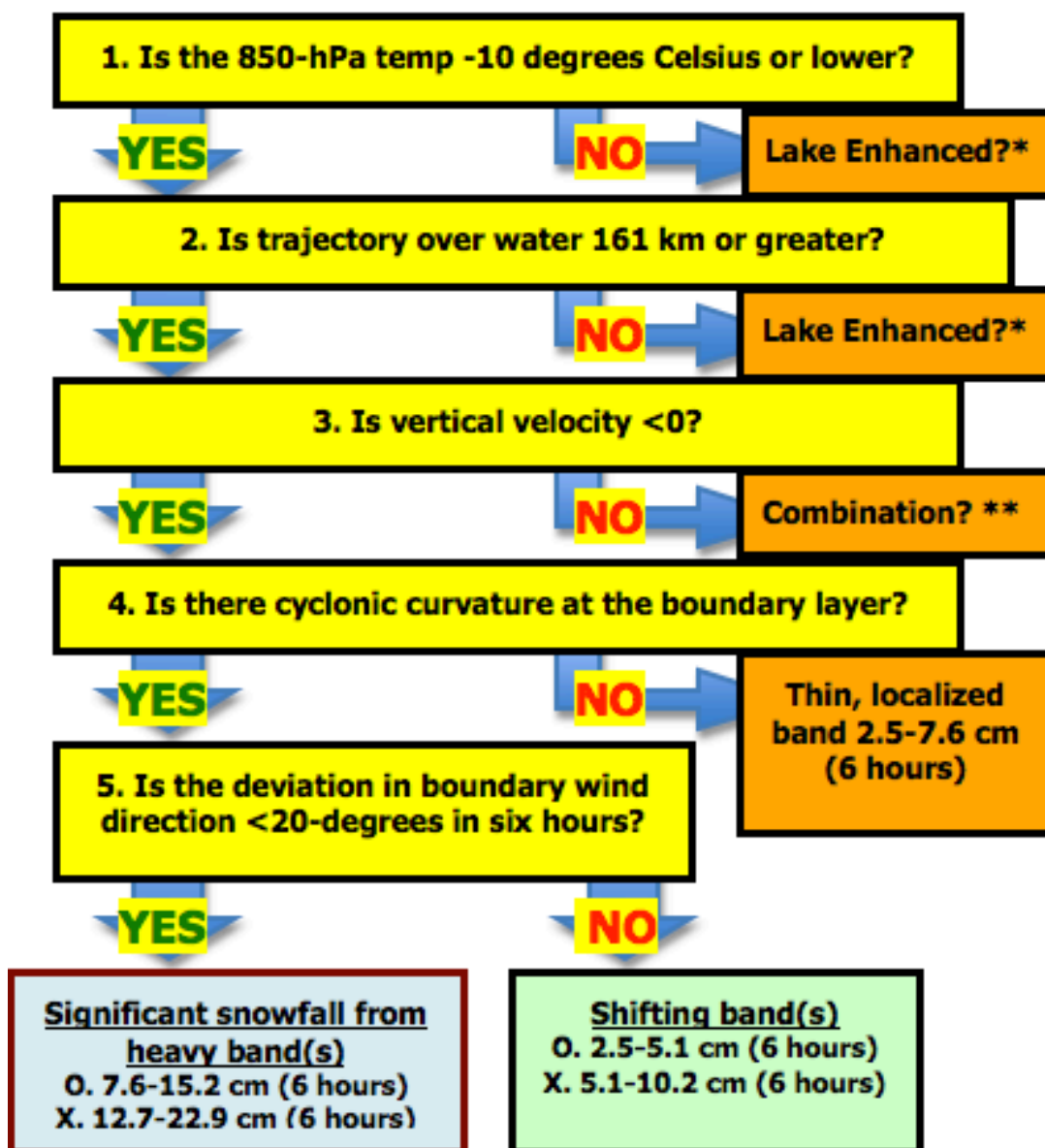
1. ΔT_{850} of 13 °C or greater (Rothrock, 1969); ΔT_{850} is the dominant influence (Lavoie, 1972); Larger lapse rates correspond with stronger lake effect events (Hjelmfelt, 1990)
2. 850-hPa level temperature no warmer than -10 °C, regardless of lake temperature (Dockus, 1985)
3. Boundary layer wind direction up to the 850-hPa level traversing 80 km or more of lake fetch, with 160 km conducive to heavier snows (longer fetches meant greater snowfall production) (Wiggin, 1950; Petterssen, 1959; Dockus, 1985)
4. Change in wind direction from the boundary layer up to 700-hPa level < 30°, or banding organization will produce less snow (>60° results in complete convective structural breakdown) (Niziol, 1987)
5. Inversion height of at least 900 m, with higher inversion heights resulting in larger snowfall totals (Rothrock, 1969; Hjelmfelt, 1990)
6. Cyclonic flow and PVA at the 500-hPa level (700-hPa and/or 850-hPa also) positively affects flow in the lower levels (below 700-hPa), enhancing lake-effect (Dockus, 1985; Niziol, 1987)

7. Ice cover reduces heat and moisture available and the process deteriorates (Saulesleja, 1986; Niziol, 1987)
8. Topographic features enhance lake-effect down-wind (Peace et al., 1966) (Lavoie, 1972; Reinking, 1993); For every 100 m gain in elevation, annual snowfall increases by 25-50 cm (Hill, 1971)
9. Land-breeze development and convergence enhances snow band development; maximized in the overnight and early morning hours (Kristovich, 2005)
10. Upstream moisture, or seeding, is beneficial to lake-effect development (Niziol et al., 1995)
11. Geostrophic wind speeds in excess of 5 meters per second (m/s) are needed unless wind shear is minimized (Dockus, 1985)

From this evolving list of forecasting parameters grew protocols practiced by forecasters around the region. The Dockus Decision Tree (Dockus, 1985) was the first to provide a detailed procedure for forecasters on all of the Great Lakes for LES and continues to influence methods today (Figures 9 and 10). The Dockus tree focused on ΔT_{850} as critical, and then distance of polar air advection over water (fetch) as defining for “pure” lake effect, or lake enhancement, where upper vertical velocity at the 700-hPa level was >0 . Figure 11 provides the Niziol Forecasting Decision Tree (Niziol, 1987) designed for western New York. Niziol’s critical parameters were ΔT_{850} , trajectory of the wind for maximum lake fetch, and directional wind shear. Niziol’s procedure set

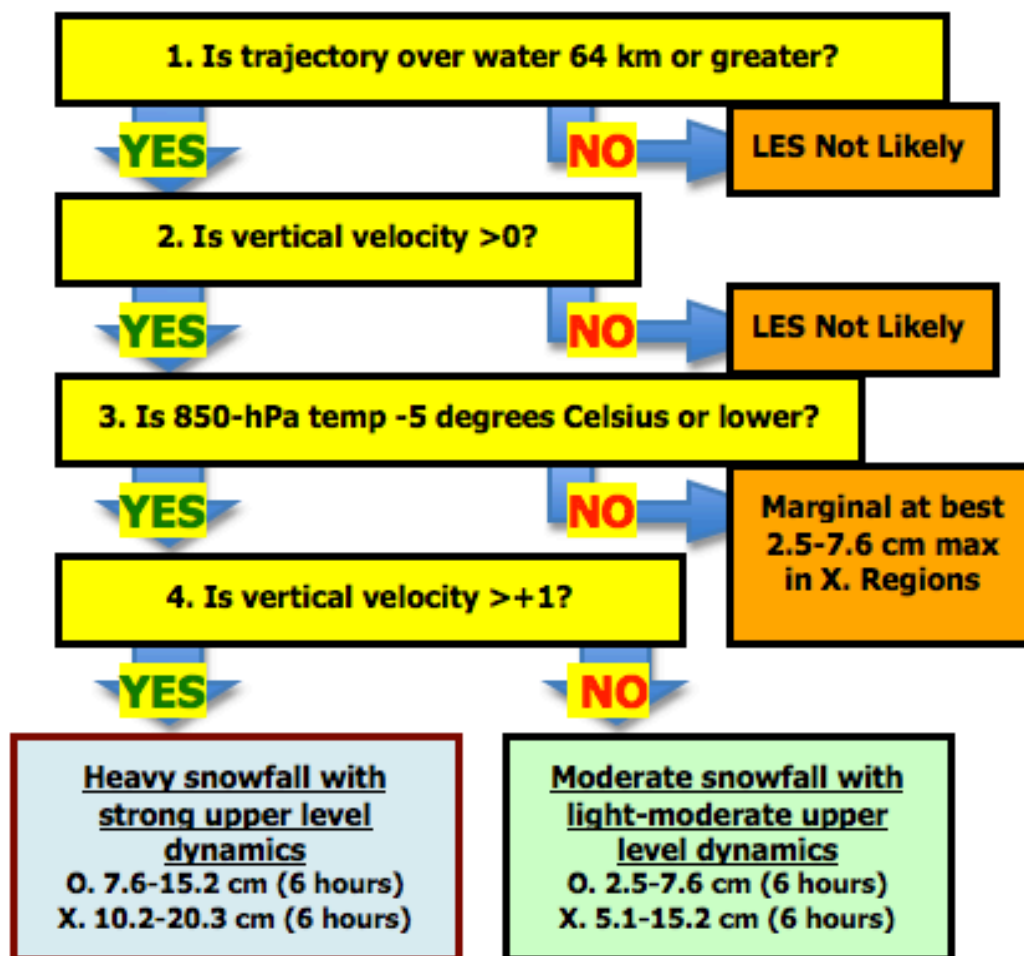
an important threshold on wind shear of a maximum of 60° for LES to occur, still in use in several regions. Figure 12 shows the protocol in use today at the NWSFO Buffalo, a derivative of the Niziol tree (McLaughlin, personal communication, 2010). The latest forecasting procedure includes ΔT_{850} , fetch (although considerably shorter), and directional wind shear as critical; it also includes the influence of upstream moisture in LES development. This factor is not yet considered as critical, but has become a parameter of interest and study in the last decade. It should be noted that in addition to this procedure, the office employs a number of forecast computer models, including the Bufkit LES forecasting program, developed by forecasters at the NWSFO Buffalo.

Figure 9. Dockus (1985) Great Lakes "Dockus Decision Tree"



*Pure LES not likely, "Lake-Enhanced" possible- See Tree B
 **"Combination" Snowfall possible- See Tree C
 X. Terrain Enhancement Likely, O. Standard Lee Terrain

Figure 10. Dockus (1985) "Dockus Decision Tree" B (Lake-Enhanced)



Dockus (1985) "Dockus Decision Tree" C (Combination)

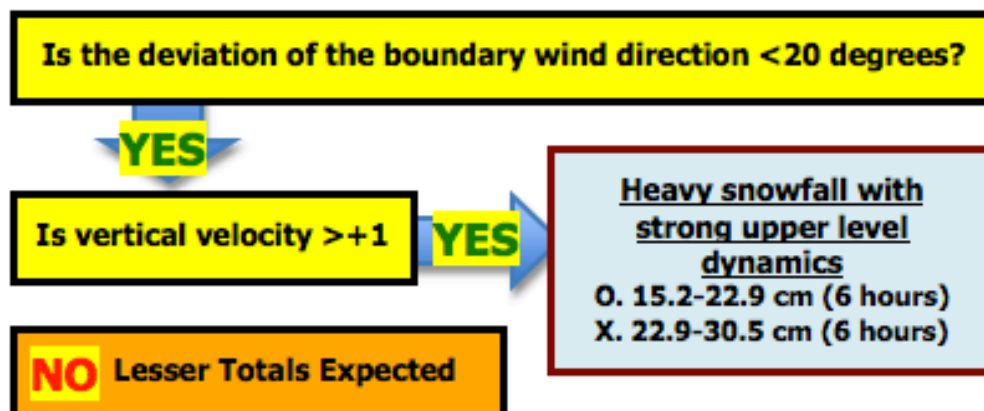


Figure 11. Niziol (1987) Western New York "Forecasting Decision Tree"

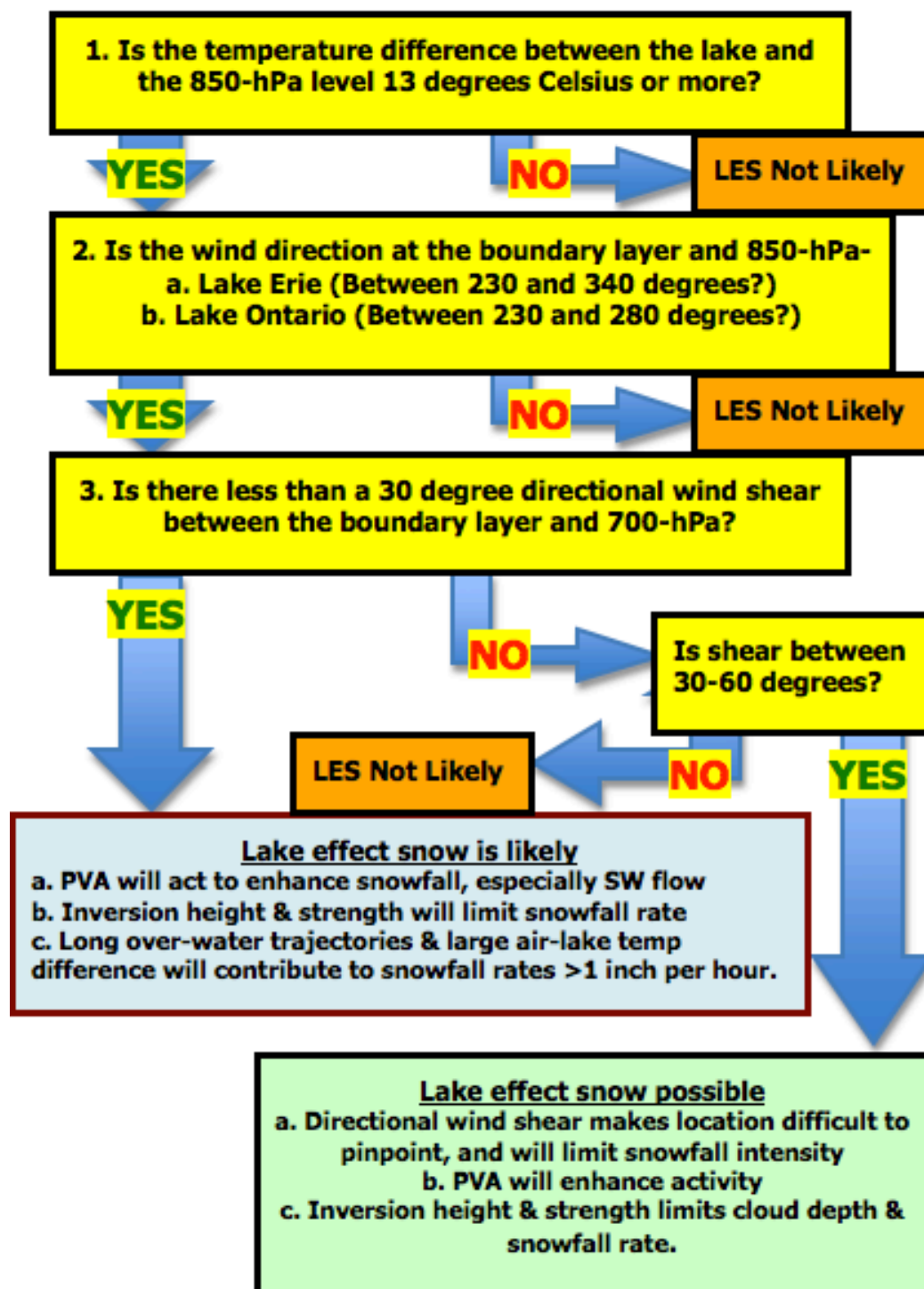
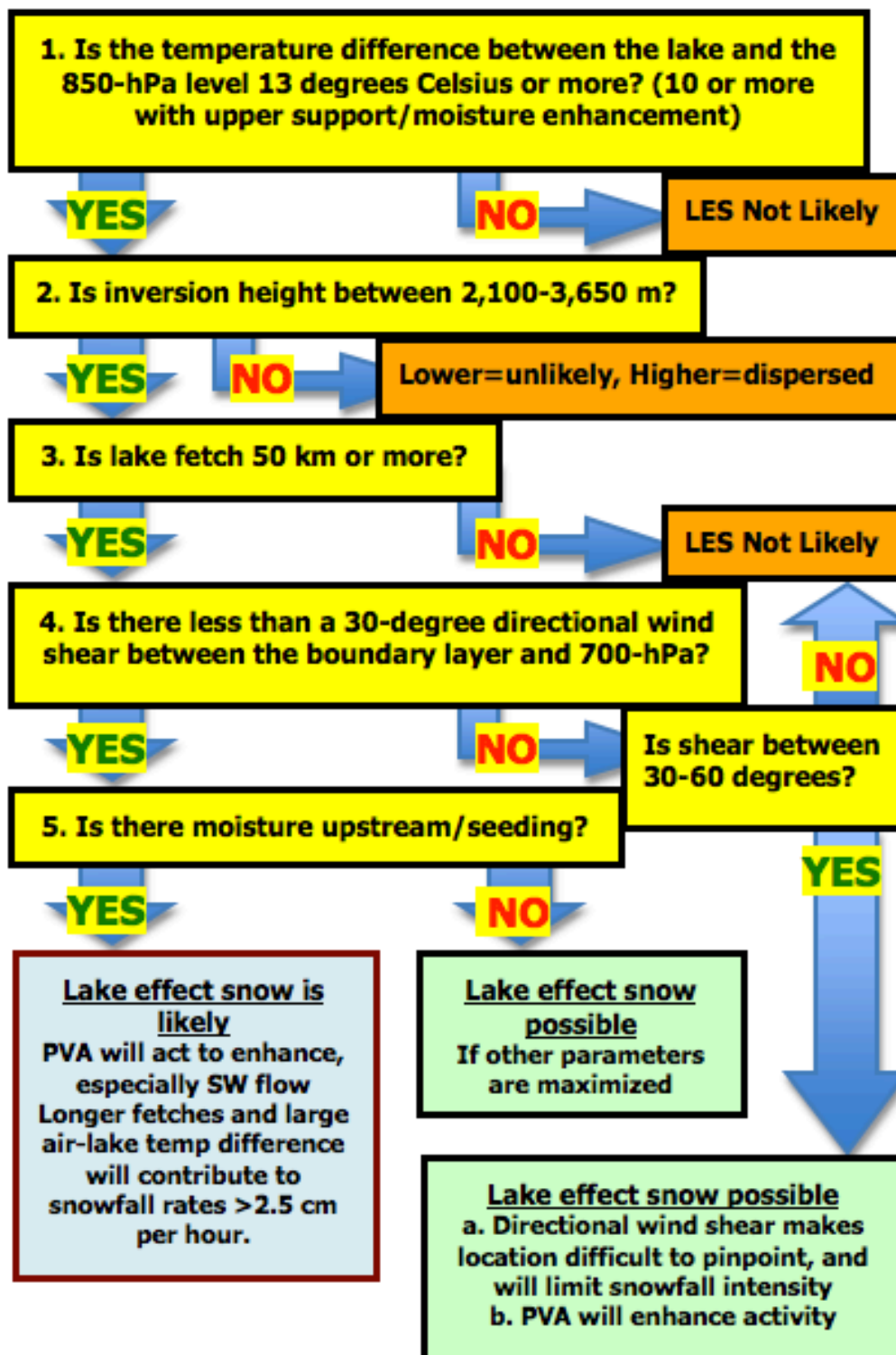


Figure 12. Buffalo NWSFO "Forecasting Decision Tree"



1.4.2 Great Salt Lake

Steenburgh et. al. (2000) advanced (Carpenter, 1993), and produced a forecasting protocol, which has been a universally accepted Great Salt Lake forecasting tool, is shown in Figure 13. It focuses on three elements that are necessary for development, and a fourth parameter that shows up in many of the heavier events:

1. ΔT_{700} of 16 °C or greater
2. A capping inversion below 700-hPa inhibits convective development
3. In flow that is not light/weak, directional shear breaks up banding
4. Low-level convergence, especially land-breeze convergence enhances lake-effect development

The NWSFO Salt Lake City employs much of the Steenburgh forecasting protocol in their current procedure, but has gotten away from a forecasting decision tree with absolute conditionals (Graham, personal communication, 2010). Forecasters now employ a list of parameters and weigh the number of factors favorable to LES development and the magnitude of these parameters. The NWSFO Salt Lake City forecasting parameters for LES are listed in Figure 14. The office has refined two of the Steenburgh forecast parameters based on climatology studies of Salt Lake LES events:

1. ΔT_{700} of 15 °C or greater
2. Adequate upstream moisture, defined as >60% relative humidity in the convective layer up to 700-hPa

Figure 13. (Steenburgh et al., 2000) Great Salt Lake-effect Forecasting

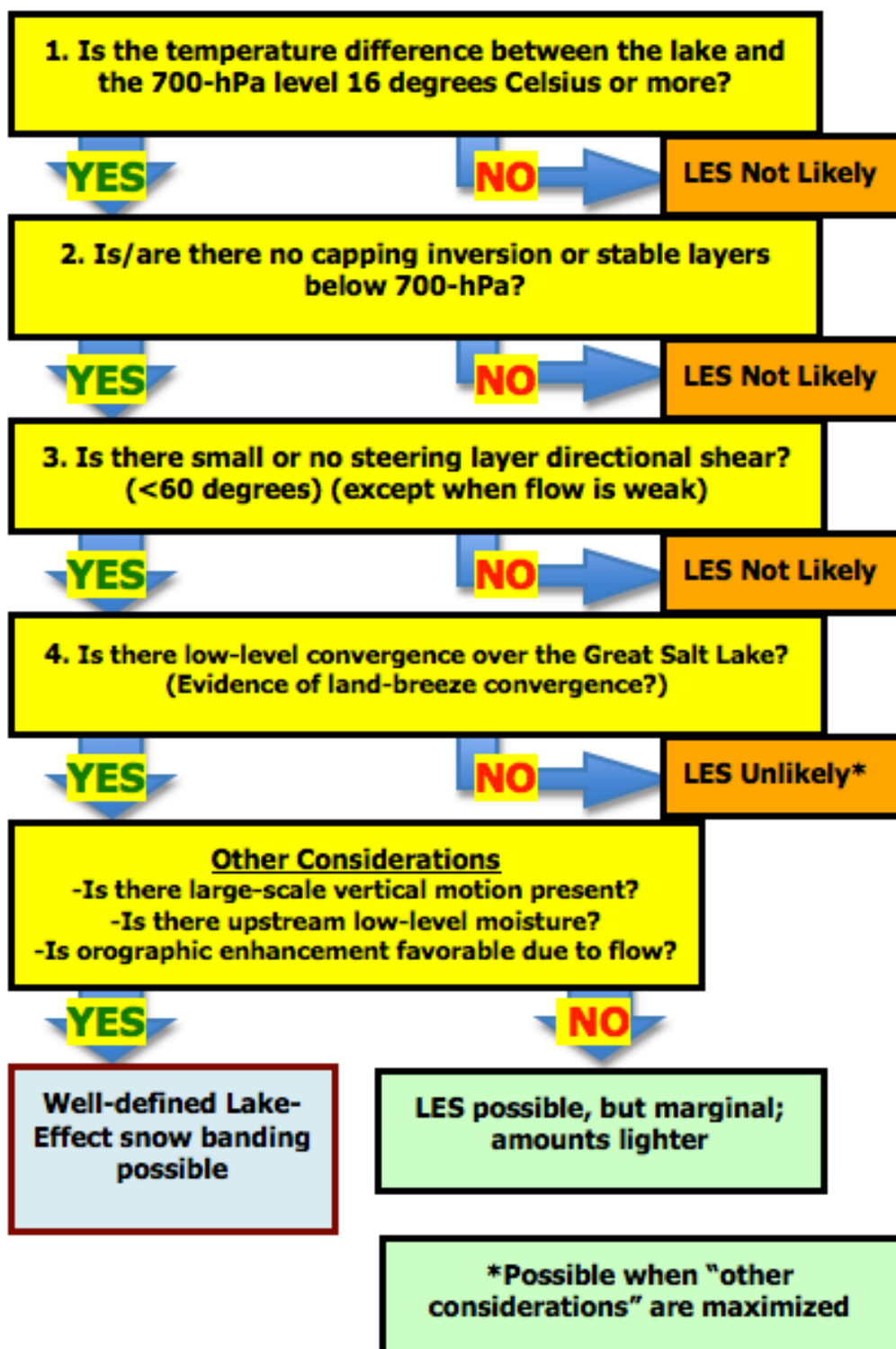
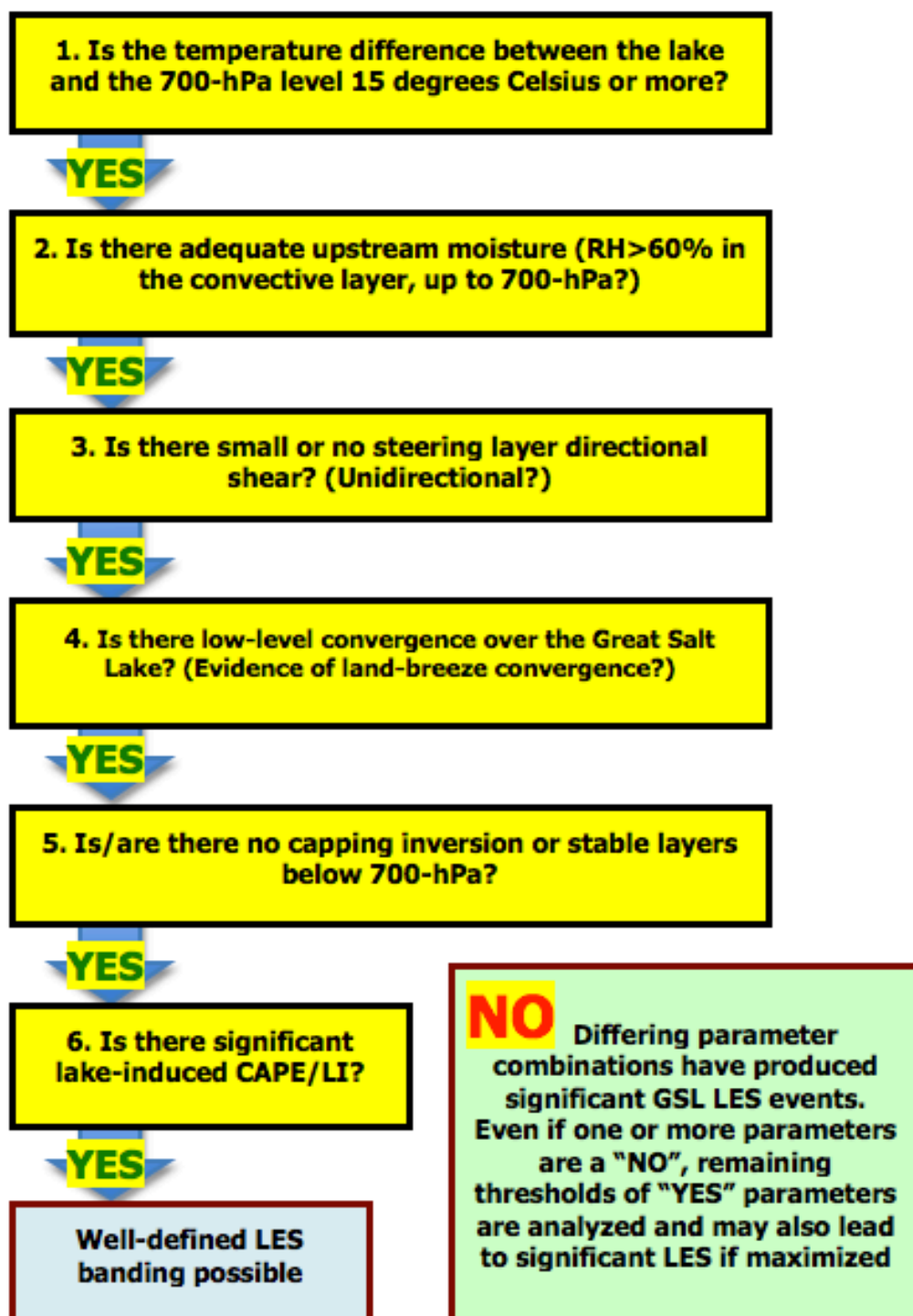


Figure 14. Salt Lake City NWSFO (Forecasting Parameters)



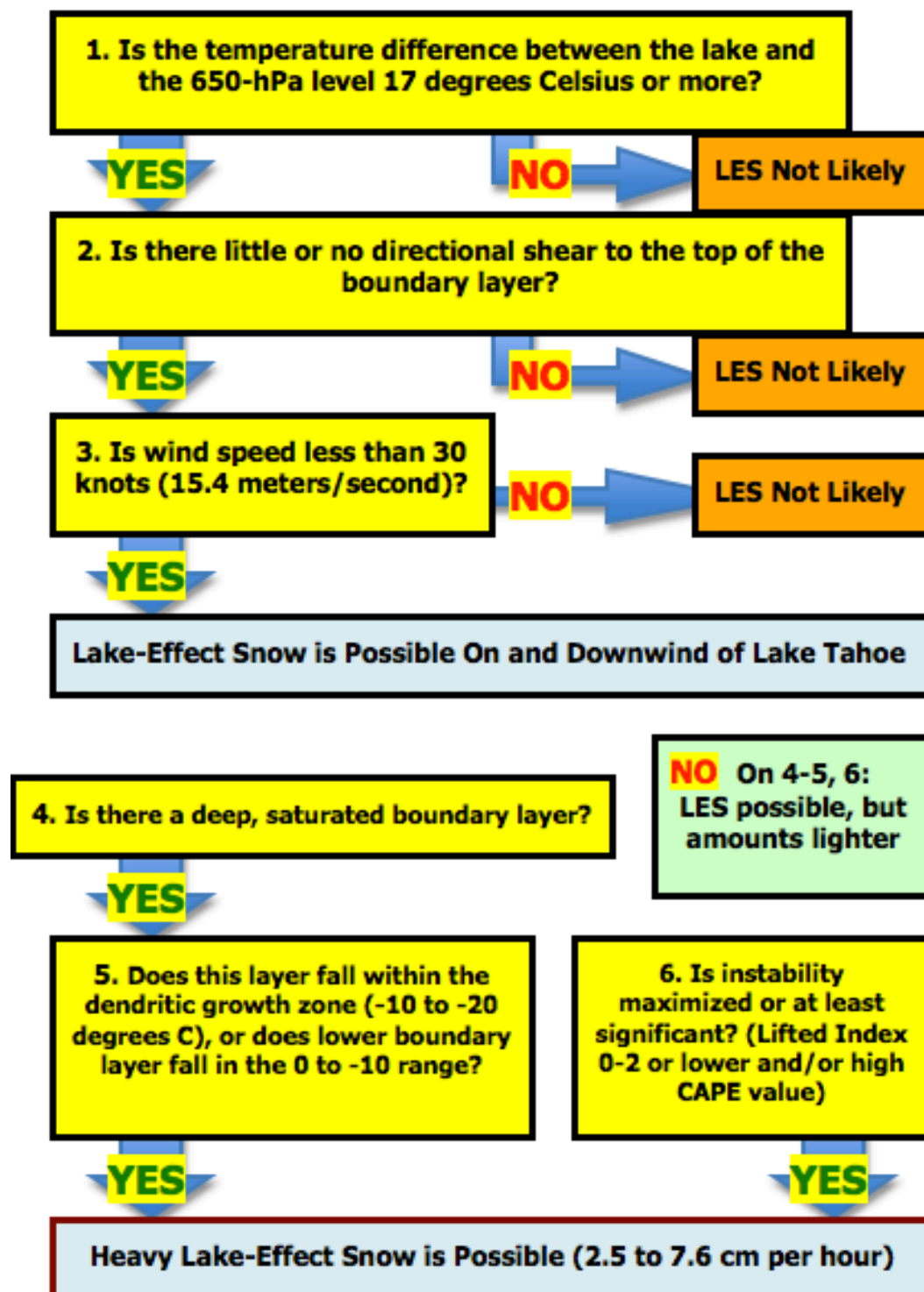
1.4.3 Lake Tahoe

Figure 15 shows the Reno NWSFO "Forecasting Decision Tree." Cairns et al. (2001) was the first paper to study a Tahoe LES case and compare forecasting parameters with other regions. In the past decade, forecasters at the NWSFO Reno advanced these findings through experience (Brong, personal communication, 2009). Critical factors in their procedure were discussed as:

1. ΔT_{650} of 17 °C or greater.
2. Little or no directional shear from the surface to the 650-hPa level or organized banding will break down.
3. Maximum wind speed must be less than 15.4 m/s or convective columns will break up.

Other parameters in the decision protocol were not listed as critical factors to LES development (O'Hara, personal communication, 2010). These factors were discussed as favorable to increase the chance of LES and amounts of snow if present.

Figure. 15. Reno National Weather Service "Forecasting Decision Tree"



1.5 Hypotheses

Atmospheric and lake surface parameters can be used to quantify the conditions necessary for LES development on Lake Tahoe.

Some of the parameters may include the following:

1. Lake surface temperature to 650-hPa level temperature difference
2. Presence or absence of an inversion at or below the 650-hPa level
3. Magnitude of directional shear between the surface and the 650-hPa level
4. Maximum wind speed between the surface and the 650-hPa level
5. Mean relative humidity between the surface and the 650-hPa level
6. Mean temperature between the surface and the 650-hPa level
7. Instability (LI and CAPE)
8. Upper level support (Cyclonic flow at 500-hPa)

2. Procedure

2.1 Case Study Event Selection

Five Lake Tahoe LES events were chosen for temporal parameter analysis based on radar observations made in real time by the NWSFO Reno. The cases were identified as LES by NWSFO Reno forecasters in forecast products and advisories and/or warnings issued to the public. The dates of the five case studies were:

1. 31 October-3 November 2003 (Case I)
2. 9-11 March 2006 (Case II)
3. 20-21 January 2008 (Case III)
4. 10-11 October 2008 (Case IV)
5. 4-5 October 2009 (Case V)

2.2 Identification of Tahoe LES Parameters

Parameters for this investigation of the Tahoe lake-effect, are based on those mentioned by (Rothrock, 1969; Dockus, 1985; Niziol, 1987), in the Great Lakes research, (Carpenter, 1993; Steenburgh et al., 2000) for the Great Salt Lake, and (Cairns et al., 2001) on Lake Tahoe. National Weather Service Office forecasting information from the Buffalo, Salt Lake City, and Reno Offices is also included in selection and analysis of the meteorological elements necessary for the development of a lake effect.

For this study, the parameters for Tahoe LES analysis include:

1. ΔT_{650} [The 650-hPa level was chosen due to the increased elevation of Lake Tahoe (Cairns et al., 2001)]: This value was compared to the minimum 17 °C forecasting threshold (ΔT_{650X}) used by the NWSFO Reno.
2. Temperature difference between the lake surface and land surface in the Tahoe Basin (KTVL, Lake Tahoe Airport) (ΔT_{land}): This was an experimental variable that was obtained in other regions for use in verification of land breeze convergence. In this study, there was not enough data to prove the existence, location, or influence of a convergence zone, but this value was collected for statistical use, future research, and the author's curiosity.
3. Existence and height of a capping inversion: This parameter was examined based on research on the Great Lakes and Great Salt Lake suggesting that the absence of a capping inversion or increased height of an existing inversion above one km is critical for lake-effect snow formation. This was an affirmative or negative determination of inversion existence at or below the 650-hPa level.
4. Existence and magnitude of directional shear from the surface to the 650-hPa level, or inversion level if present (S): This value was compared to the maximum threshold of 60° (SX) in use at the NWSFO Buffalo and NWSFO Salt Lake City.

5. Maximum wind speed from the surface to the 650-hPa level, or inversion level if present (W): This value was compared to the maximum threshold for convective development and longevity of 15.4 m/s (WX), in use at the NWSFO Reno.
6. Amount of moisture (mean relative humidity) from the surface up to 650-hPa level, or inversion level if present (RH): This parameter was compared to the 60% mean relative humidity value (RHX) noted in Great Salt Lake research.
7. Mean temperature from the surface up to the 650-hPa level, or inversion if present (T): This value was compared to the mean value of the NWSFO Reno ideal temperature range for snow crystal formation and snow growth in this layer (TX) of -10 °C.
8. Instability, as determined by the lifted index (LI) and amount of existing convective available potential energy (CAPE) in the Reno soundings: This value was compared to the NWSFO Reno maximum parameter of a maximum lifted index of +2 (LIX). Any existing CAPE was mentioned, although no threshold was defined. Values higher than 100 J/kg were considered beneficial to LES development.
9. Synoptic/Upper-level support as indicated by the Lake Tahoe area being in cyclonic or anticyclonic flow or by the presence of any mechanisms for enhancing positive vertical velocity in the region from the surface to 200-hPa: This parameter was compared to research and forecasting methods

from all LES regions which suggests that cyclonic flow and positioning of the lake to the right of a trough axis provides support for LES development.

2.3 Zero-Hour Definition and Time-Step Analysis

As in (Mote et al., 1997), a zero-hour (0-hour) was established for each case study for temporal analysis. For this paper, the 0-hour for each case was established as the 0000 Coordinated Universal Time (UTC) or 1200 UTC hour preceding the first appearance of lake-effect activity on the National Weather Service (NWS) WSR-88D Next Generation Radar (NEXRAD) located north of Reno, Nevada (KRGX). Local time was Pacific Standard Time, or UTC minus eight hours (UTC minus seven hours for Pacific Daylight Time). UTC was used for all analysis in this study.

Time-step analysis of each event analyzed parameter evolution at 12-hour intervals from 24 hours preceding the 0-hour, to the 0000 UTC or 1200 UTC hour following the last appearance of lake-effect activity on the NEXRAD. This methodology was chosen based on the availability of data at 12 hour intervals.

Radar analysis of each event was performed, independent of the time-step hour increments. The evolution of radar composite reflectivity was studied through analysis of echo patterns and reflectivity intensity (dBz). Radar data was available in six-minute increments through the course of each case.

2.4 Data

Lake Surface Temperatures: The National Aeronautics and Space Administration (NASA), Jet Propulsion Laboratory, and the University of California Davis' Tahoe Environmental Research Center provided the lake water surface data ($^{\circ}\text{C}$) utilized in this study. A mean of the data archived from four data collection station buoys, TB1-TB4 (Figure 16), was collected at a one to three cm depth for the duration of each event and utilized during all analyzed time-step hours (Table 6).

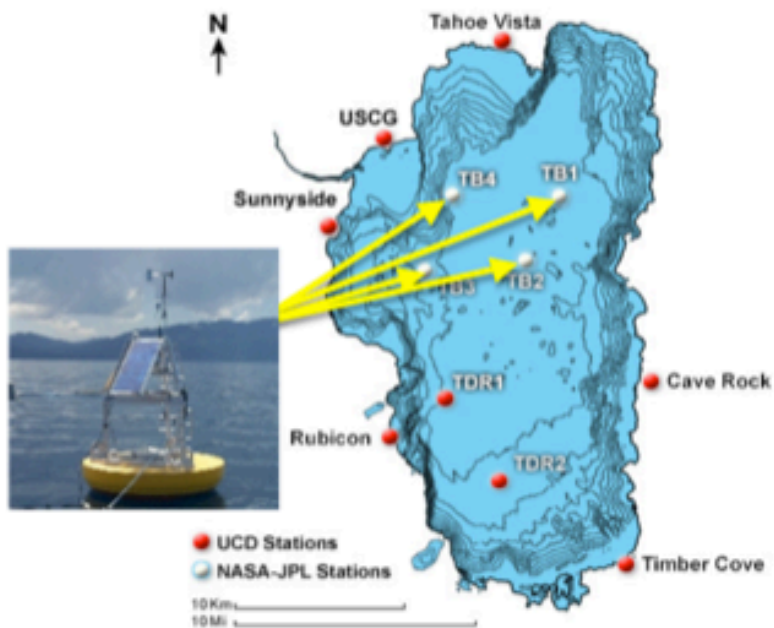


Figure 16. Lake Tahoe Data Collection Buoys (TB1, TB2, TB3, and TB4) (Jet Propulsion Laboratory-NASA and UC Davis)

Time Steps:	0-24	0-12	0	0+12	0+24	0+36	0+48	0+60	0+72
9-11 November 2000 (Cairns et al.)	10.82	10.62	10.66	10.53	10.41	10.26	10.24	10.05	10.16
Case I	13.93	13.56	13.36	13.09	13.03	12.81	12.56	12.26	12.35
Case II	5.60	5.35	5.38	5.28	5.34	5.25	5.30		
Case III	5.92	5.47	5.44	5.37	5.45	5.41	5.43		
Case IV	15.36	15.57	15.19	15.03	14.49	14.49			
Case V	16.15	15.84	15.43	15.21	14.96	14.81			

**Table 6. Lake Tahoe Surface Temperatures (°C)
(Jet Propulsion Laboratory-NASA and UC Davis)**

Land Station Temperatures: The temperature data from one land station, Lake Tahoe Airport (KTVL), was utilized for each time-step hour through the duration of each case. KTVL was chosen due to availability of hourly temperature data (Table 7).

Time Steps:	0-24	0-12	0	0+12	0+24	0+36	0+48	0+60	0+72
9-11 November 2000 (Cairns et al.)	5.00	-2.78	-2.00	-5.00	-3.28	-10.00	-3.28	-14.39	2.78
Case I	2.22	-4.00	-2.78	-11.11	-0.61	-13.00	-1.00	-4.00	-0.61
Case II	3.89	0.00	-4.00	-8.28	-6.11	-9.00	-5.00		
Case III	6.11	0.00	-4.00	-6.00	-3.89	-6.00	-3.28		
Case IV	5.00	11.11	-4.39	0.00	-3.89	0.00			
Case V	16.7	8.89	10.00	-2.00	1.00	-5.00			

Table 7. Lake Tahoe Airport (KTVL) Temperatures (°C)

Radar Analysis: KRGX NEXRAD composite reflectivity was analyzed utilizing archived data obtained from the National Climatic Data Center. KRGX is the closest NWS radar site to the Tahoe Basin, and the site location is indicated on all radar imagery included in this study. Due to greater distance to the southwest quadrant of the Tahoe Basin from KRGX, reduced echo reflectivity was a possible source of error in analysis of this region of the study area.

Upper Air Soundings: The Reno (REV) sounding was used in the analysis of thermodynamics (temperature profile and stability assessment), wind speed and direction with height, moisture content with height, depth of the boundary layer, and existence and location of inversions. REV was chosen due to its proximity to Lake Tahoe, just 61 km from the north shore. Two daily launches, at 0000 UTC and 1200 UTC, were executed during the studied events. Archived REV sounding data was obtained from the Atmospheric Sciences Department at the University of Wyoming. The data was analyzed from the level of Lake Tahoe (1,897 m) upward, using the commercial software program RAOB. REV upper air sounding data did not account for processes that occurred in the Tahoe Basin, and provided only two daily launches with associated data for detailed study of LES parameters. Figure 17 provides an example REV upper air sounding from Case II. The yellow line defines the 650-hPa level, and the surface level (Tahoe lake level) is defined by the dark blue line. LES parameter investigation focused on this layer (surface to 650-hPa level) in each of the 44 REV upper air soundings analyzed in this thesis.

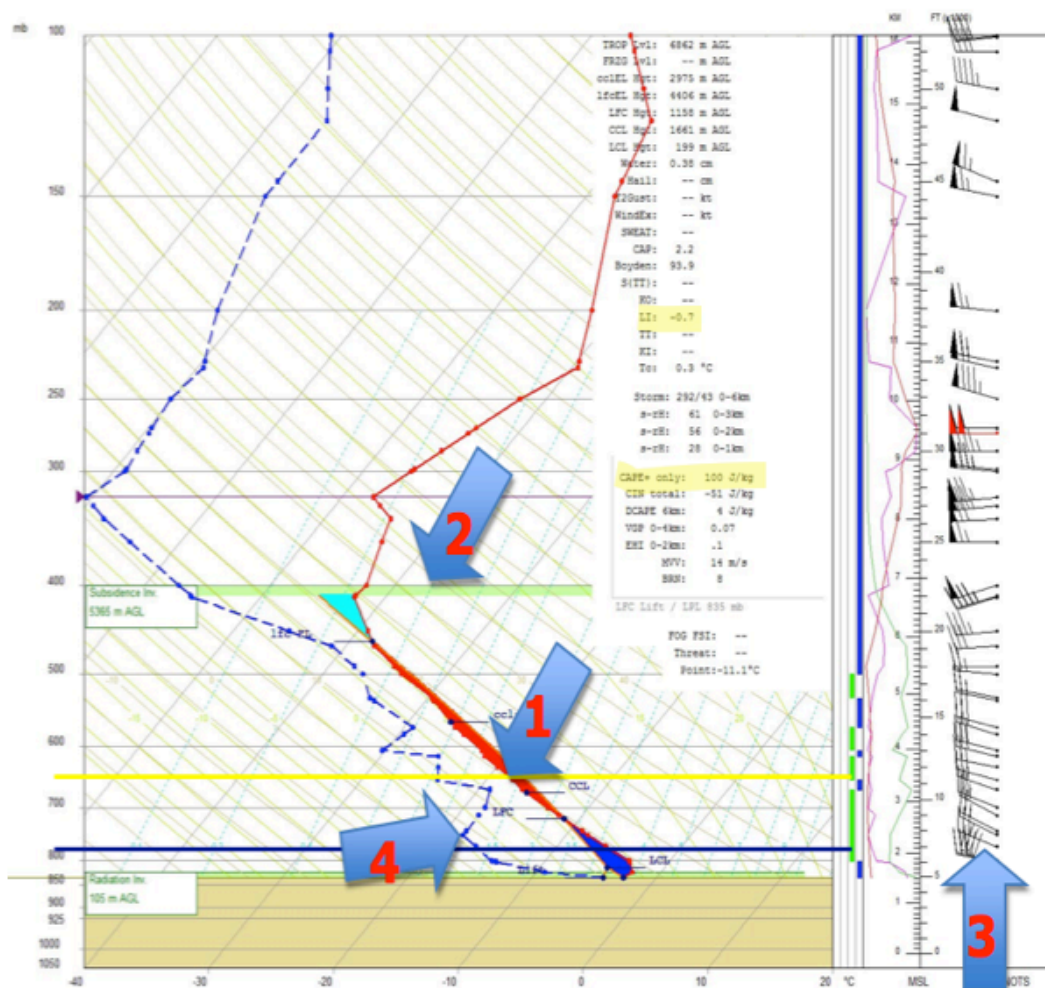


Figure 17. REV Sounding 10 March 2006 (1200 UTC)

Upper Air Plots: Figure 18 shows analysis of the atmosphere represented in pressure levels and obtained from the National Center of Environmental Prediction (NCEP) data archive. Upper air charts utilized in this study were:

- 200-hPa level analysis for jet and jet streak location and isotachs
- 500-hPa level analysis for trough/ridge location, PVA/NVA, circulation
- 850-hPa level analysis for advection, and areas of convergence

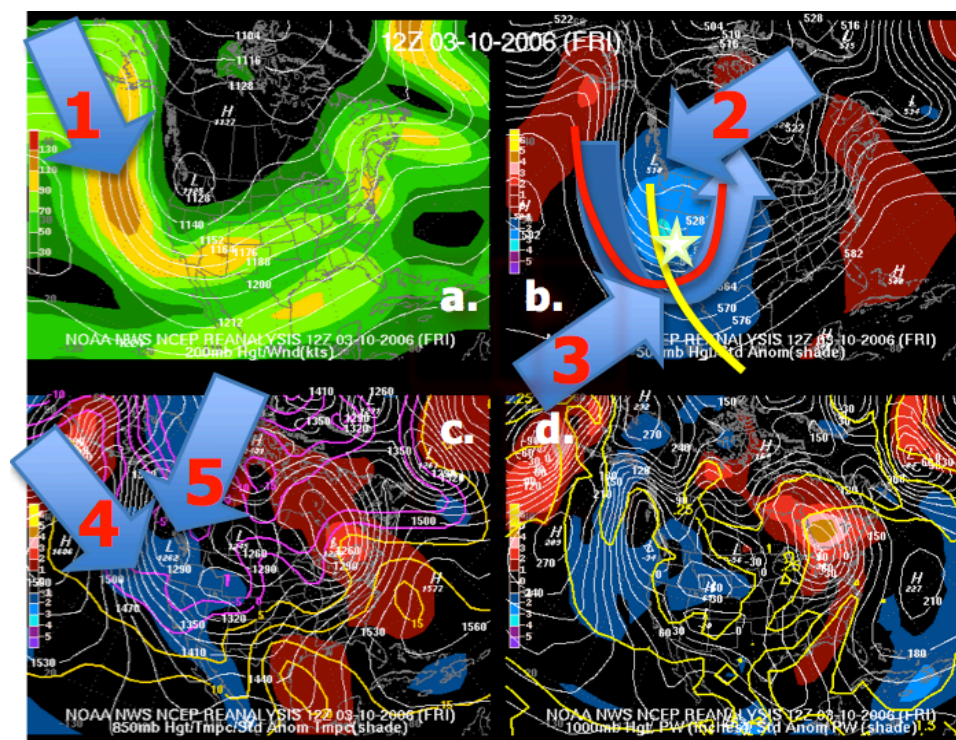


Figure 18. 10 March 2006, 1200 UTC: 200, 500, 850, 1000-hPa NOAA Upper Air Analyses

2.5 Methods for LES Case Study Parameter Analysis

1. ΔT_{650} : The temperature of the 650-hPa level was determined from the NWS sounding taken from Reno, Nevada (REV) utilizing RAOB software at each time-step hour. Arrow 1 in Figure 17 indicates the 650-hPa level temperature on the temperature profile. For this study, an interpolated value for the 650-hPa level temperature was calculated using the RAOB software, as this was not a mandatory sounding level. ΔT_{650} = lake surface temperature – 650-hPa level temperature.
2. ΔT_{land} : Lake surface temperature – KTVL temperature.

3. Existence and height of a capping inversion: Arrow 2 in Figure 17 shows an example of an inversion, where temperature increased with height in the REV sounding. Inversion levels in the REV soundings were highlighted in green in the RAOB software.
4. S: On the REV sounding, the layer from Tahoe lake-level (1898 m) and the 650-hPa level was analyzed for maximum directional wind shear (the greatest difference in wind direction in the layer). Arrow 3 in Figure 17 shows graphical wind direction and speed observations through the layer, quantified in the sounding numerical data.
5. W: Maximum wind speed in the lake-level to 650-hPa level layer was determined on the REV sounding, also considering the wind data indicated by Arrow 3 in Figure 17 and associated sounding numerical data. Wind speed was given in knots and converted to m/s in this study.
6. RH: In the REV sounding, Arrow 4 in Figure 17 shows the dewpoint temperature profile. This temperature of the air at saturation, along with the relative humidity (RH), were measured and provided in the numerical sounding data at mandatory levels, as well as additional pressure levels in the profile. Mean RH was determined from the interpolated RH available in the RAOB software for the lake-level and 650-hPa level. These values were averaged with the mandatory level RH percentages observed in this layer to arrive at the mean layer RH.

7. T: The REV temperature profile (Arrow 1 in Figure 17) was analyzed from lake-level up to the 650-hPa level. Mean temperature was determined from the interpolated temperatures available in the RAOB software for the lake-level and 650-hPa level. These values were averaged with the mandatory level temperatures observed in this layer to arrive at the mean layer temperature.
8. Instability, as determined by the lifted index (LI) and amount of existing convective available potential energy (CAPE) in the Reno soundings: These values were calculated and provided in each sounding. They are highlighted in yellow in Figure 17 in the data listing to the right of the sounding. Determined manually, LI is calculated in a sounding by lifting a parcel of air along the dry adiabat to its level of free convection (LFC, labeled in Figure 17), then along a moist adiabat to the 500-hPa level. Then LI is determined by subtracting the temperature of the lifted parcel from the observed temperature at the 500-hPa level. CAPE is the total area between the ascent path and the environment from the LFC up to the equilibrium level (EL, labeled in Figure 17). The area of CAPE in Figure 17 is highlighted in red and indicated by Arrow 1.
9. Synoptic/Upper-level support: Figure 18 shows an example of the upper air charts analyzed to determine the affirmative or negative contribution of upper level and general synoptic patterns to positive vertical velocity. Figure 18a was an analysis of wind speed and geopotential height at the

200-hPa pressure level. This map was analyzed for isotachs, or higher wind speeds indicating jet streaks, as indicated in this example by Arrow 1. The left-front, or right-rear quadrants of jet streaks provide positive vertical velocity and upper level support. Figure 18b was an analysis of the 500-hPa pressure level. The location of troughs and ridges and the direction of circulation were determined at this level. Arrow 3 in Figure 18 indicates the trough axis highlighted by a yellow line. The trough is outlined with a red line, and the curved arrow following the trough outline indicates the direction of flow, which was cyclonic in this analysis. The star in Figure 18b shows the location of Lake Tahoe, which was to the right of the trough axis, in the exit region of the trough. This was favorable for upper level divergence and PVA. Arrow 2 indicates an upper low-pressure area at the 500-hPa level, which can contribute to lower level convergence and atmospheric lifting. Figure 18c is an analysis of the 850-hPa pressure level. Arrow 4 shows cold air advection into the Lake Tahoe area at this level, which is a mechanism for low-level convergence and frontal lifting, and Arrow 5 indicates a low-pressure area close to the surface, or an area of low-level convergence.

3. LES Case Studies

3.1 Case I

3.1.1 Event Summary

Following a week of abnormally warm weather for the Tahoe Basin in late October, the pattern rapidly changed on 29 October. A ridge of high-pressure, 3 to 4 standard deviations higher in height than average, amplified into Alaska in the Eastern Pacific, allowing a trough of low-pressure, 2 to 3 standard deviations lower in height than average, to drop into the Western United States. A cold front dropped temperatures at KTVL from a maximum of 16.7 °C on 29 October to a maximum of 3.9 °C on 30 October. Lake water temperature remained warm at 13.9 °C at 0000 UTC on 31 October.

An abnormally cold, positively tilted, long-wave trough was positioned over the western United States through the duration of this event, from 30 October through 4 November (Figure 19b, Arrow 1). During most of the period, the trough axis was west of Lake Tahoe, keeping the basin in a region favorable for upper-level divergence and PVA. Two cold low-pressure areas took similar tracks, generating two lake-effect snowfall events during this period.

The first system produced widespread snowfall starting on the afternoon of 31 October, orographically enhanced with widespread snow shower activity along and west of the Sierra Nevada Crest. The low was positioned west of the lake, north of the San Francisco Bay Area, placing the lake in southerly flow east of the low. The low tracked from the coast east to the Lake Tahoe area by the

morning of 1 November (Figure 19c, Arrow 2). Banding of radar echoes, indicative of an LES event, first became prominent on the north shore from the California-Nevada border to the Interstate 80 corridor, and then shifted to the west shore of Lake Tahoe as the low moved east. The National Weather Service Office in Reno issued a lake-effect snow warning for the west shore in the early morning hours of 1 November, which expired at 1500 UTC.

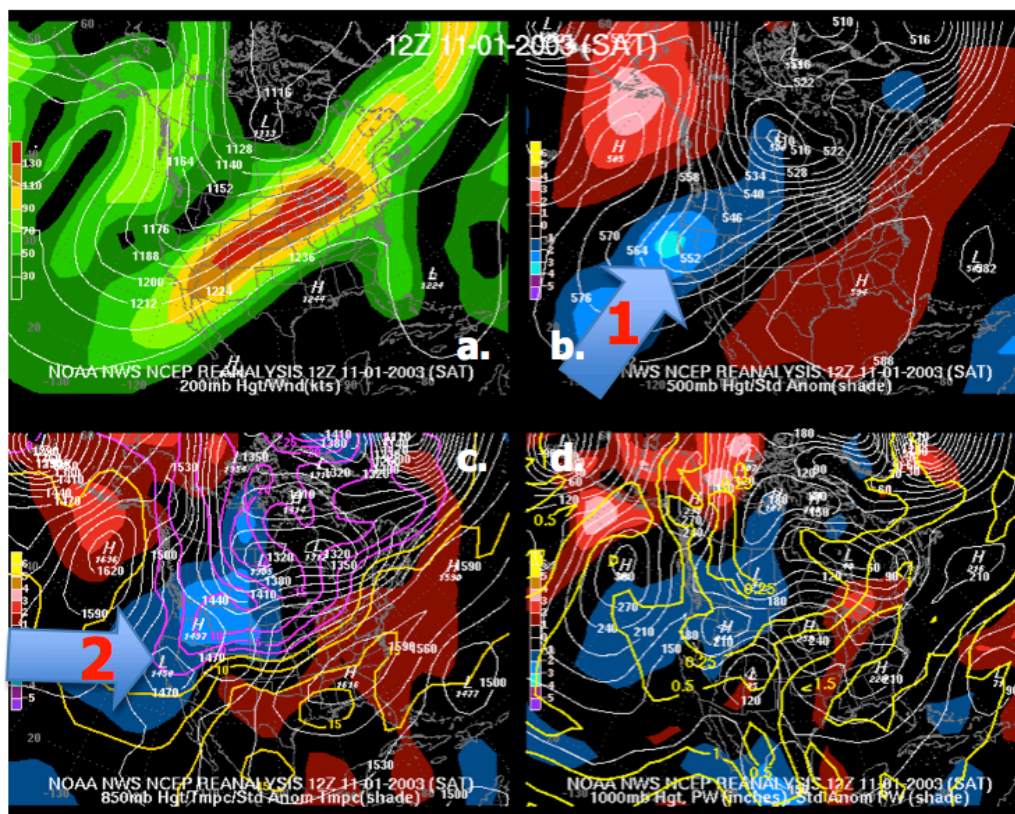


Figure 19. 1 November 2003, 1200 UTC: 200, 500, 850, 1000-hPa NOAA Upper Air Analyses

Even with a brief break in the two systems, the long-wave trough stayed in place, with little temperature modification. The second low took a similar track, dropping from Oregon on the afternoon of 2 November, to the California-Nevada-Oregon border by the early morning of 3 November (Figure 20c). Following widespread snow shower activity along a convergence boundary in a heavily sheared environment, westerly flow and cold air advection developed a second LES banding event on the east shore of the lake. From 1400 UTC until 1900 UTC, snow bands affected the eastern shore.

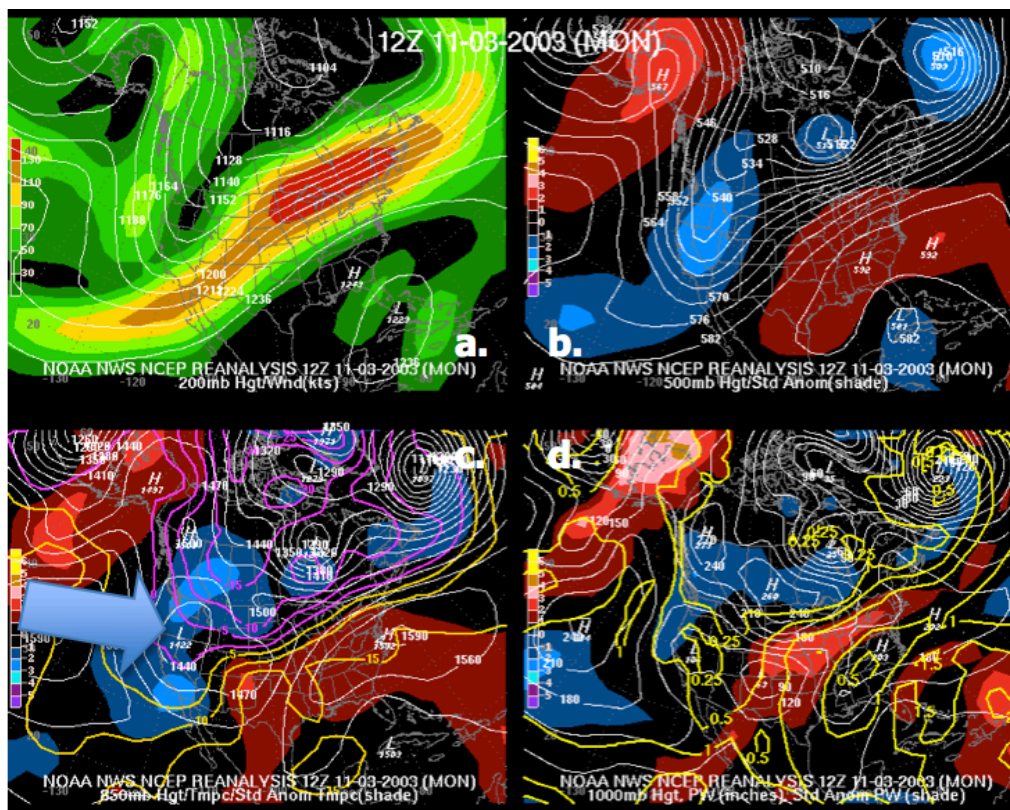


Figure 20. 3 November 2003, 1200 UTC: 200, 500, 850, 1000-hPa NOAA Upper Air Analyses

Figure 21 shows Case I reported snowfall totals. The reports reflect the change in orientation of the LES banding with this event that affected the north and west shores and downwind terrain on 1 November (Locations 1-3), and the eastern shore and downwind terrain on 3 November (Locations 4,5).

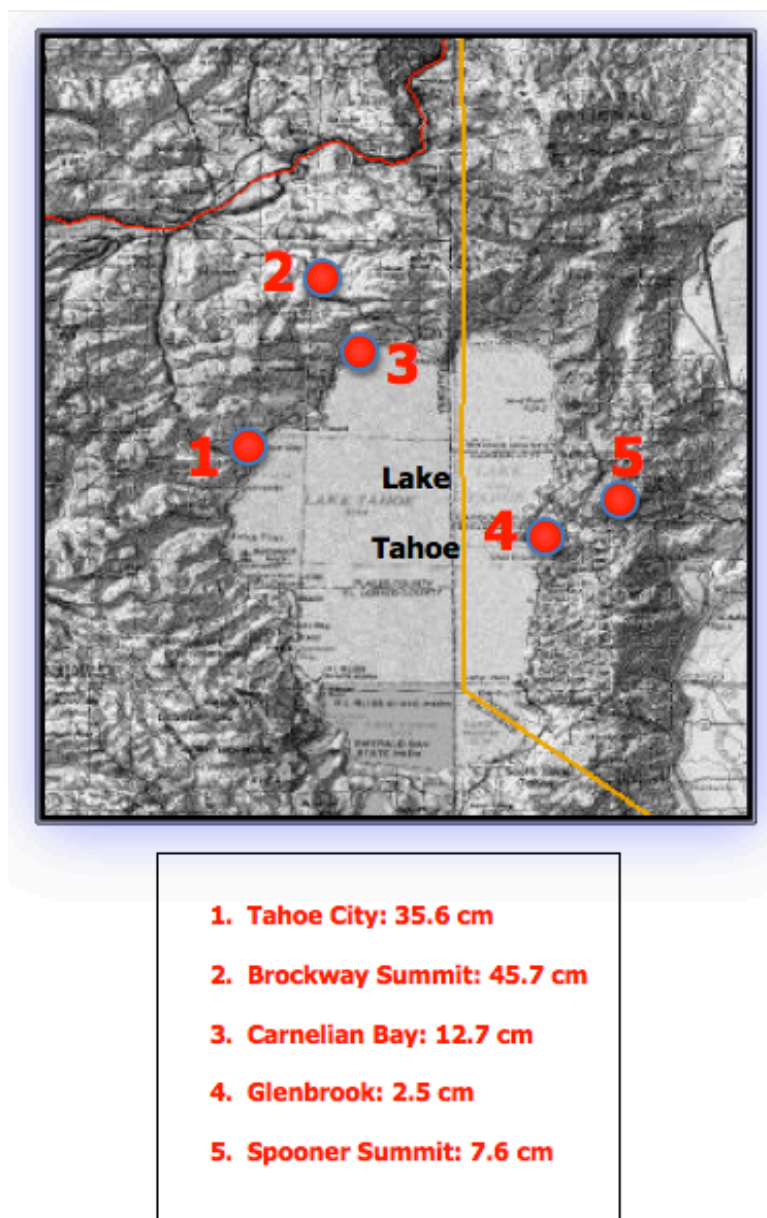


Figure 21. Case I Reported Snowfall Totals

3.1.2 Results of Time-step Analysis

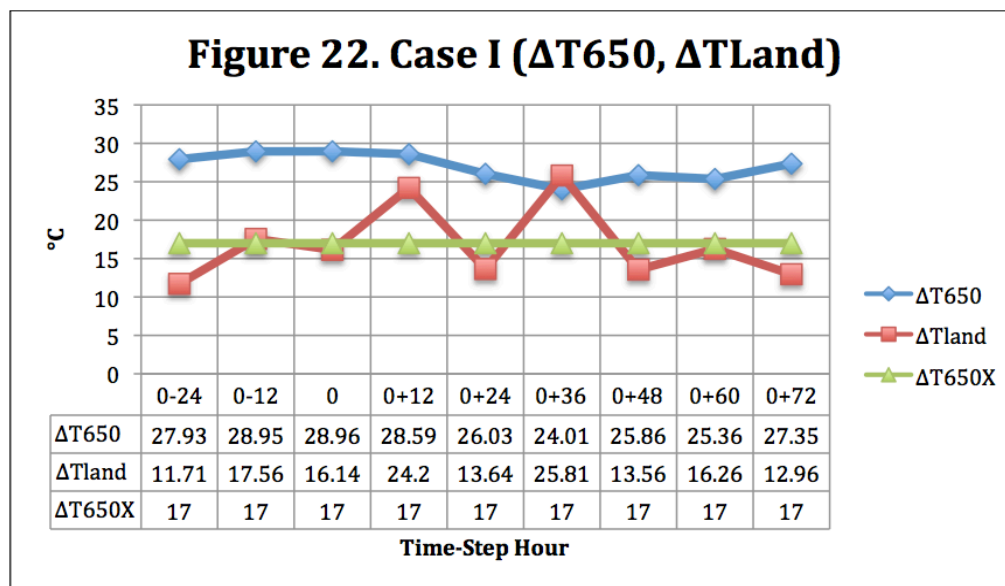
Table 8 is a complete listing of all parameter analysis results during Case

I. Figures 22-27 provide time-step analysis of individual LES parameters.

Time-Step Hours:	0-24	0-12	0	0+12	0+24	0+36	0+48	0+60	0+72
ΔT_{650} (°C)	27.93	28.95	28.96	28.59	26.03	24.01	25.86	25.36	27.35
ΔT_{land} (°C)	11.71	17.56	16.14	24.20	13.64	25.81	13.56	16.26	12.96
Capping Inversion	NO	NO	NO	NO	NO	YES	NO	NO	NO
S (°)	90	90	120	110	162	59	59	75	31
W (m/s)	8.23	8.75	5.66	3.09	2.57	8.23	9.26	10.8	8.23
RH (%)	63	96	84	83	51	28	66	82	77
T (°C)	-6.65	-9.73	-9.58	-9.80	-7.48	-7.20	-7.23	-7.58	-7.20
Instability (LI CAPE) CAPE (J/kg)	-0.1 91	0.6 51	-0.6 219	3.4 0	6.5 0	12.8 0	2.8 0	3.1 0	5.5 48
Upper Level Support	YES	YES	YES	YES	NO	NO	YES	YES	NO

Table 8. Case I Parameter Analysis Results
Blue columns indicate time-step hours when LES occurred
Green columns indicate hours that immediately preceded and followed LES

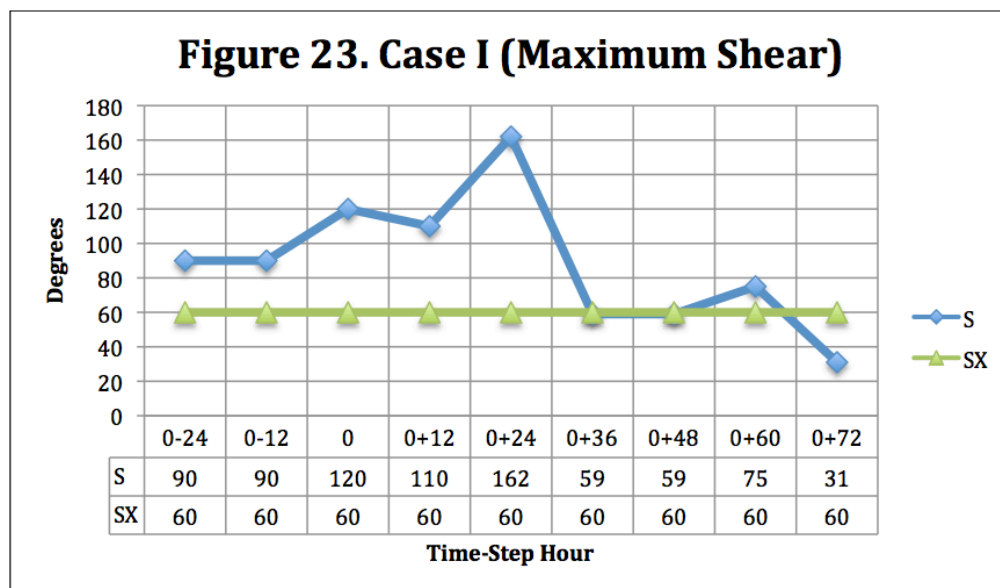
ΔT_{650} (Figure 22): Through the duration of Case I, ΔT_{650} was much greater than ΔT_{650X} . During the two time-step hours when LES banding occurred, this temperature difference was 28.59 degrees (0+12) and 25.36 degrees (0+60).



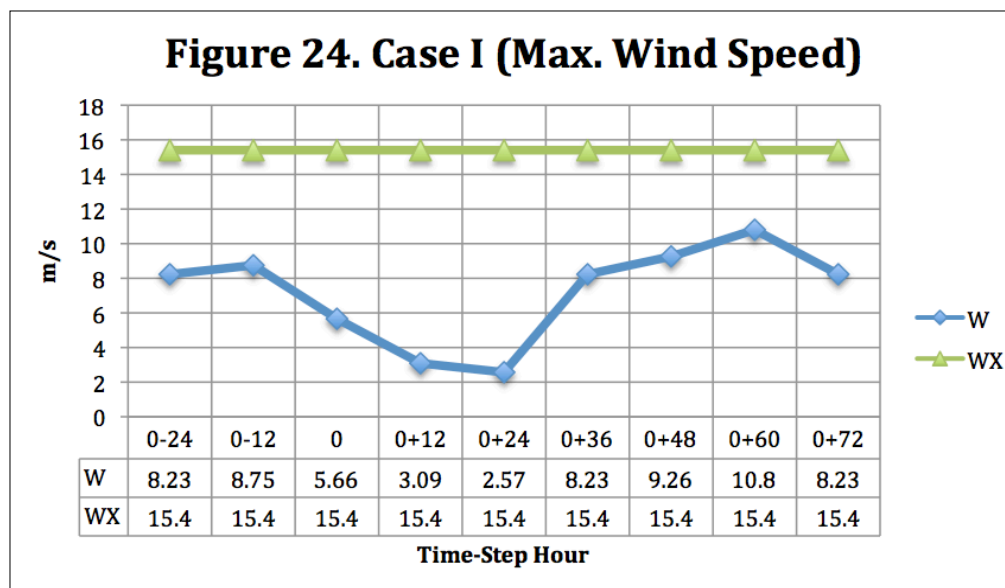
ΔT_{land} (Figure 22): This parameter reflected expected diurnal swing and demonstrated peaks in the early morning hours through the duration of the case. The greatest ΔT_{land} during time-step hours when LES was observed on the KRGX NEXRAD occurred during the 0+12 time-step hour. The second event also occurred in the early morning hours, when this value was maximized during the 0+60 period. The greatest ΔT_{land} of the event occurred between systems and in the presence of an inversion at 0+36, when under partial clearing, KTVL temperature dropped to -13 °C.

Existence of a Capping Inversion: Only one time step (0+36) did show an inversion, at the surface and around the 650-hPa level. No inversions were present during the time-step hours when LES was observed.

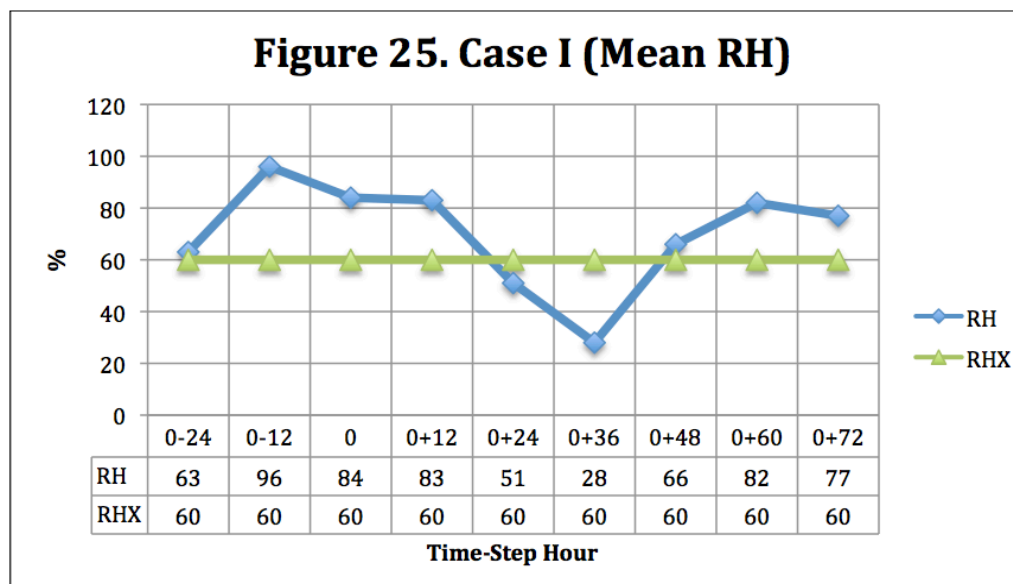
S (Figure 23): Maximum directional shear exceeded SX during both time-step hours when LES occurred. In the first period (0+12), a low passed overhead and likely provided the backing, or counter-clockwise turning of flow with height. The wind speed was very light however, and (Dockus, 1985) mentioned that higher shear was not detrimental if wind speeds were light. In the second time-step hour when LES occurred (0+60), maximum directional shear was 74° before the start of LES, but KRGX analysis demonstrated that the flow shifted easterly during the 0+60 time-step hour. This shift resulted in increased shear. Maximum directional shear was only 31° by the 0+72 time-step hour.



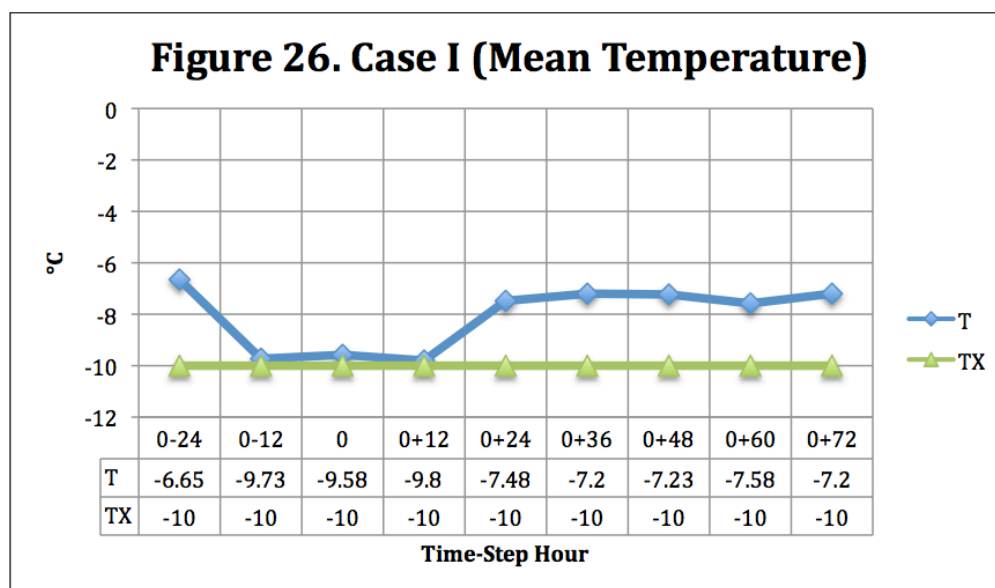
W (Figure 24): Wind speed was very light during the first event, as a low passed over the lake. Wind speed was greatest during the second event, but only peaked at 10.8 m/s in the surface-to-650-hPa level (surface-650) layer during the 0+60 time-step hour. W was below WX for the duration of Case I.



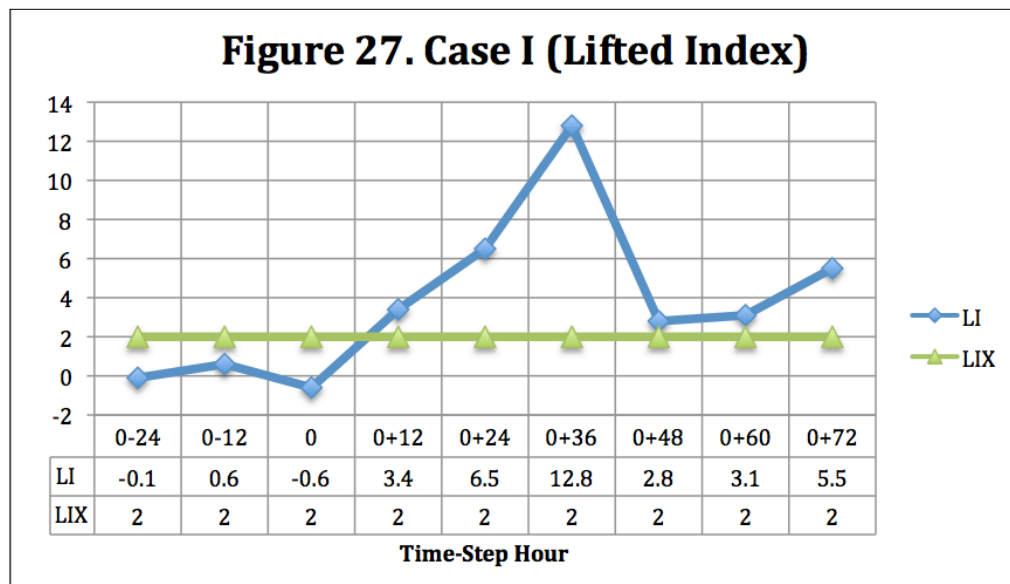
RH (Figure 25): Surface-650 layer air was moist during both time-step hours when LES occurred, with a relative humidity of 83% (0+12) and 82% (0+60). RH dropped below RHX under subsidence and decrease in cloud cover (shortwave ridging) between the low-pressure areas at 0+36.



T (Figure 26): Mean surface-650 layer temperature was $-9.8\text{ }^{\circ}\text{C}$ (0+12) and $-7.58\text{ }^{\circ}\text{C}$ (0+60). The 650-hPa level temperatures were ideal for snowfall formation at -15.5 degrees (0+12) and close to ideal at -13.1 degrees (0+60). T was close to TX at 0+12, but warmed by 0+60 to $7.6\text{ }^{\circ}\text{C}$.



Instability (Figure 27): In this case, during the two time-step hours when LES was observed, LI was greater than 3, and CAPE was 0 on the REV upper-air sounding. LI was greater than LIX during all time-step hours from 0+12 though the end of the event. The greatest instability was shown at the 0-hour, when daytime heating was maximized and other processes were occurring in the exit region of the trough.



Upper Level Support: Lake Tahoe was to the right of the trough axis in cyclonic flow during hours when LES occurred and in the 12-hour intervals proceeding development. This was favorable for upper level divergence and lower level convergence and upward vertical velocity.

3.1.3 Radar Analysis

Snow shower activity was widespread and both cyclonic and orographic in nature through the 24-hour period of 31 October. A low-pressure area was located in Northern California by 1200 UTC, and tracked to the San Francisco Bay area by 0000 UTC on 1 November. Cyclonic flow around the low produced a 650-hPa level wind flow of 180° at 1200 UTC on 31 October, shifting to 170° by

0000 UTC on 1 November. During this time period, the southerly flow produced snow shower activity along the Sierra Nevada crest, and west and southwest-facing slopes. Figure 28 shows maximum reflectivity of 30 dBz, and movement of echoes denoted by the arrow. The 650-hPa wind direction of 170° was noted as the direction of movement at this hour. Higher reflectivity was detected over the western half of Lake Tahoe, but also over the mountainous terrain north and south (upwind) of the lake. Lake enhancement may have been contributing at this hour, but vorticity in association with the low, afternoon heating, and orographics, were likely stronger elements in this radar echo pattern.

As other activity decreased after sunset, returns on and down-wind of Lake Tahoe became evident from 0200 UTC to 0800 UTC on 1 November. Figure 29 shows composite reflectivity at 0504 UTC. Two cells developed along the west shore of Lake Tahoe, one around Homewood and one near Tahoe City. A 29 dBz maximum reflectivity was noted, and the arrow shows the direction of echo movement. Other echoes at this hour were declining in reflectivity, while echoes over and downwind with both Lake Tahoe and Pyramid Lake were showing an increase in coverage and reflectivity.

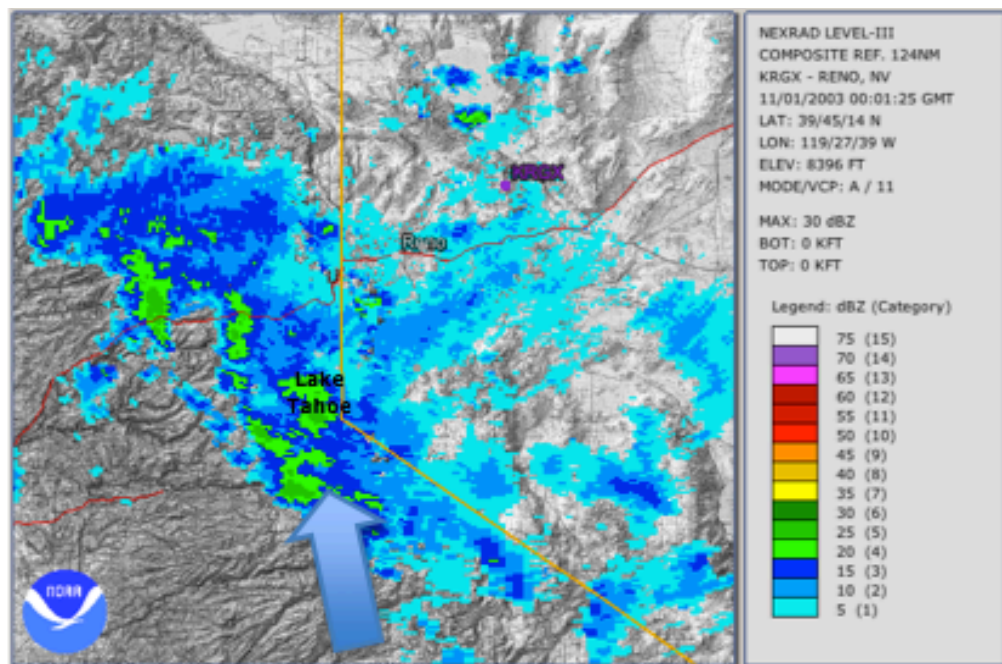


Figure 28. KRGX Composite Reflectivity at 0001 UTC on 1 Nov 2003

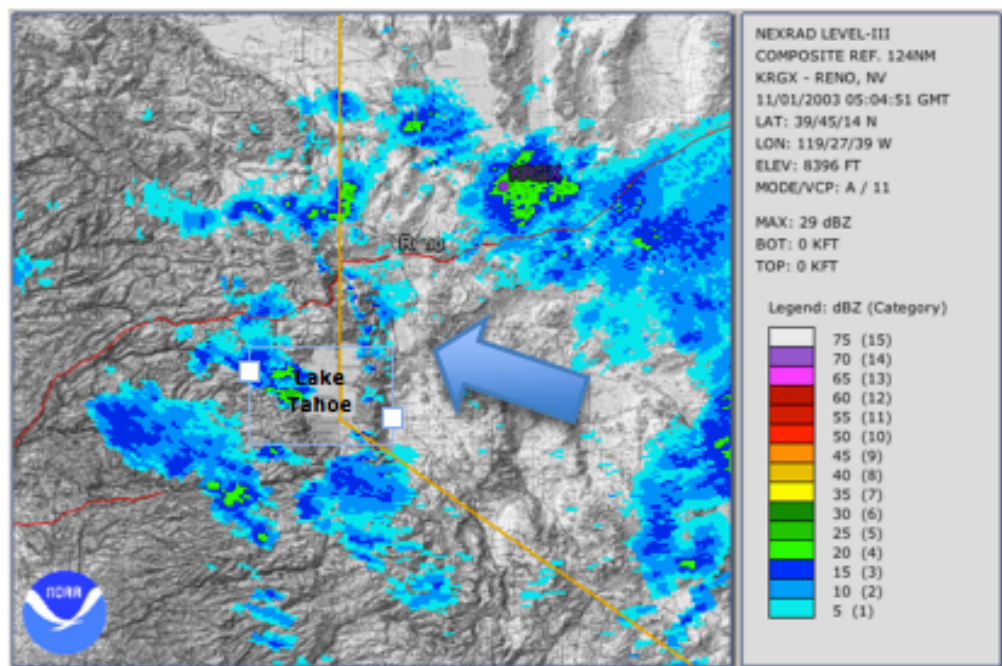


Figure 29. KRGX Composite Reflectivity at 0504 UTC on 1 Nov 2003

Figure 30 shows the snow development of a LES band. The arrow denotes the movement of echoes at 0756 UTC. A maximum dBz of 30 was associated with a cell over the northwest quadrant of the lake and the west shore, from Homewood north to Tahoe City. A broken band of echoes with higher reflectivity of 20 to 25 dBz extended northwest 25 km into the Truckee area. This image reflected the peak reflectivity and length of this LES band. The band persisted through the end of this time step, until the 1200 UTC hour.

Figure 31 shows the last hour of reflectivity for the LES band that developed in the first two hours following 0-hour. A 33 dBz cell was evident over the west shore of the lake around Homewood ski area. The arrow denotes echo movement, which was around 2.5 m/s, and almost stationary by 1230 UTC. Flow was weak at all levels, and 650-hPa flow direction had become westerly at 275°. Flow at the 700-hPa level was still 165°, steering the disintegrating band.

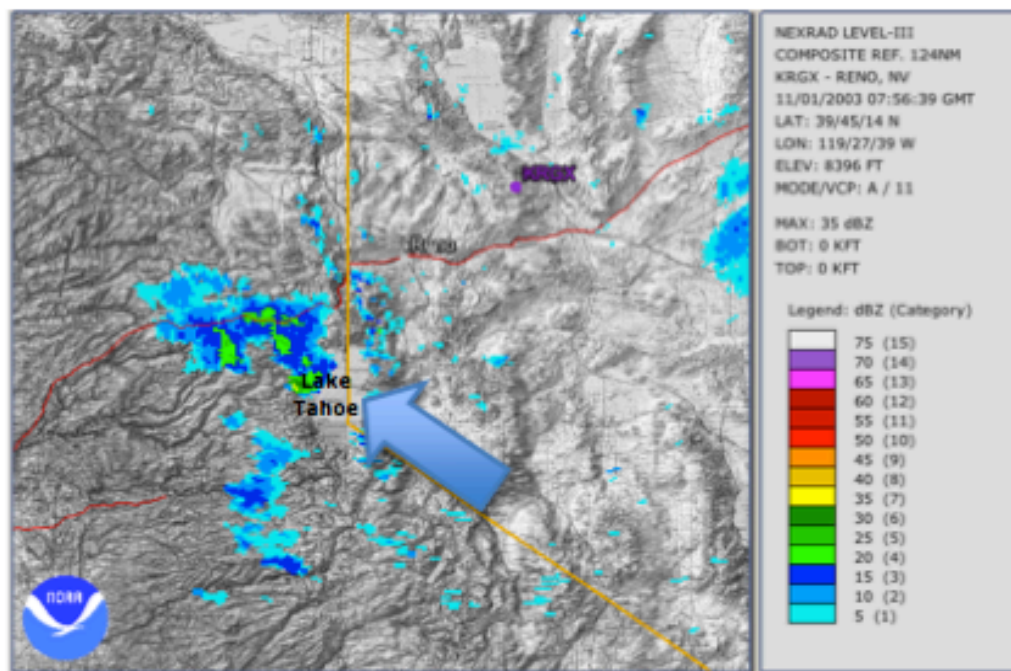


Figure 30. KRGX Composite Reflectivity at 0756 UTC on 1 Nov 2003

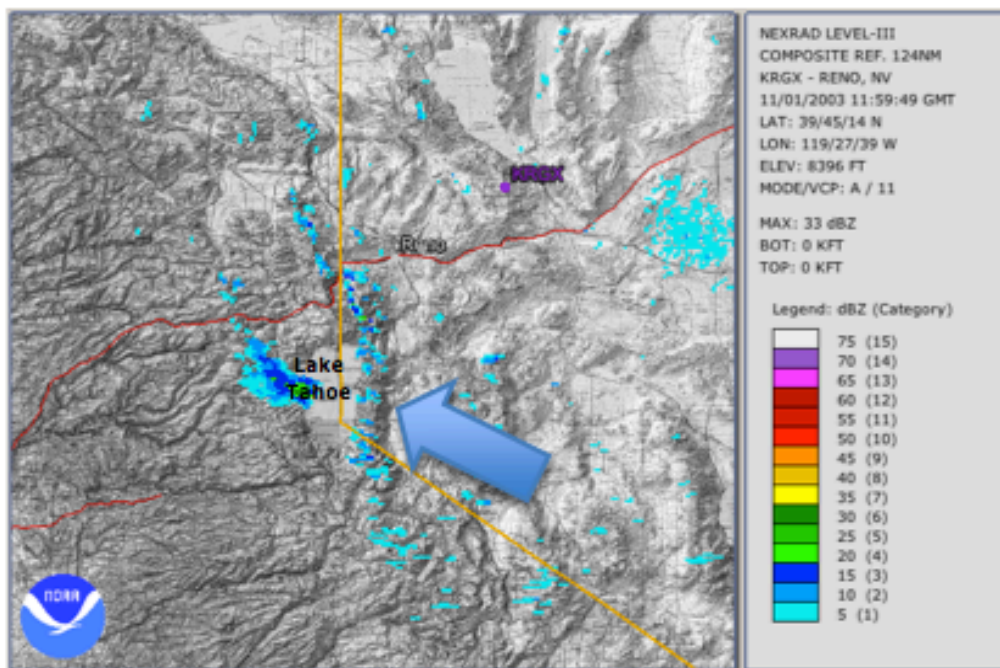


Figure 31. KRGX Composite Reflectivity at 1200 UTC on 3 Nov 2003

After the break between systems, snow shower activity again became widespread as the second front dropped down from the Pacific Northwest and reinforced the abnormally cold pattern. A second low-pressure area was located on the California-Nevada-Oregon border by 1200 UTC. Cyclonic flow around the low provided lift and echo enhancement in association with convergence and forcing along a front, with lower level flow out of the southeast, and upper, and mid-level flow becoming westerly. The environment was heavily sheared. Wind direction veered from 158° near the surface up to 233° at the 650-hPa level. Figure 32 shows widespread snow shower activity, but dBz did not exceed 30. Echoes extended northeast to southwest and were independent of the northwest to southeast orientation of the Sierra Nevada, denoting a convergence boundary. The large blue arrow shows the direction of movement of individual echoes, while the smaller arrows show the progression of the entire line of reflectivity.

Within the next two hours, the front advanced to the east. By 1452 UTC (Figure 33), reflectivity was dissipating in the Sierra Nevada. The exception was snow band formation over and downwind of Lake Tahoe and Pyramid Lake. Lake Tahoe produced two, well-defined LES bands. The upstream edge of the first band existed near the geographic center of the lake. This band extended northeast over Glenbrook and the Spooner Summit area to just west of Carson City, a distance of approximately 29 km. This band showed a convective core of 36 dBz. A second band just to the north originated south of Sand Harbor and extended northeast. The arrow denotes echo movement.

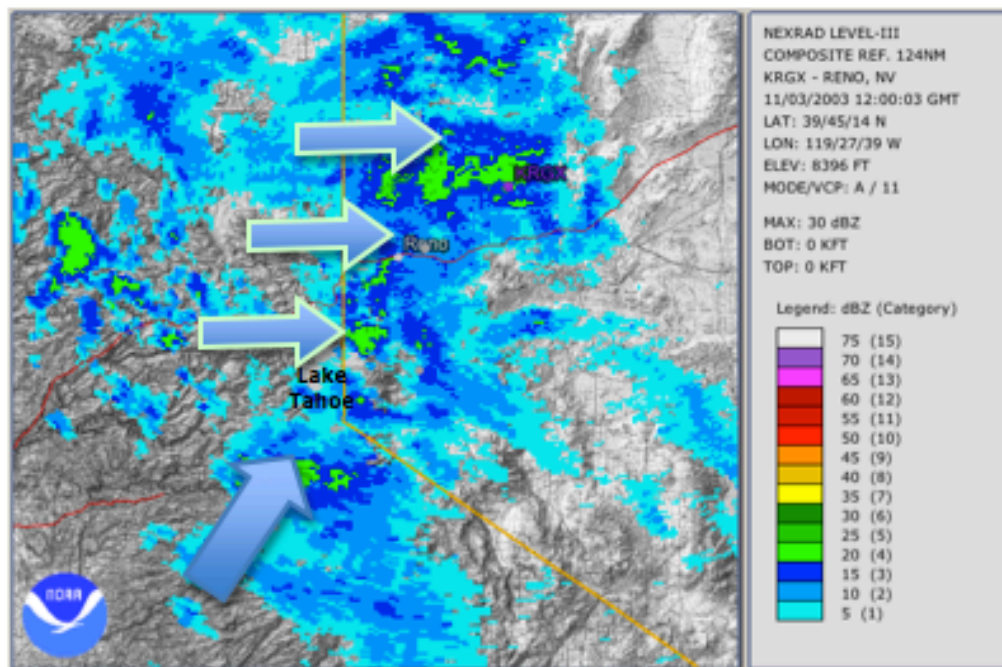


Figure 32. KRGX Composite Reflectivity at 1200 UTC on 3 Nov 2003

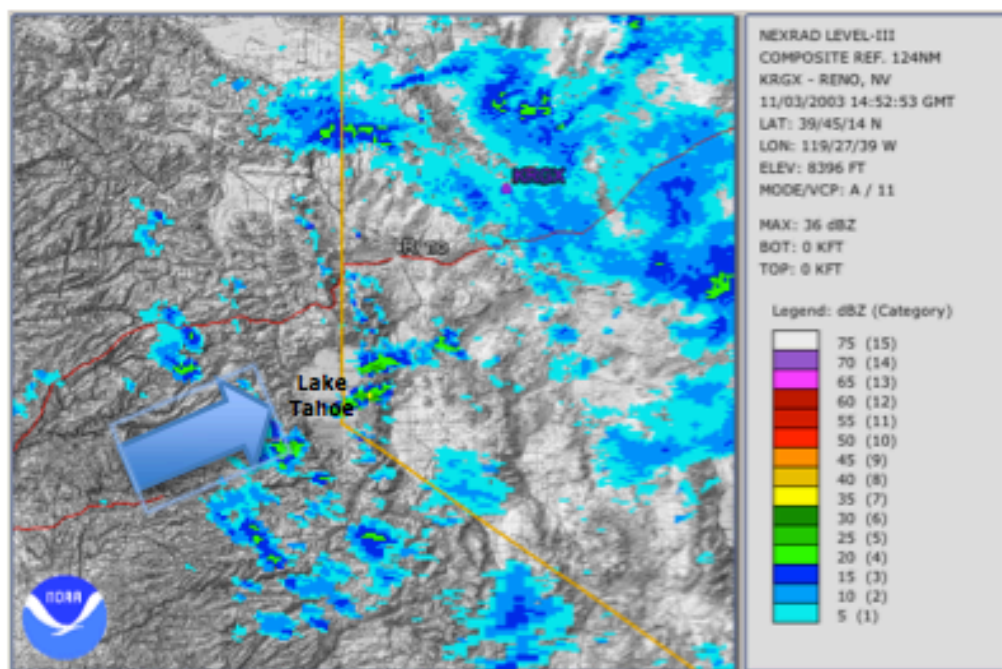


Figure 33. KRGX Composite Reflectivity at 1452 UTC on 3 Nov 2003

Two LES bands merged into one and persisted through 1900 UTC on 3 November. Figure 34 shows the LES band. It peaked in reflectivity at 32 dBz and extended from Glenbrook to Carson City. The arrow denotes the movement of this band, under westerly flow. Directional shear decreased following this hour, and was 31° by 0000 UTC on 4 November. Figure 35 shows composite reflectivity at 1829 UTC on 3 November, the last hour of organized convection. The band dissipated over the lake, with 30 to 35 dBz echoes over the Carson City area, and downwind over the Pine Nut Mountains. This band extended east 60 km from Lake Tahoe to northern Smith Valley at its peak. There were some breaks in reflectivity east Carson City, where orographic forcing likely helped to enhance or sustain downwind cells.

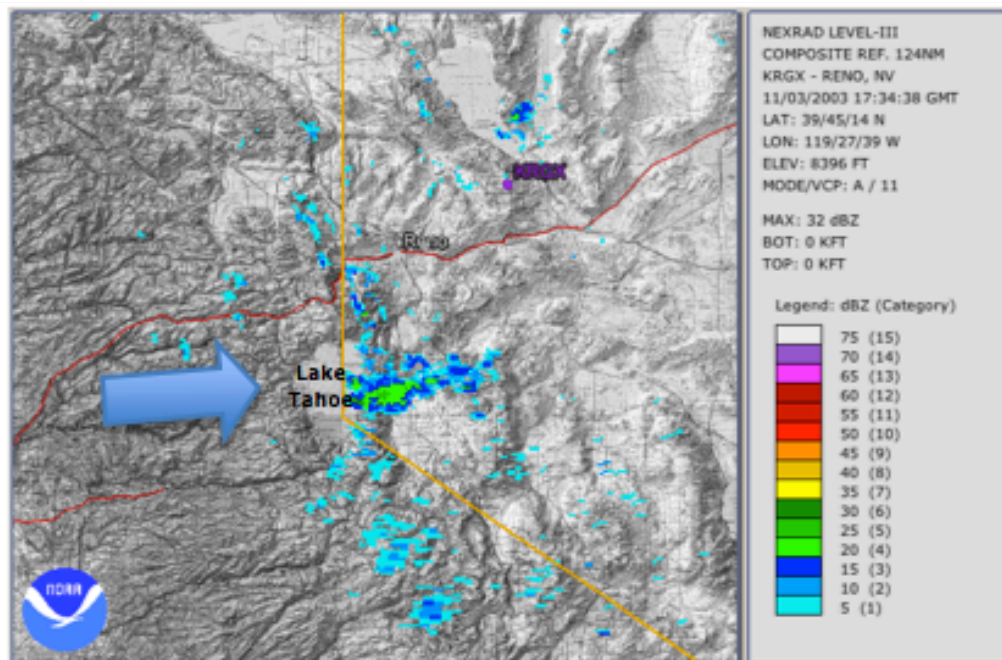


Figure 34. KRGX Composite Reflectivity at 1734 UTC on 3 Nov 2003

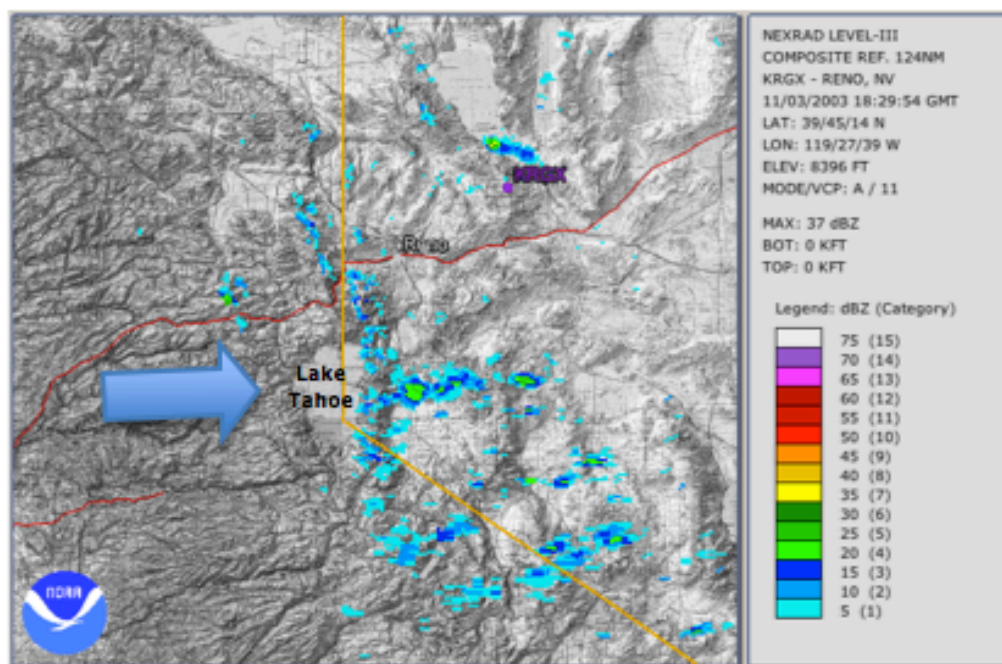


Figure 35. KRGX Composite Reflectivity at 1829 UTC on 3 Nov 2003

3.2 Case II

3.2.1 Event Summary

The first week of March 2006, was above average to average temperature-wise for the Tahoe Basin. Lake temperature was 5.60 °C at 0000 UTC on 9 March.

By the morning of 9 March, wind became gusty at all levels ahead of a cold front. The cold air advection was associated with a trough 2 to 3 standard deviations below average that deepened along and west of the California coast due to a 56 m/s jet streak positioned offshore.

By 0000 UTC on 10 March, the jet dropped south allowing cold air advection. The broad trough axis was positioned west of the lake at the 500-hPa level and flow was westerly (Figure 36b, Arrow 1). In the cold, moist, unstable westerly flow in the lower levels (Figure 36c, Arrow 2), snow shower activity developed along the west slope of the Sierra and drifted across Lake Tahoe. As activity diminished to the north and west, snow bands developed and intensified over and downwind of Lake Tahoe through the evening. The main LES band persisted from 0700 UTC until 1000 UTC. It extended more than 60 km to the east of the lake, producing heavy snow in Carson City. As this band diminished, another similar band developed after 1411 UTC. This band was five to ten km wide and showed changes in orientation downwind with increasing directional shear. During this period, a LES warning was in effect from the Reno NWSFO for the east shore of Lake Tahoe and western Nevada downwind of the lake.

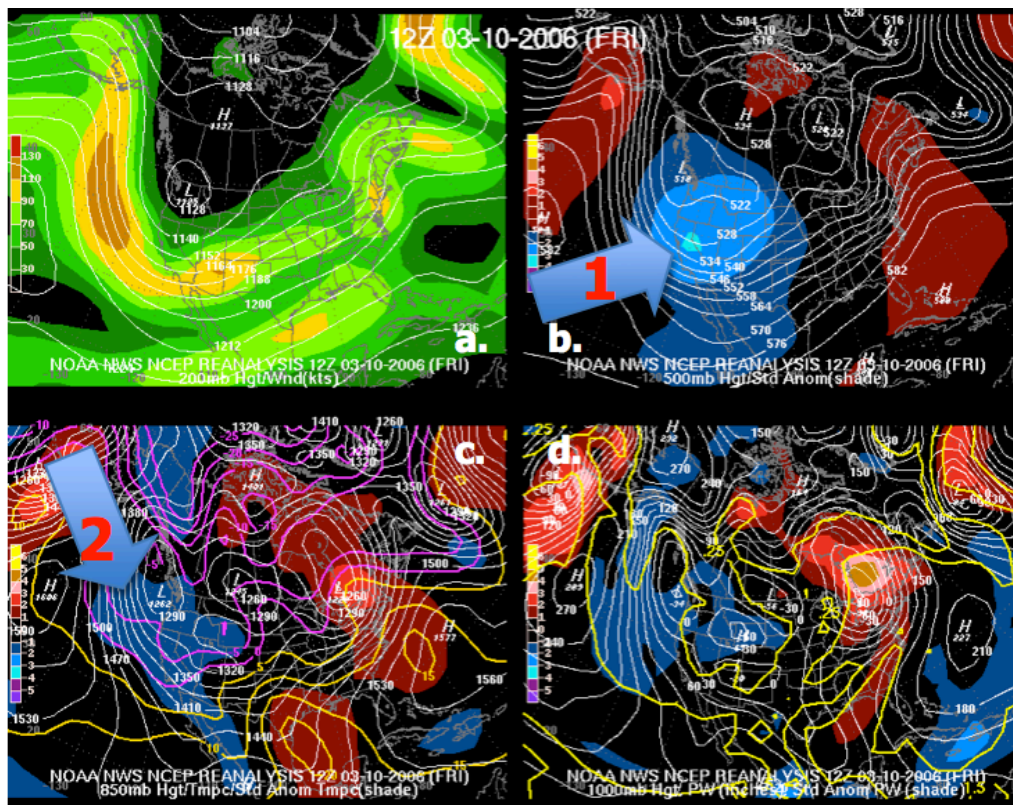
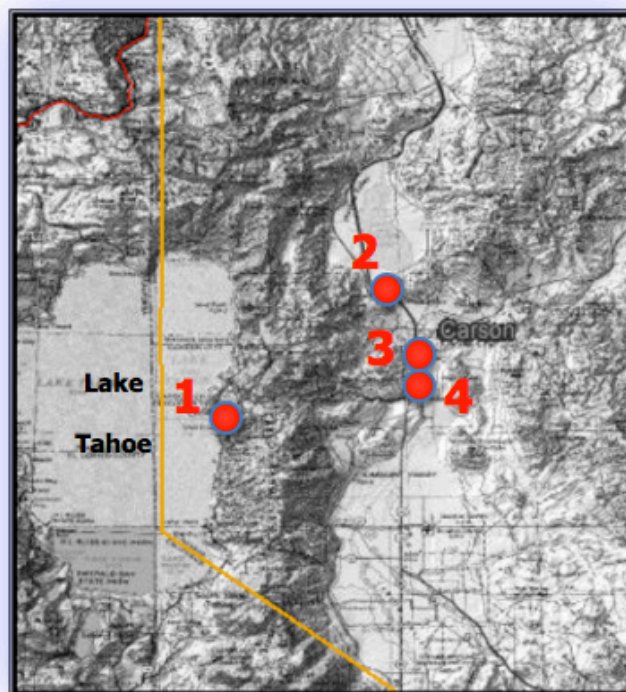


Figure 36. 10 March 2006, 1200 UTC: 200, 500, 850, 1000-hPa NOAA Upper Air Analyses

From 0000 UTC on 11 March through the end of the event, flow shifted to the southwest, as a 56 m/s jet streak deepened the trough axis to the west of the lake. Snow banding developed over the northeast quadrant of the lake and extended over Mount Rose into Washoe Valley. These LES echoes showed higher radar reflectivity, but they were short-lived and short in band development downwind of the lake. Shear increased through this period, disrupting downwind band structure. By 12 March, the air mass began to warm and dry, and the trough axis began to shift east of Lake Tahoe.

Figure 37 shows Case II reported snowfall totals. This case produced a well-defined persistent LES band from Lake Tahoe downwind to the Carson City area. Orientation was consistent, and with the dissipation of the first band, a second band developed with similar location. This resulted in considerable snowfall downwind of the lake around Carson City. Reported amounts downwind of the Carson Range were approximately three times higher than the total at Glenbrook on the east shore of the lake.



1. Glenbrook: 7.6 cm
2. N. Carson City: 26.7 cm
3. Carson City: 30.5 cm
4. S. Carson City: 20.3 cm

Figure 37. Case II Reported Snowfall Totals

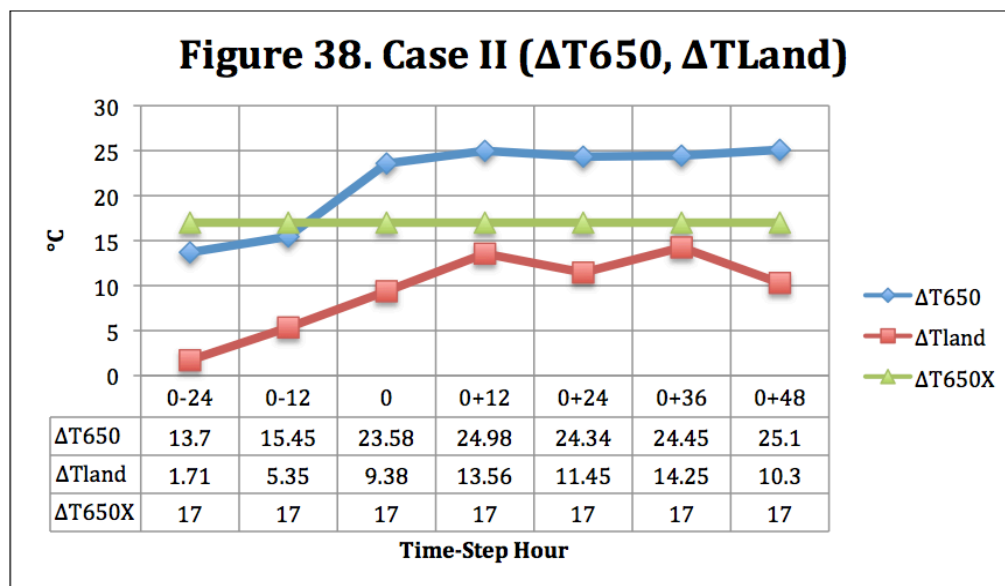
3.2.2 Results of Time-step Analysis

Table 9 is a complete listing of all parameter analysis results during Case II. Figures 38-43 provide time-step analysis of individual LES parameters.

Time-Step Hours:	0-24	0-12	0	0+12	0+24	0+36	0+48
ΔT_{650} (°C)	13.70	15.45	23.58	24.98	24.34	24.45	25.10
ΔT_{land} (°C)	1.71	5.35	9.38	13.56	11.45	14.25	10.30
Capping Inversion	YES	NO	NO	NO	NO	NO	NO
S (°)	24	28	12	15	22	65	47
W (m/s)	10.29	24.69	14.40	10.29	11.83	9.77	6.69
RH (%)	56	33	55	74	44	79	78
T (°C)	-1.53	-5.00	-10.80	-13.18	-11.58	-13.55	-13.05
Instability (LI CAPE) CAPE (J/kg)	10.4 0	6.1 0	-0.7 0.79	1.2 0	-1.3 122	0.8 0	1.4 0
Upper Level Support	NO	YES	YES	YES	YES	YES	YES

Table 9. Case II Parameter Analysis Results
Blue columns indicate time-step hours when LES occurred
Green columns indicate hours that immediately preceded and followed LES

ΔT_{650} (Figure 38): ΔT_{650} ranged from 23.58 °C at the 0-hour, to 25.10 °C following final dissipation of LES radar echoes. These values were also greater than ΔT_{650X} . ΔT_{650} was greater than 24 °C during time-step hours when LES occurred.

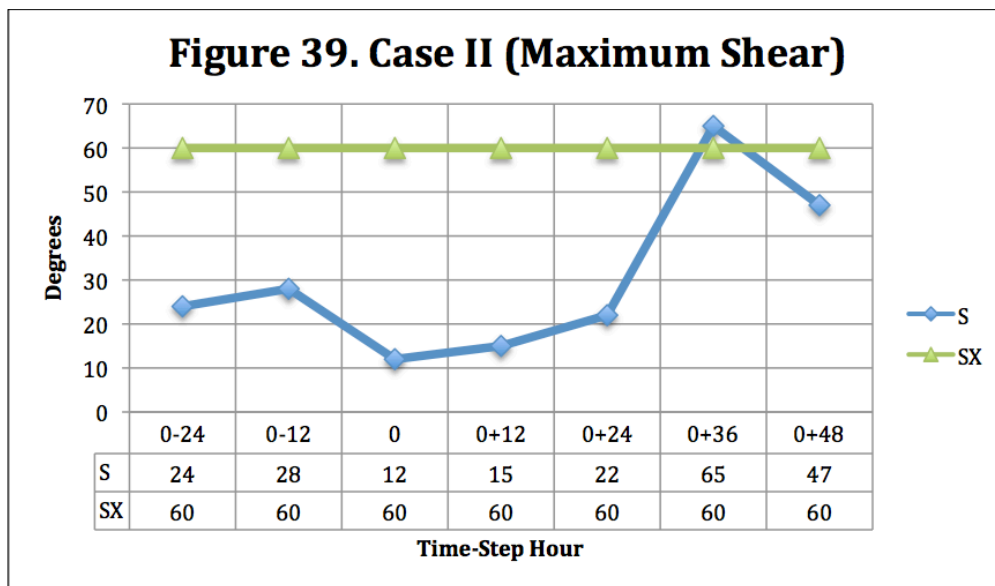


ΔT_{land} (Figure 38): This parameter was significant in this case, greater than 11 °C during time-step hours when LES banding occurred, and greater than 9 °C including the 0-hour. These values were significantly higher from the zero-hour through the end of the case.

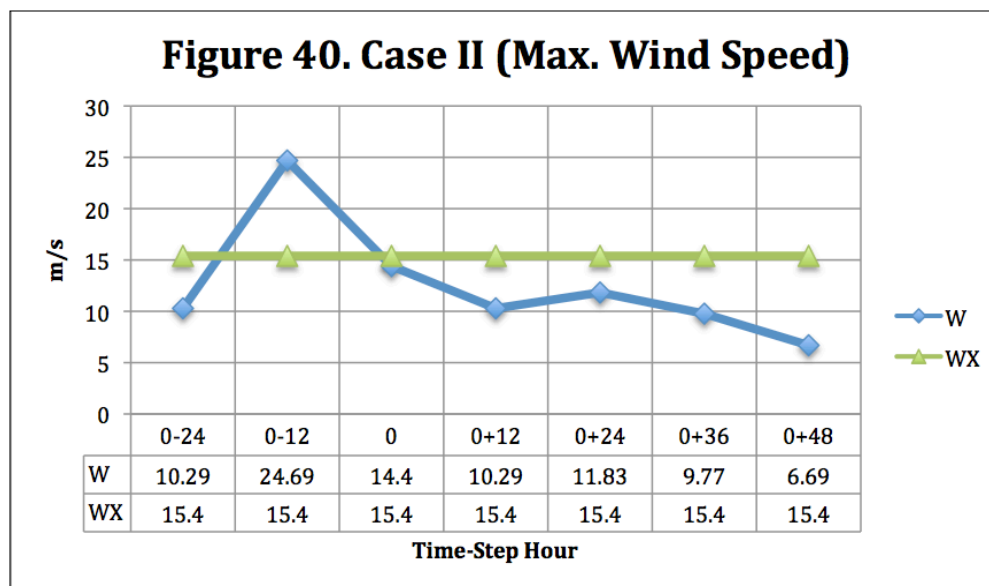
Existence of a Capping Inversion: In this case, only one time step (0-24) showed an inversion at the 708-hPa level. No inversions existed at or below the 650-hPa level during time-step hours when LES occurred.

Maximum Shear (Figure 39): In this case, S exceeded SX in one time-step (0+36). During this hour, LES banding with 50 to 60 km lengths ended. LES banding occurred with 20 to 25 km distances downwind of the lake. Activity

dissipated and redeveloped several times during the last 18 hours of the case. Shear likely discontinued the strong, longer distance LES band formation, although reflectivity was higher in two of the shorter bands.

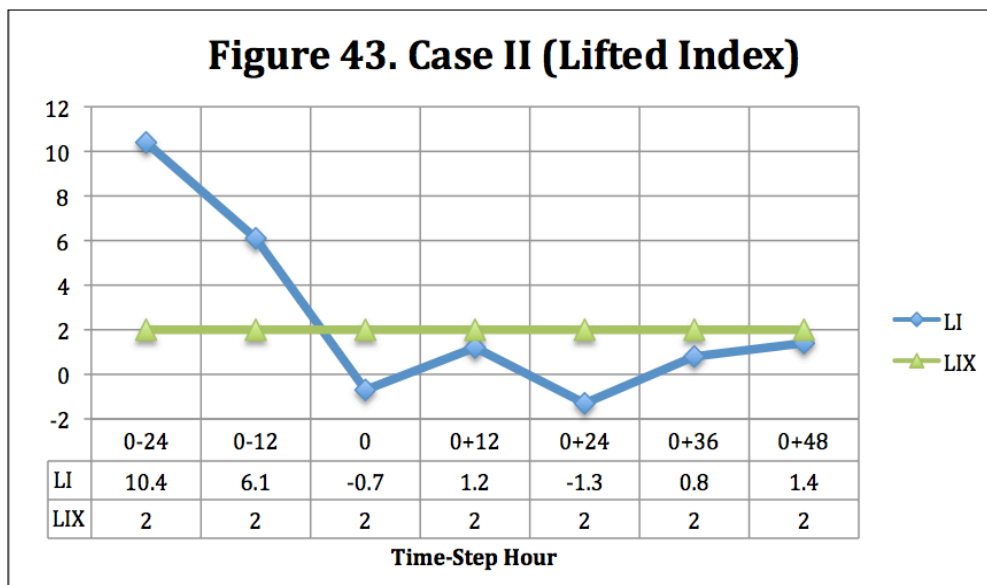


W (Figure 40): Wind speed was very strong during the early hours of this event and peaked at 24.69 m/s at the 0-12 hour. Following the 0-hour, when W was 14.40, wind speed fell below 12 m/s for the duration of the event. W was less than WX from the 0-hour through dissipation of LES echoes on KRGX.



RH (Figure 41): A shift in flow occurred at the 0+24 time-step hour. RH that had been around 70% fell below RHX to 44%, as drier air mixed in at around the 750-hPa level. RH was back up to 79% by the 0+36 hour. A lull in radar activity coincided with the drop in RH and the wind shift, between 1600 UTC on 10 March and 0200 UTC on 11 March. In this case, the REV sounding was downwind of Lake Tahoe at the 650-hPa level after the 0+24 hour.

Instability (Figure 43): From the 0-hour through the end of the event, time-step hour afternoon soundings were unstable, with morning soundings slightly stable, or with LI between 0 and 2. CAPE of 0.79 (0-Hour) and 122 (0+24) was calculated. LI was less than LIX in all time-step hours from 0-hour through the end of the case.



Upper Level Support: From 0-hour through the end of the event, flow was cyclonic and to the right of the 500-hPa trough axis. This was favorable for upper level divergence and upward vertical velocity.

3.2.3 Radar Analysis

Following the 0-Hour, in the wake of cold air advection, a band of snow showers developed along Interstate 80 (Truckee area), moving from west to

east. Wind at the 650-hPa level corresponded with this direction, coming from 283°. By 0339 UTC (Figure 44), snow shower activity increased along the west slope of the Sierra under orographic enhancement in an abnormally cold, unstable atmosphere. The arrow denotes movement of echoes. Reflectivity at this hour peaked at 35 dBz, but was generally only around 20 to 30 dBz. This activity was enhanced by lift along the Sierra Nevada crest, and shifted east under continued westerly flow. By 0668 UTC (Figure 45), as most of the activity was dissipated, snow showers crossing Lake Tahoe showed enhancement and intensification. Two pronounced bands developed near the east and northeast shores that extended east into Carson City. One band extended from close to the geographic center of Tahoe east 28 km to south Carson City. The second band extended 25 km from Crystal Bay to north Carson City. Reflectivity maximums of 25 to 29 dBz were observed with these LES bands, showing likely orographic enhancement with lifting over the Carson Range, from Spooner Summit north to Marlette Peak.

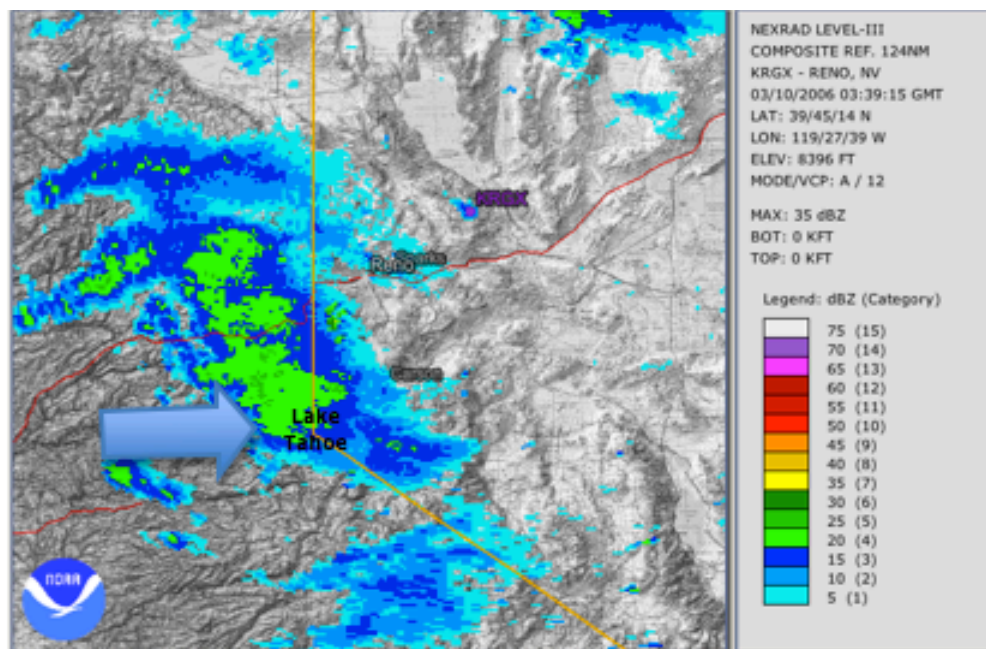


Figure 44. KRGX Composite Reflectivity at 0339 UTC on 10 Mar 2006

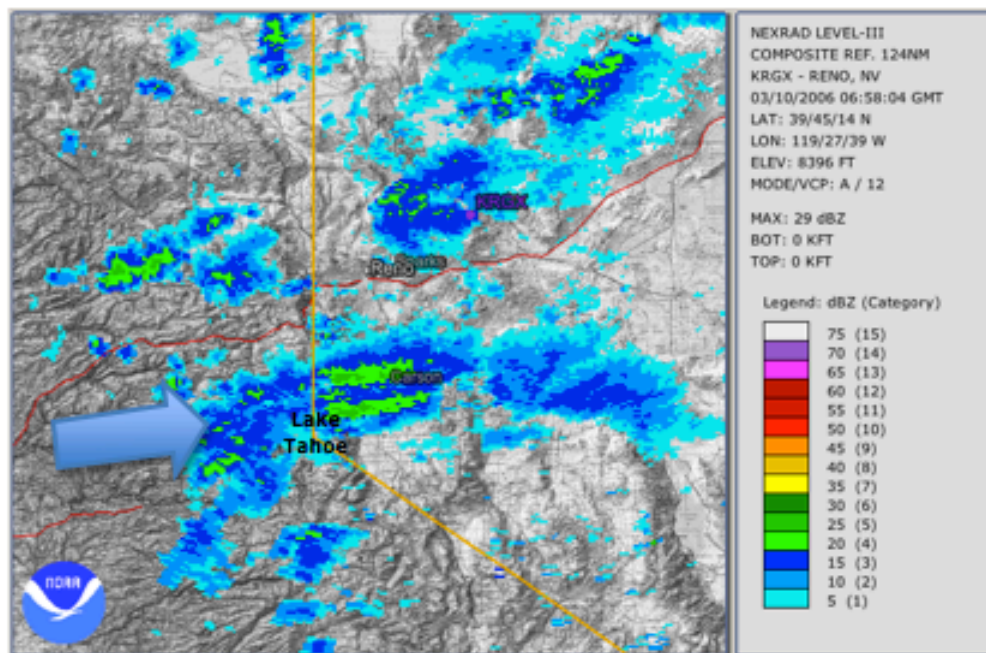


Figure 45. KRGX Composite Reflectivity at 0658 UTC on 10 Mar 2006

These bands merged into one band and intensified over the following hours. By 0812 UTC (Figure 46), the LES band was showing a reflectivity maximum of 31 dBz and extended from Lake Tahoe, downwind more than 60 km over the Pine Nut Mountains and Smith Valley. The band was also wide, with a 15 to 20 km lateral extent. Maximum reflectivity existed over and downwind of the lake to around Carson City, with a second maximum shown over the higher elevation of the northern slope of the Pine Nut Mountain Range. This band persisted until 1200 UTC, when it dissipated to a small band from the lake over Spooner Summit and snow showers near and to the east of Smith Valley.

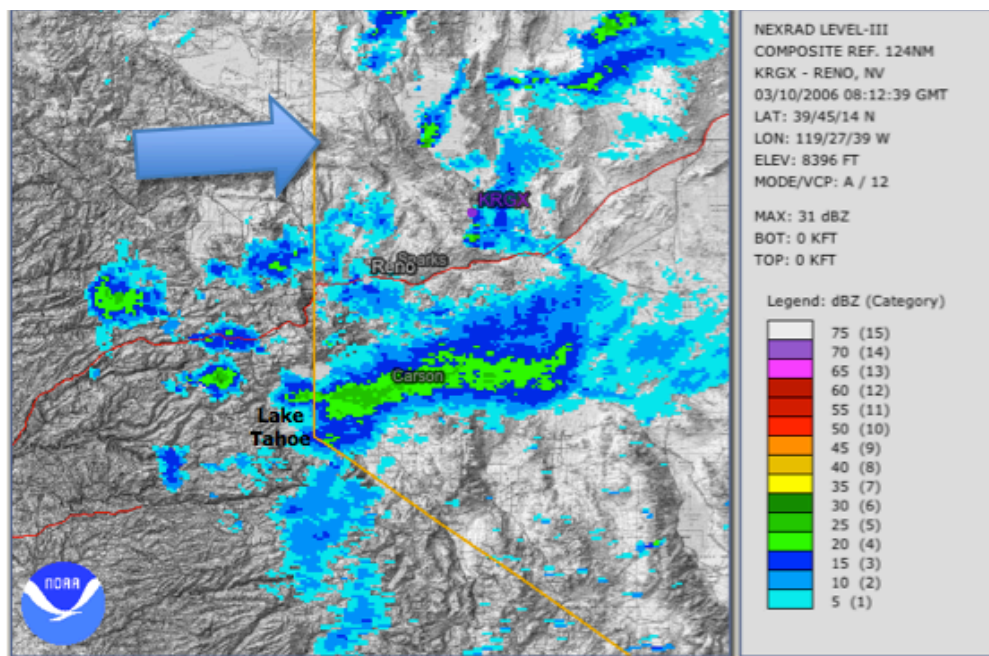


Figure 46. KRGX Composite Reflectivity at 0812 UTC on 10 Mar 2006

At 1200 UTC (Figure 47), the band that extended from Lake Tahoe east to Smith Valley had dissipated to snow showers near and east of the Pine Nut Mountains with reflectivity of 20 to 25 dBz. The arrow denotes movement of echoes. Convection continued over the eastern half of the lake, and extended downwind over Spooner Summit with a maximum reflectivity of 20 dBz. Snow showers upwind of the lake had developed in the cold, cyclonic environment, and were moving east from the Sierra crest to the west shore of Lake Tahoe. Wind direction at the 650-hPa level was 290° , with direction shifting to the north in the lower levels.

As upwind showers crossed the lake, by 1411 UTC (Figure 48), individual showers had transitioned into a second extended snow band. This LES band showed a maximum dBz of 37 over the lake. Radar reflectivity showed west-east orientation of the band for 15 km from the lake to Spooner Summit. It then showed more of a northwest to southeast orientation, as the band extended into the northern Carson Valley and into the Pine Nut Mountains. The LES band then extended easterly to the northern Smith Valley. While this band extended almost 60 km like the 0700 UTC to 1000 UTC band, width of the band was only around five km, increasing to 10 km downwind of the Pine Nut Mountains. The change in orientation of this band reflected an increase in shear seen on the REV sounding. While 650-hPa level wind direction was 290° , 750-hPa level direction was 305° . This LES band dissipated by 1600 UTC. Echoes around the lake were isolated until after 00z on the 11 March.

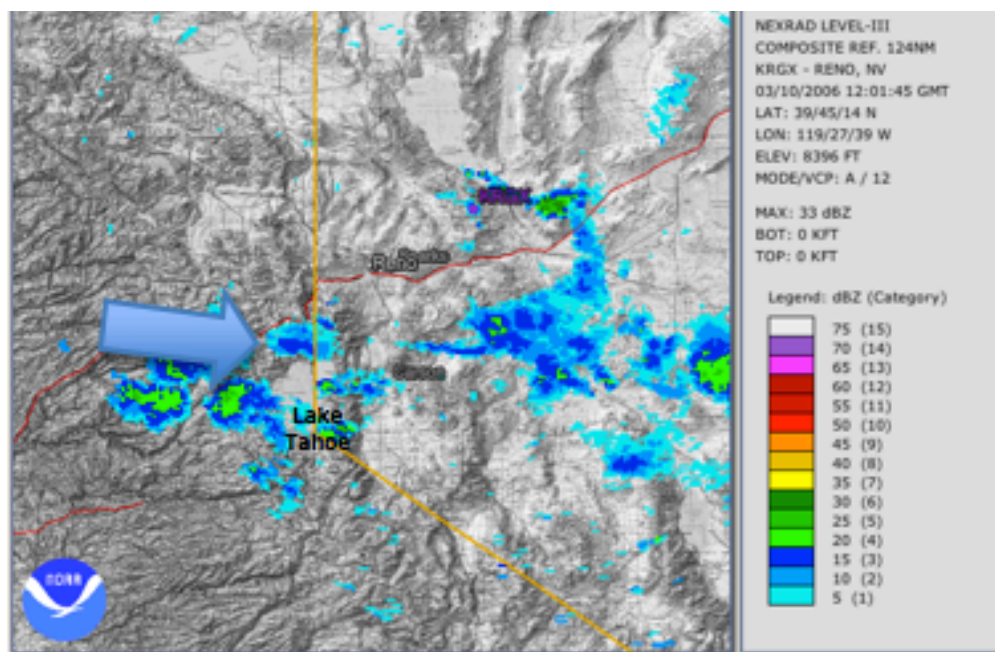


Figure 47. KRGX Composite Reflectivity at 1201 UTC on 10 Mar 2006

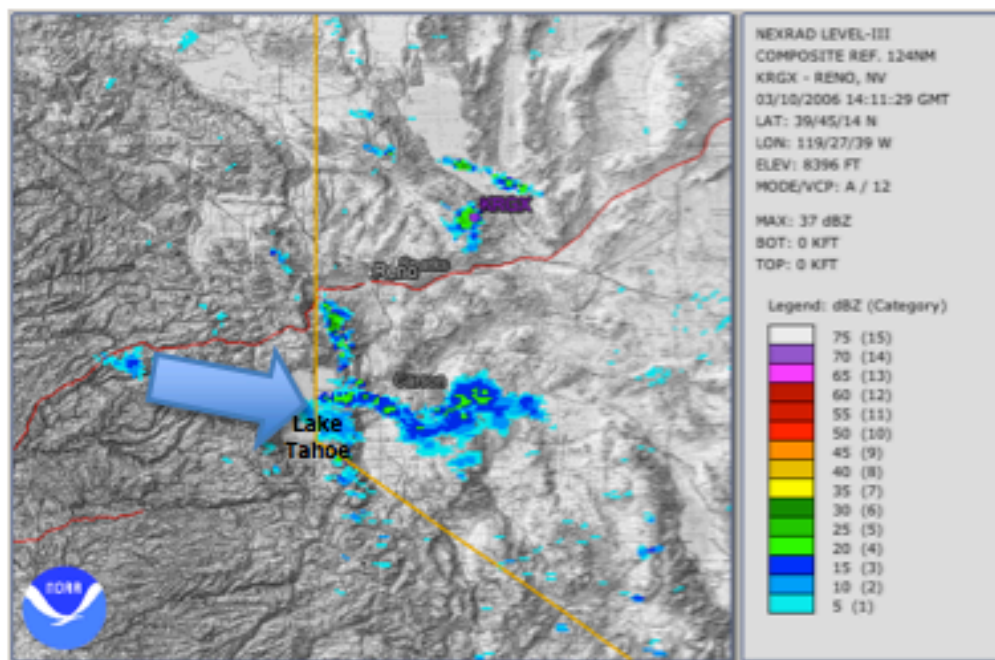


Figure 48. KRGX Composite Reflectivity at 1411 UTC on 10 Mar 2006

Wind shifted by 0000 UTC on 11 March. Shear was still limited, but flow had become southwest to south southwesterly. The 650-hPa level wind direction had shifted to 208°. After a lull in activity following the dissipation of the last 10 March band, new development appeared on the radar by 0215 UTC (Figure 49). The arrow denotes Echo movement. Convection developed over the northeast quadrant of Lake Tahoe, with maximum reflectivity of 36 dBz. By 0412 UTC (Figure 50), this convection formed a LES band, which extended from Crystal Bay on Lake Tahoe northeast over Mt. Rose. Echo movement had shifted from south-southwest to north-northeast. The band was compact and only extended around 25 km, but exhibited higher reflectivity than previous banding at 35 to 40 dBz. The band likely gained orographic enhancement, as it was lifted from the basin over Mt. Rose. This band dissipated by 0600 UTC, with snow showers of 25 dBz or less developing over the northeast shore of Lake Tahoe through 1200 UTC.

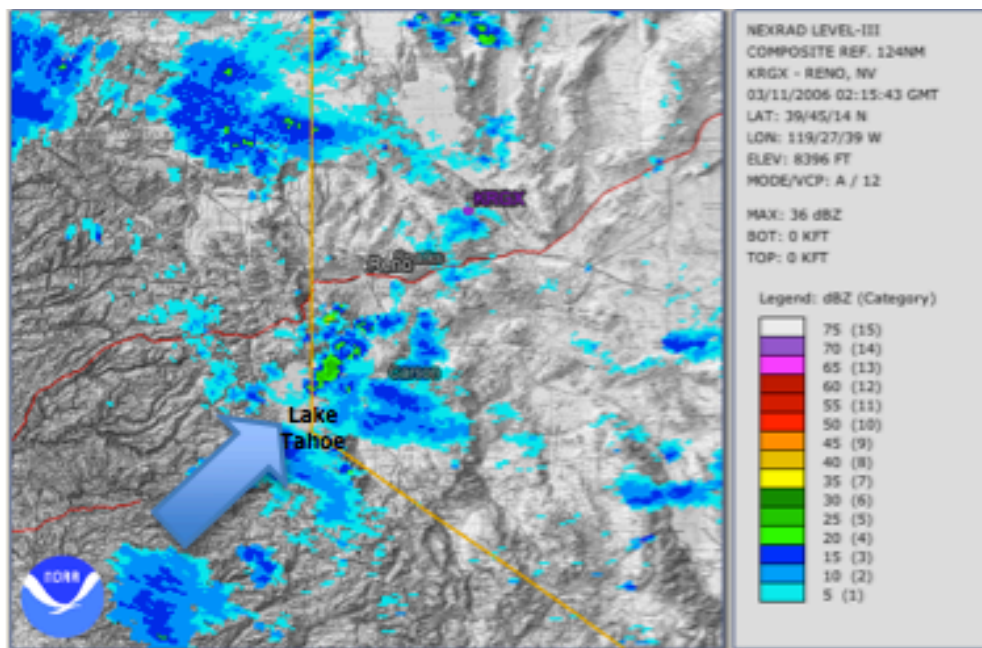


Figure 49. KRGX Composite Reflectivity at 0215 UTC on 11 Mar 2006

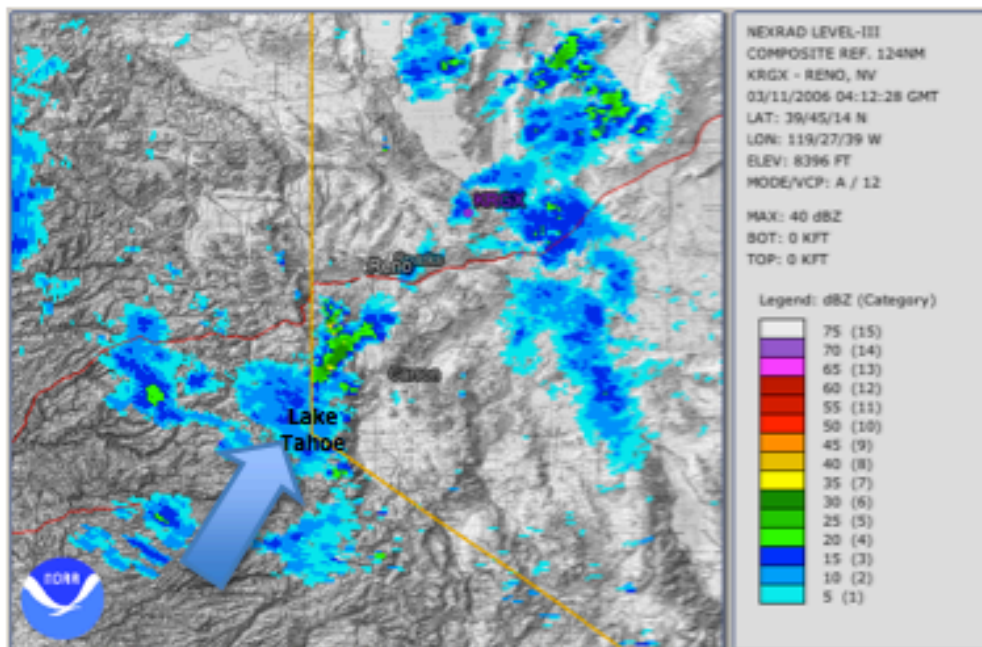


Figure 50. KRGX Composite Reflectivity at 0412 UTC on 11 Mar 2006

Snow shower activity continued along the northeastern shore of Lake Tahoe around 1200 UTC, with reflectivity generally less than 25 dBZ (Figure 51). The arrow denotes echo movement. The final significant band of this event formed by 16:01z (Figure 52), as a cell developed just north of the geographic center of Lake Tahoe, with reflectivity of 34 dBZ. From this cell, a band extended north-northeast through Incline Village to around Slide Mountain. Around half of this 20 kilometer distance was over the lake. Directional shear had increased this hour to 65°. The band was still oriented to the 220° 650-hPa wind direction. Shear impacted development of this band with southeasterly flow around lake level and 700-hPa level flow becoming more westerly. By 2303 UTC (Figure 53), LES dissipated in an increasingly sheared environment.

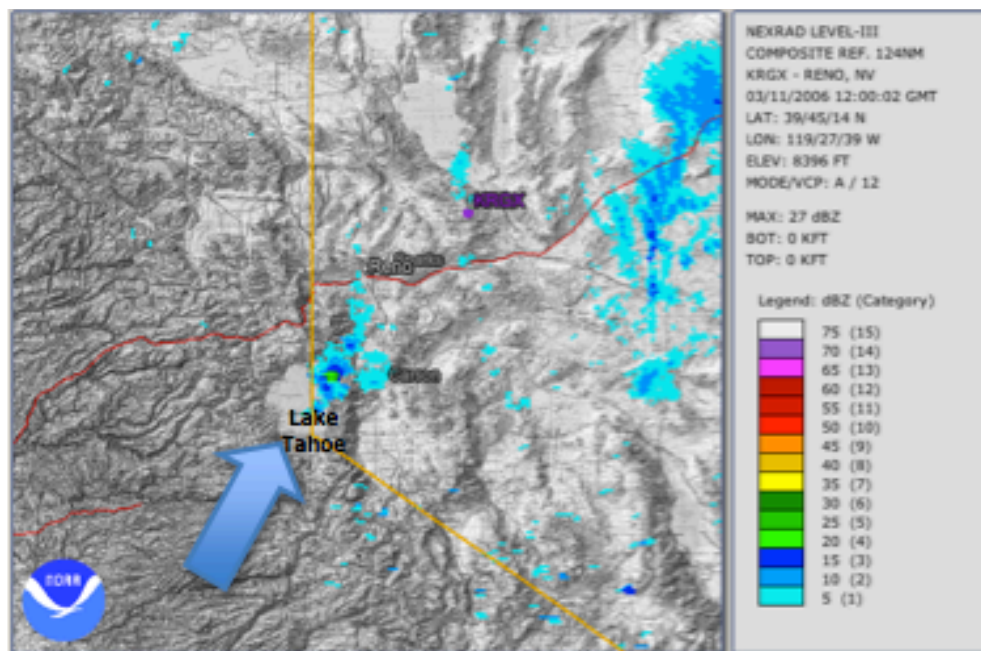


Figure 51. KRGX Composite Reflectivity at 1200 UTC on 11 Mar 2006

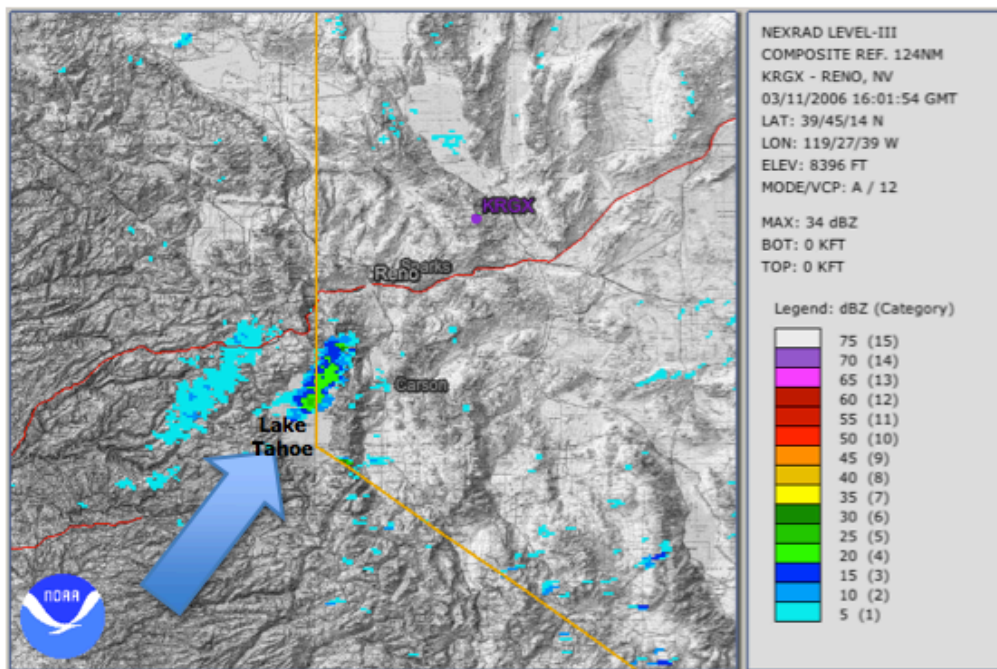


Figure 52. KRGX Composite Reflectivity at 1601 UTC on 11 Mar 2006

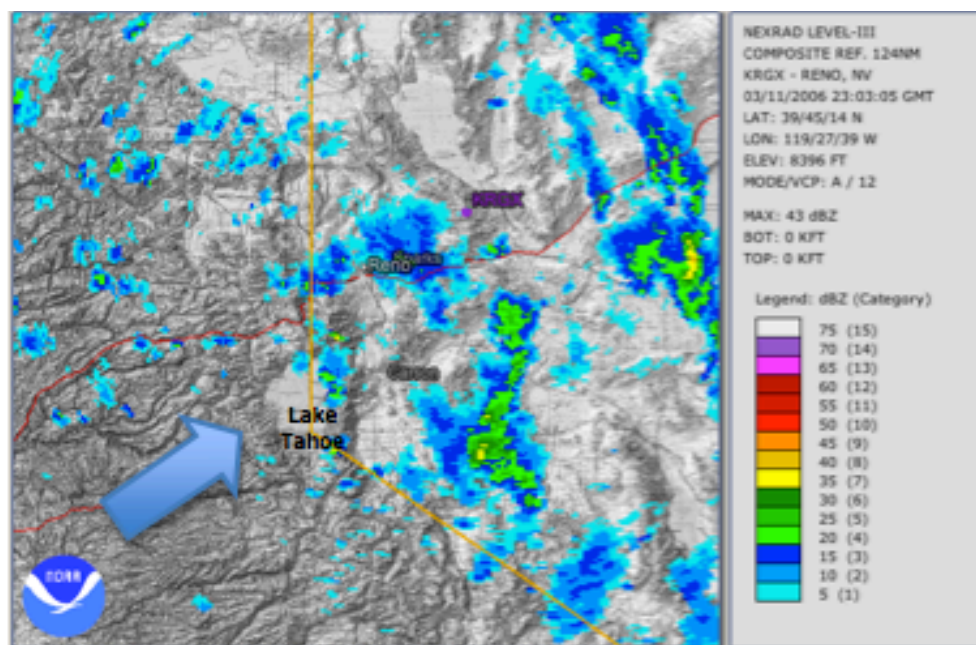


Figure 53. KRGX Composite Reflectivity at 2303 UTC on 11 Mar 2006

3.3 Case III

3.3.1 Event Summary

Mid-January 2008 was mild for Lake Tahoe. On 20 January, the lake temperature was 5.92 °C, and the temperature at KTVL was 6.11 °C. During the afternoon hours, the lake was cooler than the land. A ridge of high pressure existed along the west coast and amplified north into the Gulf of Alaska.

A low-pressure trough brought changes by 1200 UTC. Ahead of a surface cold front, a wind speed of 20.58 m/s was recorded at KTVL, and rain and snow showers developed along and ahead of the boundary. The trough, 1 to 2 standard deviations below average at the 500-hPa level, dropped temperatures considerably by 0000 UTC on 21 January.

In the following days, a jet streak deepened the positively oriented trough and then cut it off from the main jet to the northeast (Figure 54b, Arrow 1). The closed low drifted through Northern California during the final 12 hours of 21 January (Figure 54c, Arrow 2) to near the San Francisco Bay Area at 1200 UTC on 22 January. During this period, LES bands first developed over the eastern half of Lake Tahoe and extended downwind to the Reno-Sparks metropolitan area. The Reno NWSFO issued a lake effect snow advisory for the duration of this event, for the north and east shores of the lake and areas of western Nevada downwind of the Lake Tahoe. This included the Reno-Sparks area. The advisory did not expire until 0000 UTC on 23 January.

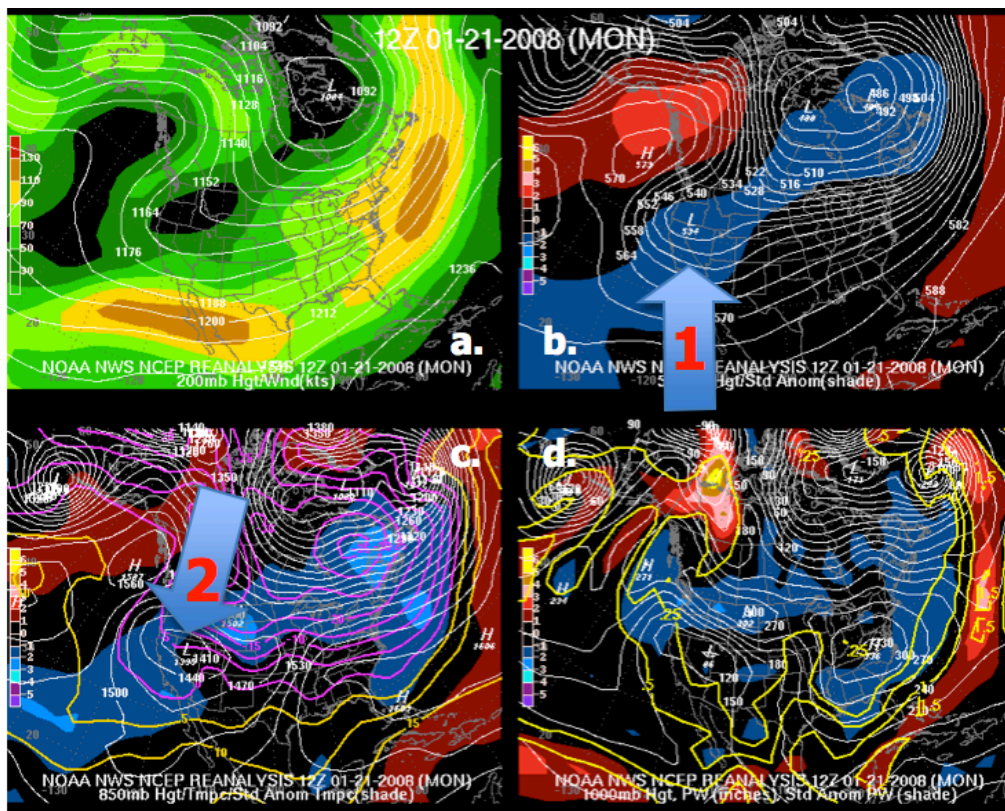
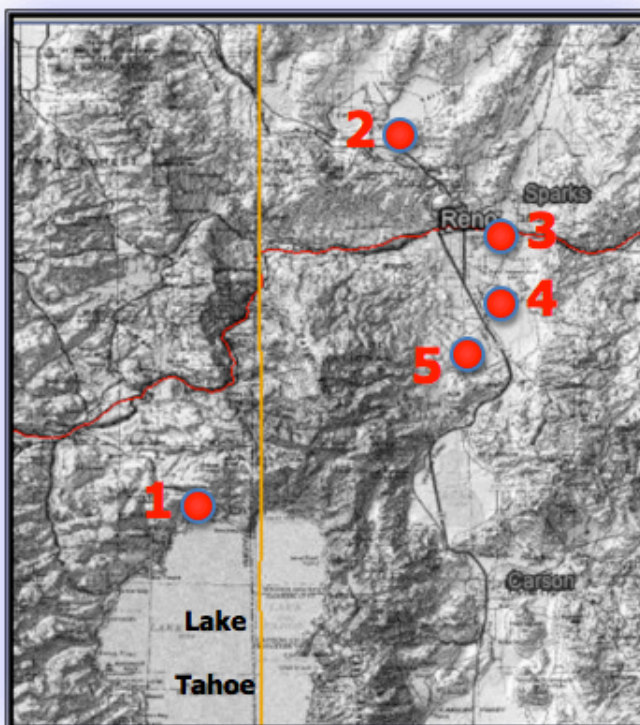


Figure 54. 21 January 2008, 1200 UTC: 200, 500, 850, 1000-hPa NOAA Upper Air Analyses

As the low drifted southwest, flow became southerly, and then southeasterly. After the Reno-Sparks band dissipated, likely due to shear from the turning of the wind flow, new banding affected the north shore of the lake north to Interstate 80 under the southerly flow, and then affected Tahoe City and Highway 89 when flow shifted to the southeast. As the low drifted away, air temperature began to moderate, and snow shower activity associated with the lake ended by 13z on 22 January.

Figure 55 shows Case III reported snowfall totals. LES banding with this event was impressive, both extensive in downwind distance from the lake, and long-lived. The main band existed for 7 hours, extending from Lake Tahoe downwind to Reno, Sparks, and the Reno-Sparks North Valleys. Storm totals were highest in south and southwest Reno, double the totals on the north shore.



1. Carnelian Bay: 10.2 cm
2. Stead: 0.8 cm
3. Airport (RNO): 5.1 cm
4. Damonte Ranch: 12.7 cm
5. SW Reno: 19.1 cm

Figure 55. Case III Reported Snowfall Totals

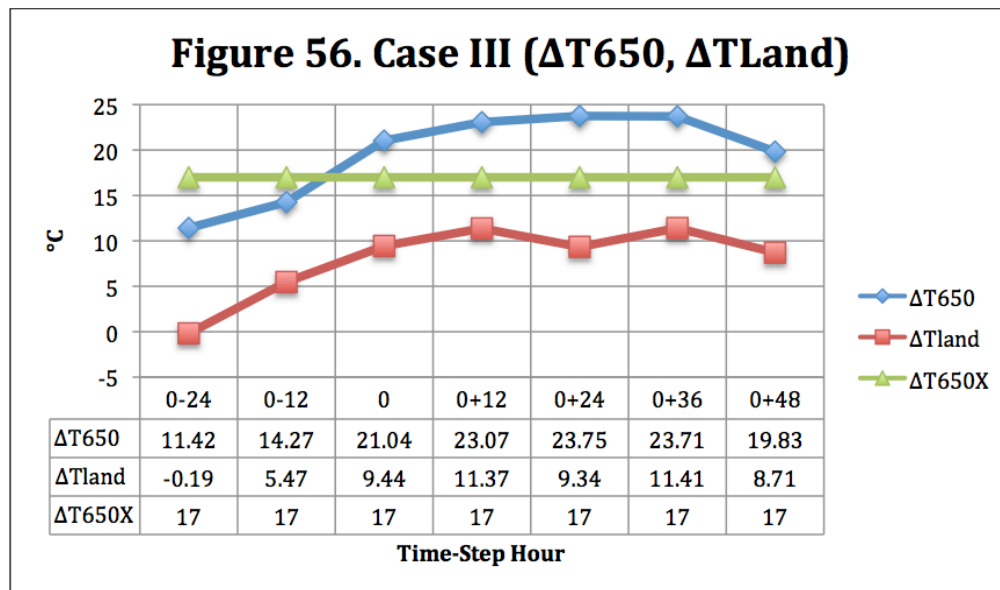
3.3.2 Results of Time-step Analysis

Table 10 is a complete listing of all parameter analysis results during Case III. Figures 56-61 provide time-step analysis of individual LES parameters.

Time-Step Hours:	0-24	0-12	0	0+12	0+24	0+36	0+48
ΔT_{650} (°C)	11.42	14.27	21.04	23.07	23.75	23.71	19.83
ΔT_{land} (°C)	-0.19	5.47	9.44	11.37	9.34	11.41	8.71
Capping Inversion	YES	YES	NO	NO	NO	NO	YES
S (°)	10	8	10	28	86	27	25
W (m/s)	12.35	20.58	14.40	9.26	5.66	10.29	10.29
RH (%)	35	52	55	81	84	89	81
T (°C)	3.94	-2.88	-7.98	-11.83	-11.98	-13.03	-10.00
Instability (LI CAPE) CAPE (J/kg)	7.2 0	7.5 0	2.4 15	5.2 0	-0.4 102	5.6 0	6.9 0
Upper Level Support	NO	NO	YES	YES	YES	YES	NO

Table 10. Case III Parameter Analysis Results
Blue columns indicate time-step hours when LES occurred
Green columns indicate hours that immediately preceded and followed LES

ΔT_{650} (Figure 56): During the time-step hours when LES banding occurred, ΔT_{650} ranged from 21.04 °C at the 0-hour, to 19.83 °C following final dissipation of LES echoes, and was greater than ΔT_{650X} .

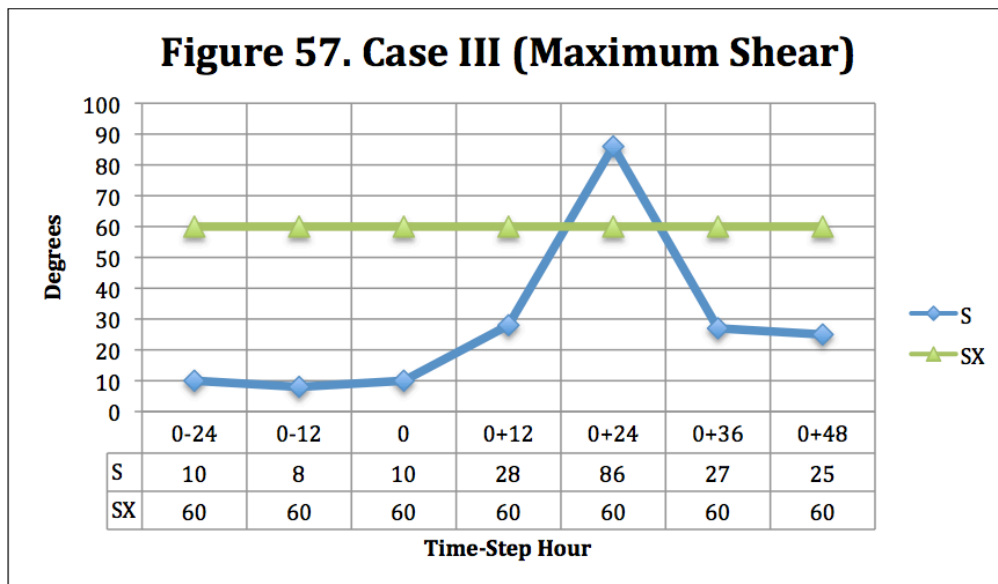


ΔT_{land} (Figure 56): ΔT_{land} was greater than 9 °C during time-step hours when LES banding occurred, and greater than 8 °C including the 0-hour and hour following dissipation (0+48).

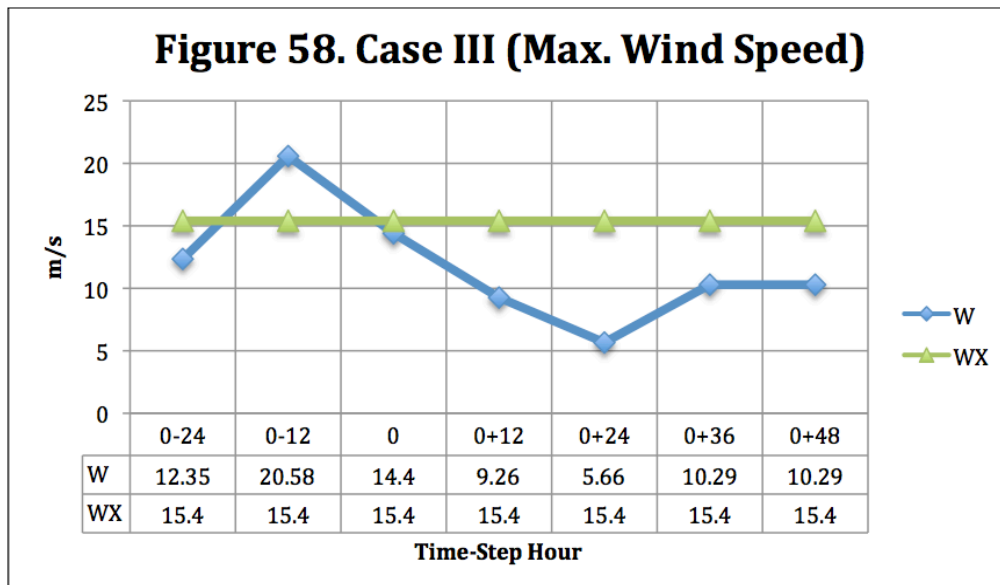
Existence of a Capping Inversion: The time step after dissipation (0+48) showed an inversion at the 725-hPa level, likely ending convection as warm air advection occurred in the mid-levels. Inversions were also present prior to the event, at the surface at 0-24, and at the 702-hPa level at 0-12.

S (Figure 57): S exceeded SX in one time-step hour (0+24). During this hour, and for the duration of the event, earlier organized LES banding of downwind distance from the lake of 50 to 70 km no longer occurred. LES reflectivity extended only 20 to 25 km downwind of the lake and showed less organization.

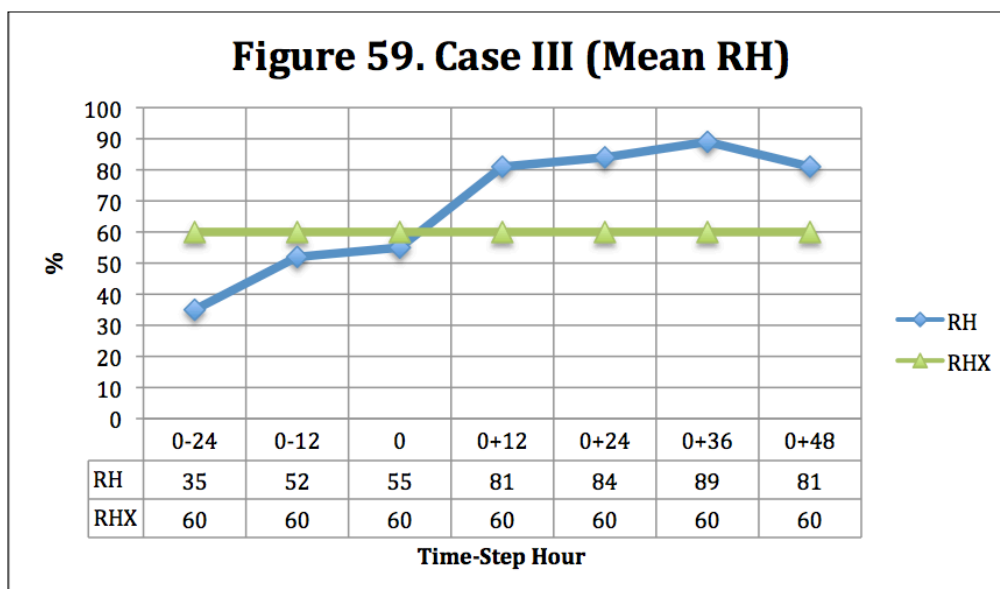
LES orientation corresponded with shifting flow, as the low to the northwest of Lake Tahoe became closed and drifted southwest of the lake. The shear was maximized as flow switched from southwest to north. LES redeveloped as shear decreased between 0+24 and 0+36.



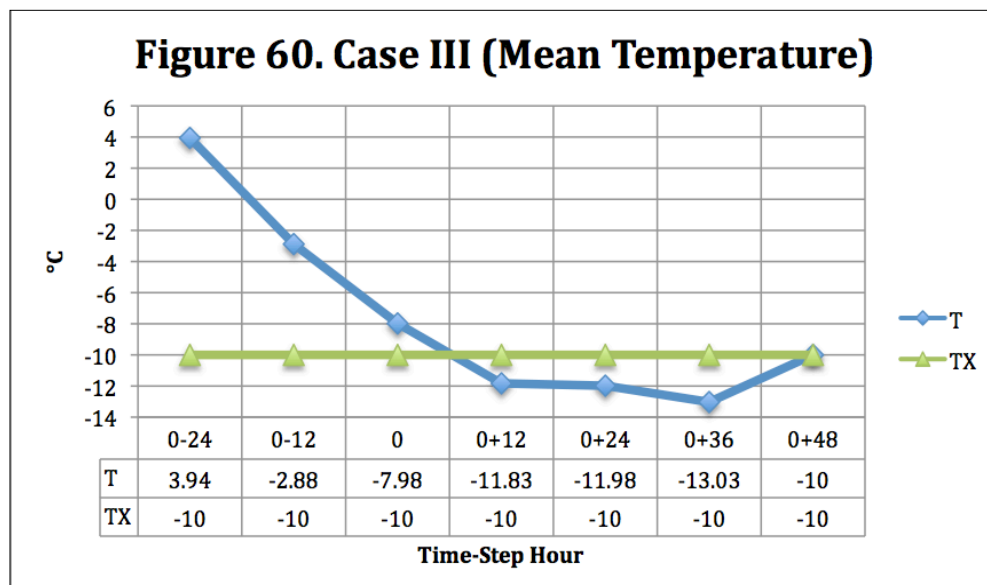
W (Figure 58): W was significant during the early hours of this event and peaked at 20.58 m/s at the 0-12 hour. Following the 0-hour, when it was 14.40 m/s, W fell below 11 m/s for the duration of the event. W was less than WX during all time-step hours from the 0-hour through the end of Case III.



RH (Figure 59): RH increased to greater than 80% from the 0+12 hour through the duration of the event during time-step hours (>RHX). The REV sounding was downwind of Lake Tahoe from the 0+12 hour through the 0+24 hour.

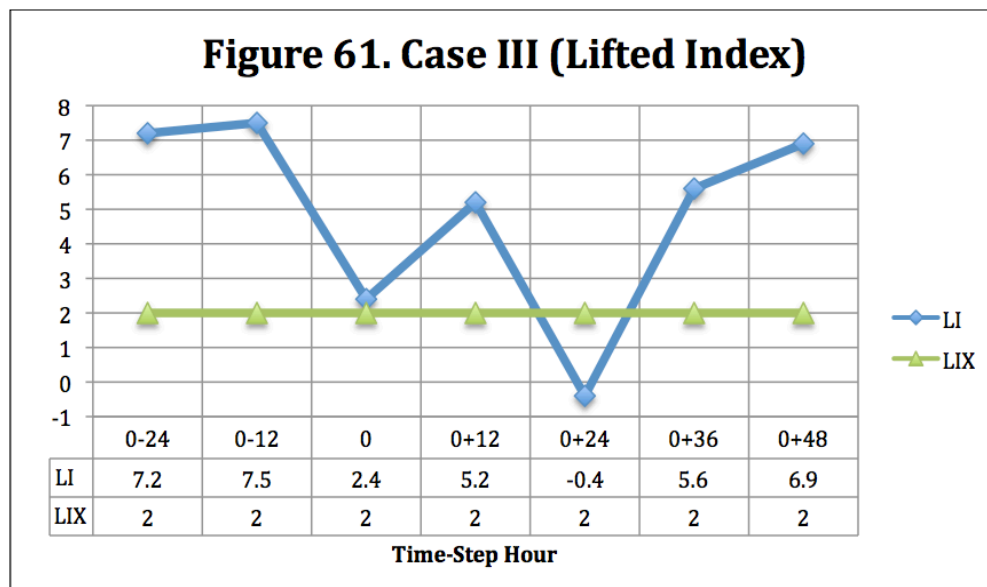


T (Figure 60): T cooled from -7.98 °C at the 0-hour, to a minimum of -11.98 °C at 0+24. This placed the surface-650-hPa layer in the optimum temperature range for snow formation, with 650-hPa level temperatures in the -15 to -18 degree range and layer average between -8 and -13 during the hours of LES development. T was colder than TX during time-step hours when LES echoes were identified on KRGX.



Instability (Figure 61): In this case, during time-step hours, from the 0-hour through the end of the event, one afternoon sounding was unstable (0+24), with a lifted index of -0.4. This was the only time-step hour when LI was lower than LIX. Strong stability was apparent during the other hours, as LI ranged from 2.4 to 6.9. The only CAPE was measured at 15 j/kg at the 0-hour and 102 j/kg at 0+24. The LES banding with the highest reflectivity and longest downwind

length from the lake occurred between the 0+12 and 0+24 hours, when instability was increasing, but slight stability was likely.



Upper Level Support: From the 0-hour through the end of the event, flow was cyclonic and to the right of the 500-hPa trough axis or closed low. This was favorable for upper level divergence and PVA. By the end of the event, as the low dropped southwest, this support was no longer evident by 0+48.

3.3.3 Radar Analysis

Snow showers in association with the lake first appeared on radar with this event at 0525 UTC on 21 January (Figure 62). The arrow denotes Echo movement. Snow showers with reflectivity of 20 dBz or less were developing over the eastern half of Lake Tahoe, downwind to the crest of the Carson Range.

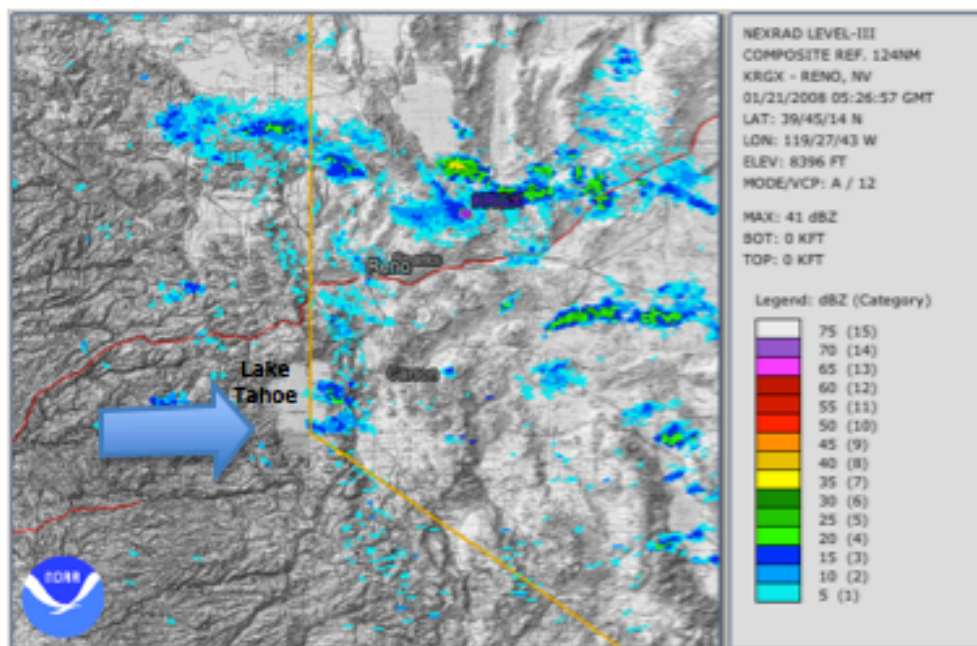


Figure 62. KRGX Composite Reflectivity at 0525 UTC on 21 Jan 2008

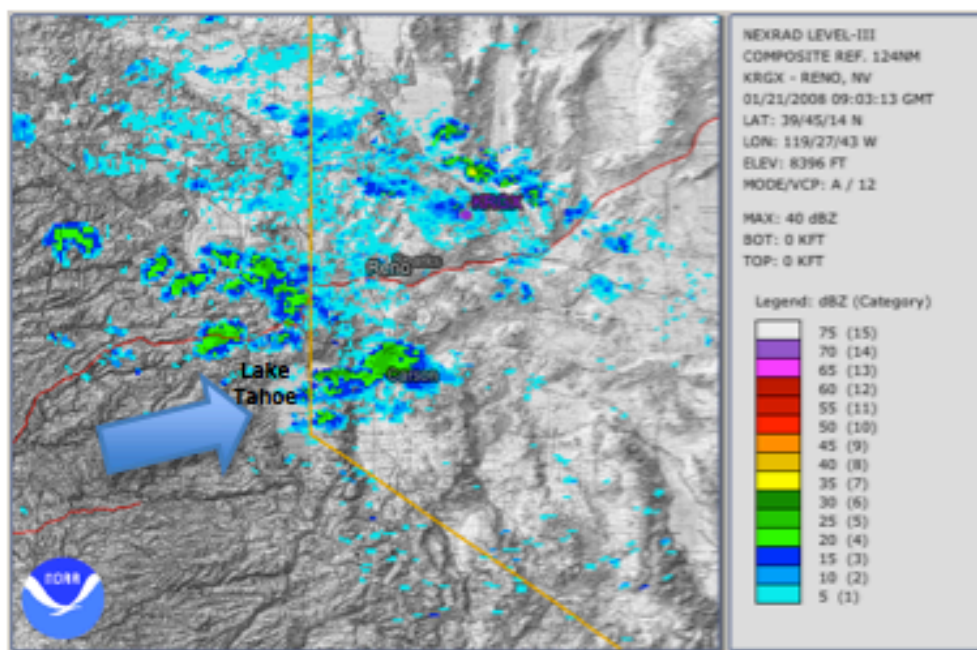


Figure 63. KRGX Composite Reflectivity at 0903 UTC on 21 Jan 2008

By 0903 UTC (Figure 63), disorganized echoes along the eastern shore developed into a LES band that extended from north of the geographic center of the lake, downwind to the Carson City area. Reflectivity of the band was in the 30 to 35 dBz range, peaking over the lake. The band extended 30 km and expanded from 10 km in width over the lake to 20 km in width from Carson City north to Washoe Valley. Wind direction at the 650-hPa level at 0000 UTC corresponded with band orientation at 245°. The band was short-lived, dissipating by 1200 UTC. Snow shower activity continued along the east shore, with a reflectivity maximum of 25 dBz.

Echoes around the lake at 1201 UTC on 21 January (Figure 64) were located in two areas along the eastern shore. The arrow denotes Echo movement. Light activity with a reflectivity of 20 dBz or less was located over Crystal Bay and affecting Incline Village. Higher reflectivity of 25 dBz existed with band development along the eastern shore over the Glenbrook area. This activity continued to develop and decline through 1500 UTC.

The major LES band defining this case first appeared at 16:29 UTC on 21 January (Figure 65). Flow was becoming more southwesterly, as the low-pressure area to the northwest deepened and began to shift south. A 30 to 35 dBz LES band formed from the geographic center of the lake to Crystal Bay and extended northeast over Sand Harbor and Incline Village to Mount Rose. At this hour, the band was approximately 25 km long and 10 km wide.

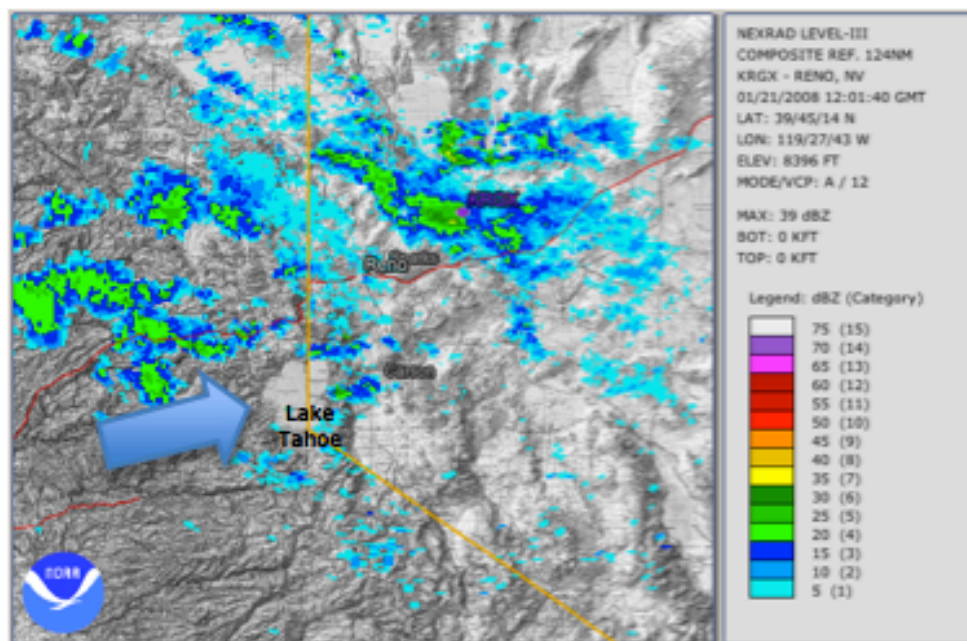


Figure 64. KRGX Composite Reflectivity at 1201 UTC on 21 Jan 2008

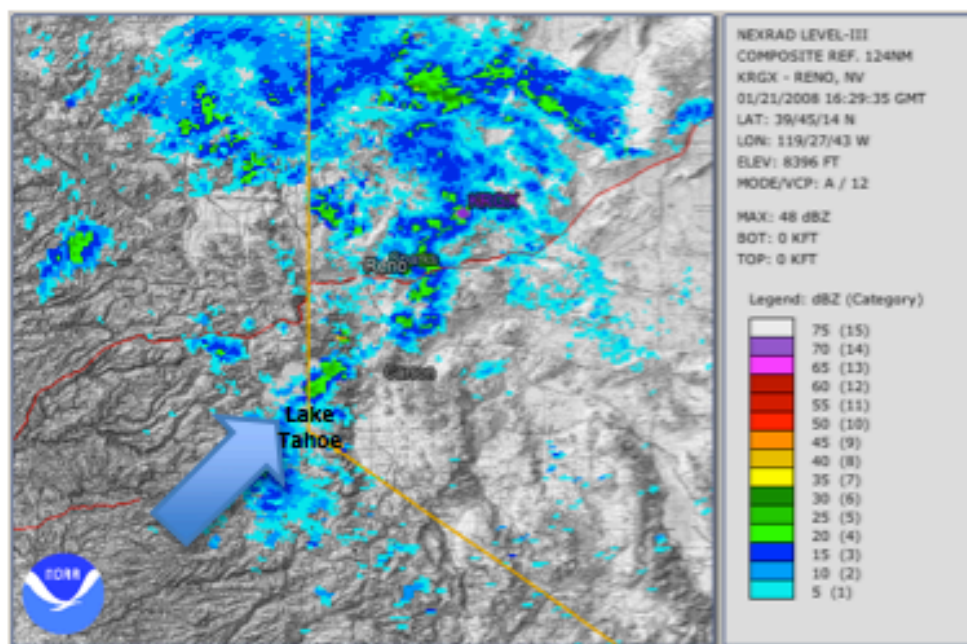


Figure 65. KRGX Composite Reflectivity at 1629 UTC on 21 Jan 2008

By 1704 UTC (Figure 66), the LES band was intensifying with reflectivity values of 35 to 40 dBz. It extended downwind from the center of Lake Tahoe over Crystal Bay, Incline Village, Mt. Rose, and into Washoe Valley. This was a distance of 40 km. The band also grew in width, consistently 15 km wide, downwind of the shore. At 1856 UTC (Figure 67), the LES band extended into the Reno-Sparks metropolitan area. Band length had grown to 50 km, and width was 15 to 20 km. Reflectivity of the band peaked at 52 dBz over the lake, but averaged 30 to 40 dBz. Figure 68 represents the maximum extent of this LES band at 20:02 UTC on 21 January. Reflectivity was shown as peaking at 56 dBz, although most of the band was in the 25 to 35 dBz range. The LES band extended from the northeast quadrant of Lake Tahoe, downwind 65 km through Reno-Sparks and into the suburban communities to the north and east. Activity reached as far as the south shore of Pyramid Lake. The 650-level wind direction was 176° four hours later at 0000 UTC, suggesting that wind was started to shift from southwesterly to southerly. Activity over the lake was ending, suggesting the decline of the band. Orographic enhancement over Mt. Rose likely created some of the highest reflectivity at this hour along and immediately downwind of the Carson Range. The band dissipated by 0000 UTC on 22 January.

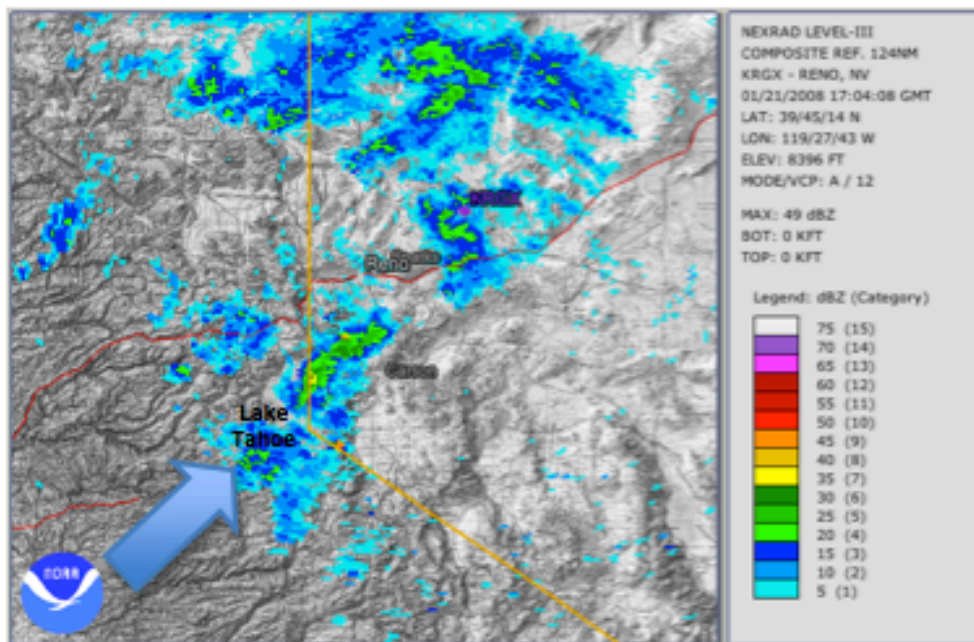


Figure 66. KRGX Composite Reflectivity at 1704 UTC on 21 Jan 2008

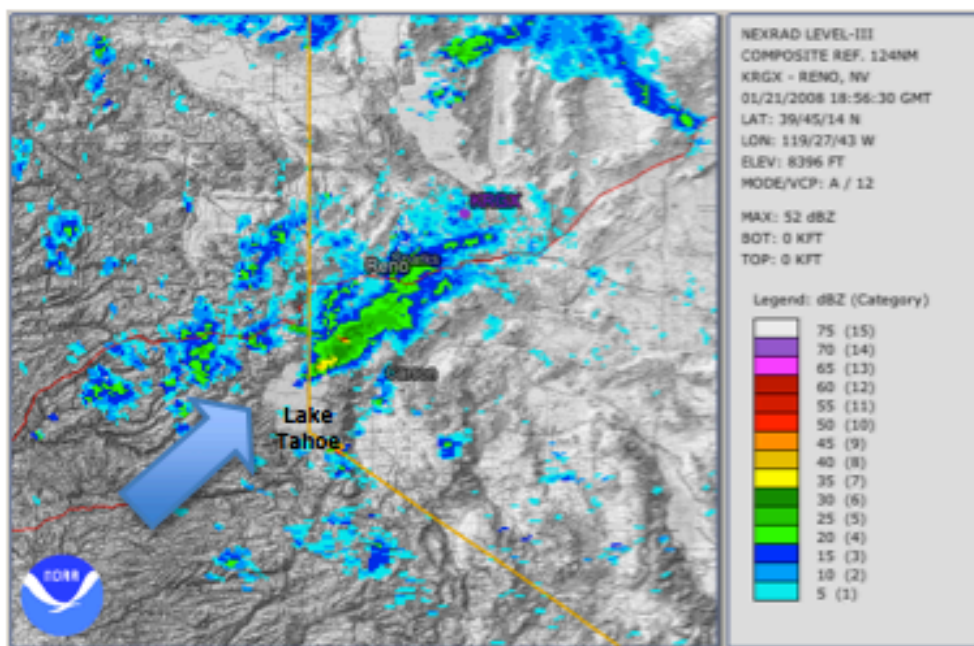


Figure 67. KRGX Composite Reflectivity at 1856 UTC on 21 Jan 2008

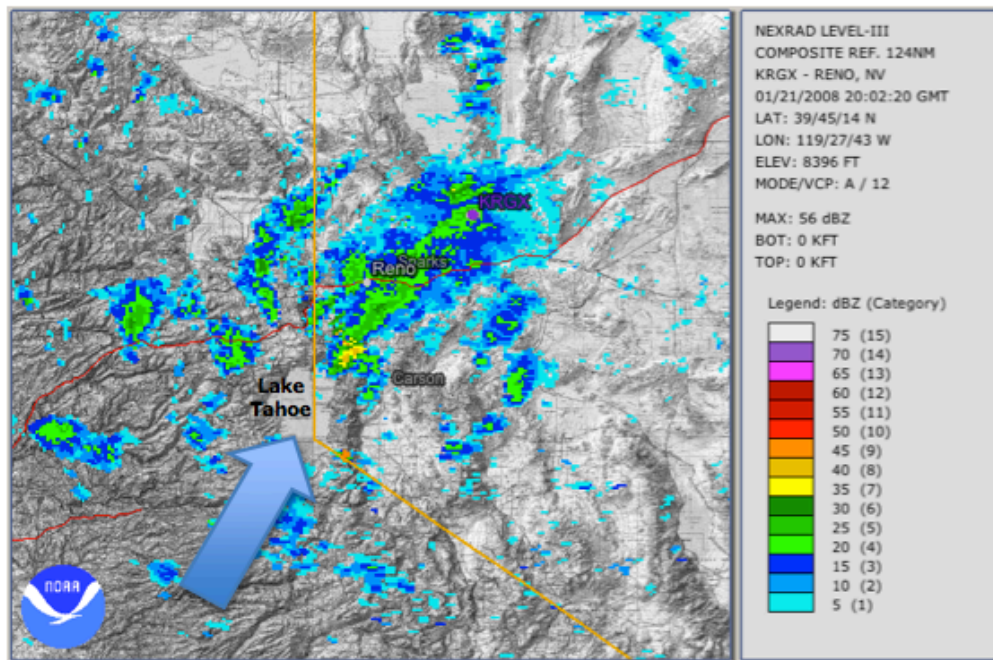


Figure 68. KRGX Composite Reflectivity at 2002 UTC on 21 Jan 2008

New development occurred over the same quadrant of Lake Tahoe following dissipation of the LES band in Figure 68. The new LES band formed over Crystal Bay and extended northeast over the Carson Range at 0000 UTC (Figure 69). The arrow denotes echo movement. Wind was shifting at this hour, and S was 86° , from 90° at Lake Level to 176° at the 650-hPa level. From 0000 UTC to 1200 UTC on 22 November, wind was turning from southwest to southeast, as the now closed low was drifting southwest and away from Lake Tahoe.

Between 00z and 01z, wind flow became southerly at the 650-hPa level. At 0130 UTC on 22 January (Figure 70), echo development had shifted in orientation to the 650-hPa direction of flow.

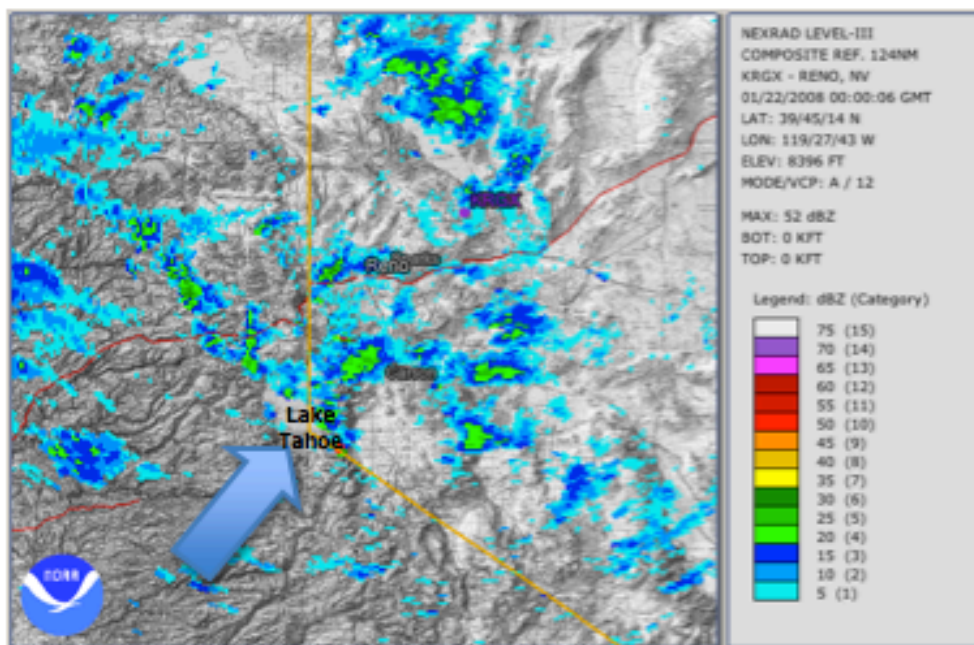


Figure 69. KRGX Composite Reflectivity at 0000 UTC on 22 Jan 2008

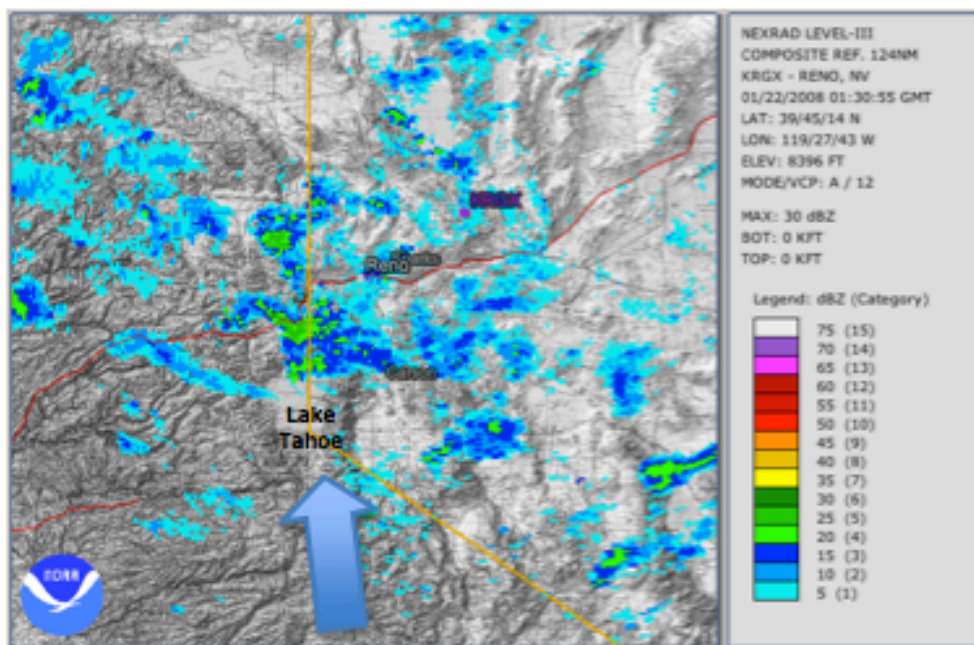


Figure 70. KRGX Composite Reflectivity at 0130 UTC on 22 Jan 2008

Convection occurred over the northern third of the lake, and snow showers extended north, affecting the north shore of Lake Tahoe from Incline Village to Carnelian Bay. Maximum dBZ of 30 was associated with this shower activity.

By 0331 UTC (Figure 71), the band peaked at a reflectivity maximum of 39 dBz. Snow extended from the northwest quadrant of the lake northwest approximately 25 km to Truckee. Echo movement suggested further turning of the 650-hPa wind, which was confirmed at 127° by 1200 UTC. Within the following hours, convection over the lake declined, and remnant snow showers drifted northwest and dissipated.

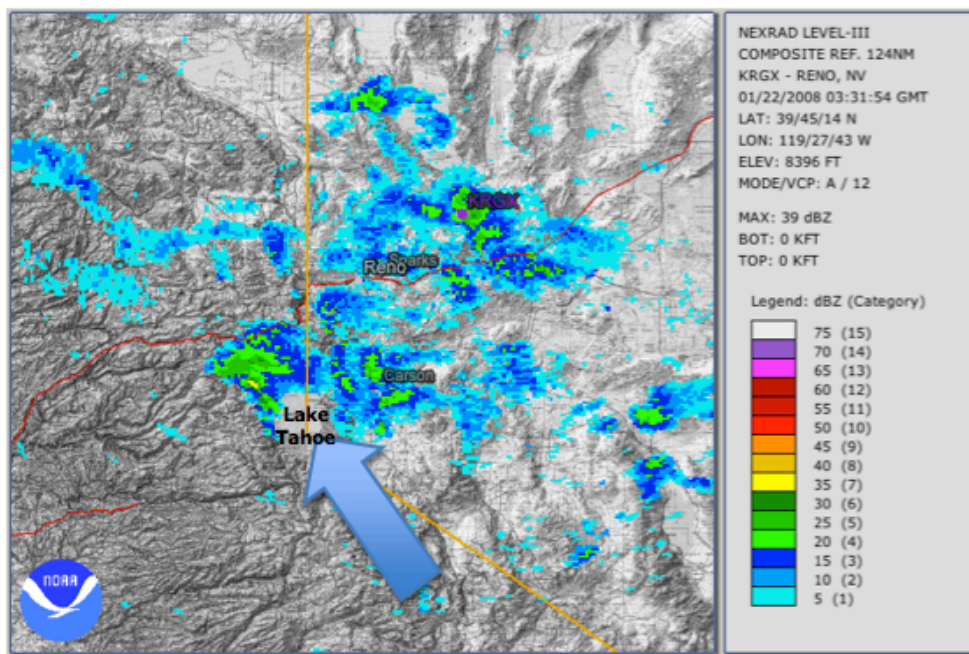


Figure 71. KRGX Composite Reflectivity at 0331 UTC on 22 Jan 2008

3.4 Case IV

3.4.1 Event Summary

The high temperature at KTVL was 23 °C on both 7 October and 8 October. The lake surface temperature was also near its climatological annual peak at 15.36 °C. By 1200 UTC on 9 October, a 56 m/s jet streak passed over the area, developing wind gusts of 17 m/s at lake level ahead of cold air advection.

By 1200 UTC on 10 October, as the trough axis at jet-level remained west of the lake (Figure 72a, Arrow 1), a low-pressure trough, 3 to 4 standard deviations below average at the 500-hPa level, dropped into the Great Basin east of Lake Tahoe (Figure 72b, Arrow 2). This placed Lake Tahoe under northerly to northeasterly flow at 650-hPa through the duration of the event. KTVL temperatures were at or below 0 °C for the duration of the event, with 650-hPa temperatures around -15 °C. Lake Tahoe was also downwind of a strong lake effect off of Pyramid Lake through this case. The Reno NWSFO issued a lake effect snow advisory for areas downwind of both Pyramid Lake and Lake Tahoe during this event.

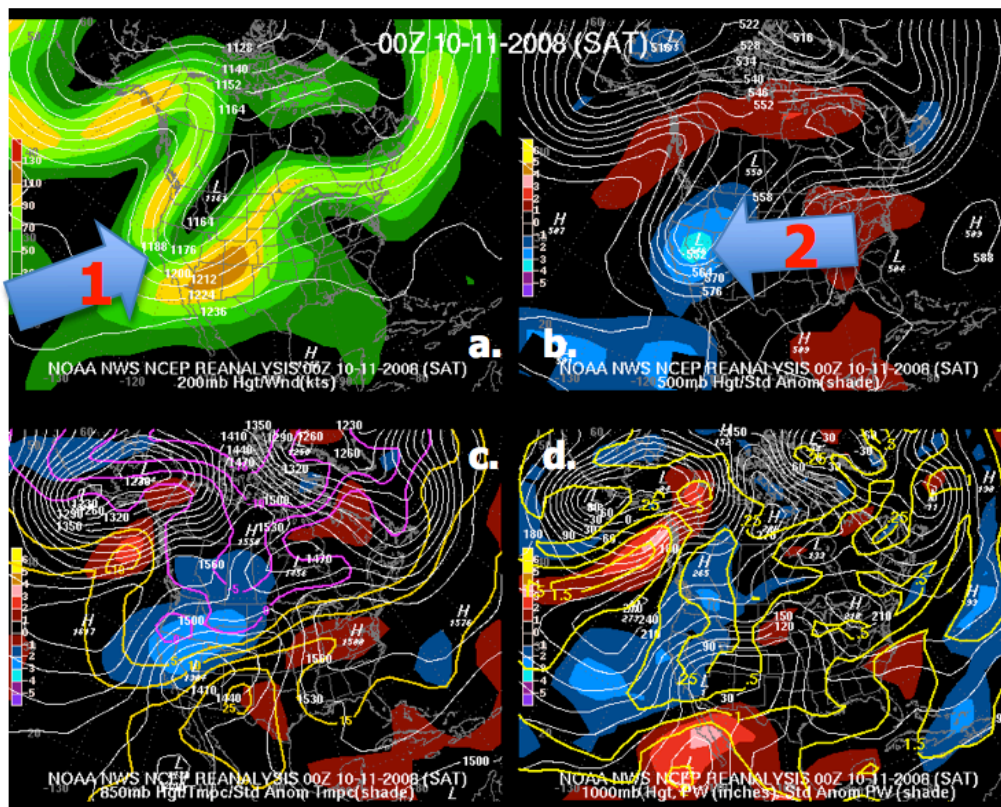


Figure 72. 11 October 2008 0000 UTC: 200, 500, 850, 1000-hPa NOAA Upper Air Analyses

As the trough weakened, air began to modify. Shear increased by 0000 UTC on 12 October. Lake-effect activity ended and milder and drier air began to mix into the Lake Tahoe area at all levels.

Figure 73 shows Case IV reported snowfall totals. Due to the warmth of the ground and the lack of observations over the southwest quadrant of Lake Tahoe, only two amounts were archived for this event. The Reno NWSFO noted rates of two to five cm per hour with banding during this event, but totals from this activity would have been in the Desolation Wilderness area and the sparsely populated southwest quadrant of the basin.

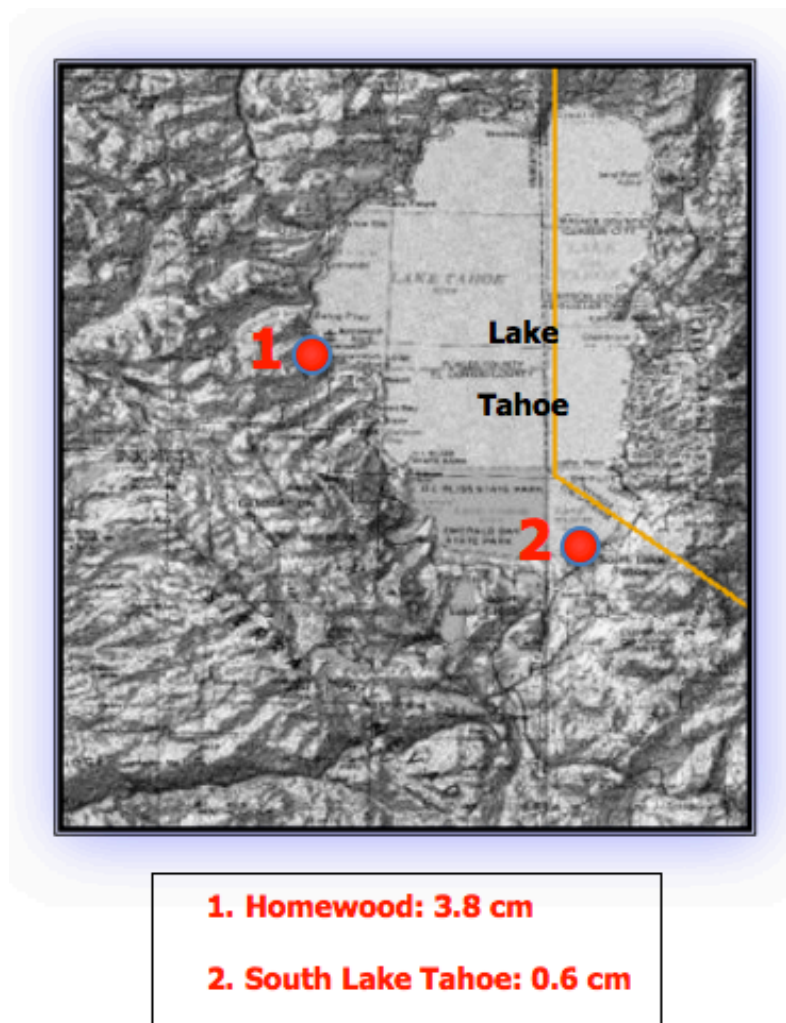


Figure 73. Case IV Reported Snowfall Totals

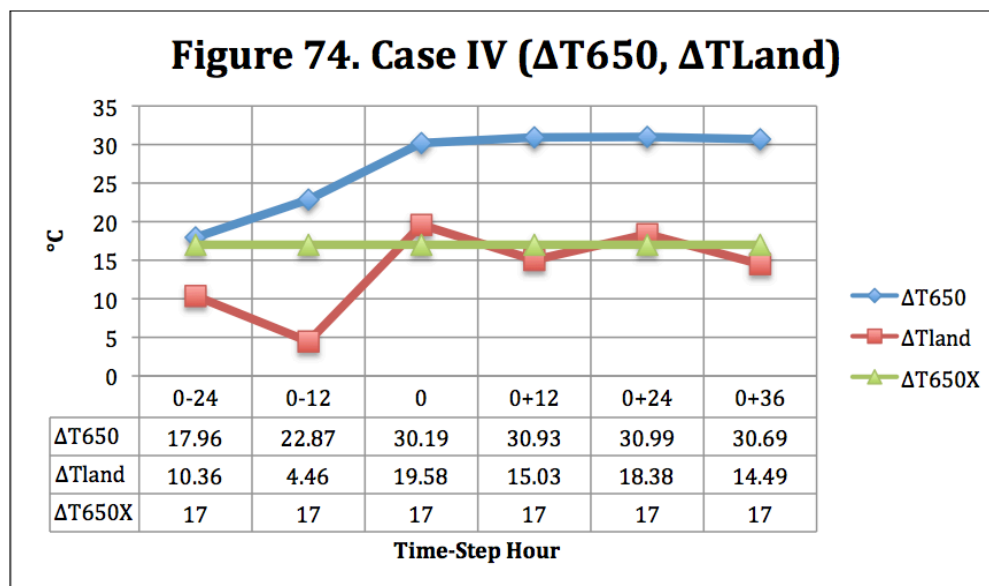
3.4.2 Results of Time-step Analysis

Table 11 is a complete listing of all parameter analysis results during Case IV. Figures 74-79 provide time-step analysis of individual LES parameters.

Time-Step Hours:	0-24	0-12	0	0+12	0+24	0+36
ΔT_{650} (°C)	17.96	22.87	30.19	30.93	30.99	30.69
ΔT_{land} (°C)	10.36	4.46	19.58	15.03	18.38	14.49
Capping Inversion	NO	NO	NO	NO	NO	NO
S (°)	10	94	89	6	20	40
W (m/s)	16.46	14.92	8.75	13.38	13.38	11.32
RH (%)	41	46	76	72	80	53
T (°C)	3.40	-1.20	-8.80	-9.10	-9.98	-8.75
Instability (LI CAPE) CAPE (J/kg)	8.0 0	5.3 0	8.9 0	-0.6 149	3.5 0	1.8 3
Upper Level Support	YES	YES	YES	YES	YES	NO

Table 11. Case IV Parameter Analysis Results
Blue columns indicate time-step hours when LES occurred
Green columns indicate hours that immediately preceded and followed LES

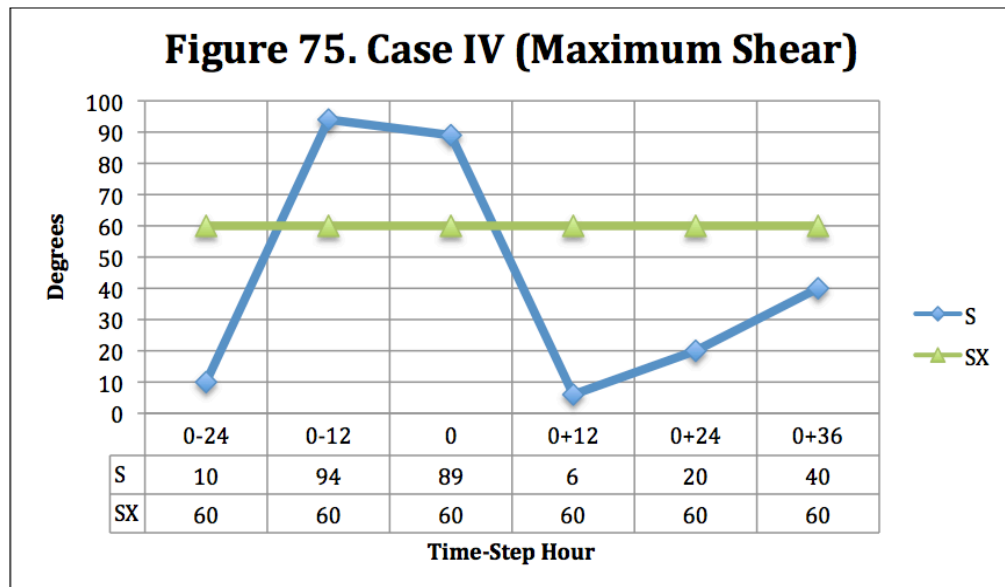
ΔT_{650} (Figure 74): During the time-step hours when LES banding occurred, ΔT_{650} ranged from 30.19 °C at the 0-hour, to 30.99 °C at 0+24 and 30.69 °C during final dissipation of LES echoes. ΔT_{650} was significantly greater than ΔT_{650X} during these hours.



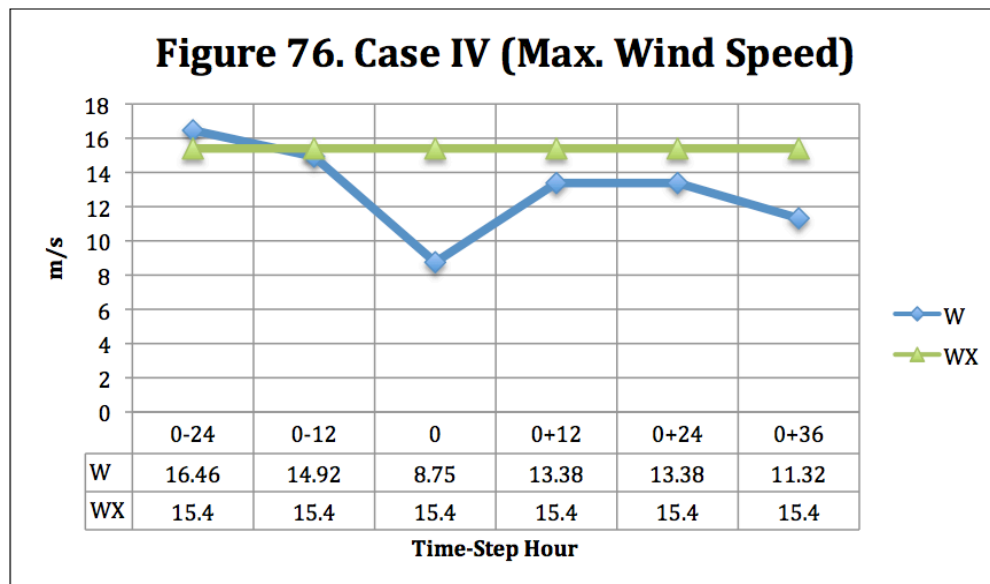
ΔT_{land} (Figure 74): ΔT_{land} was greater than 14 °C during all time-step hours from the 0-hour through the dissipation of LES.

Existence of a Capping Inversion: In this case, no capping inversions were observed at or below the 650-hPa level.

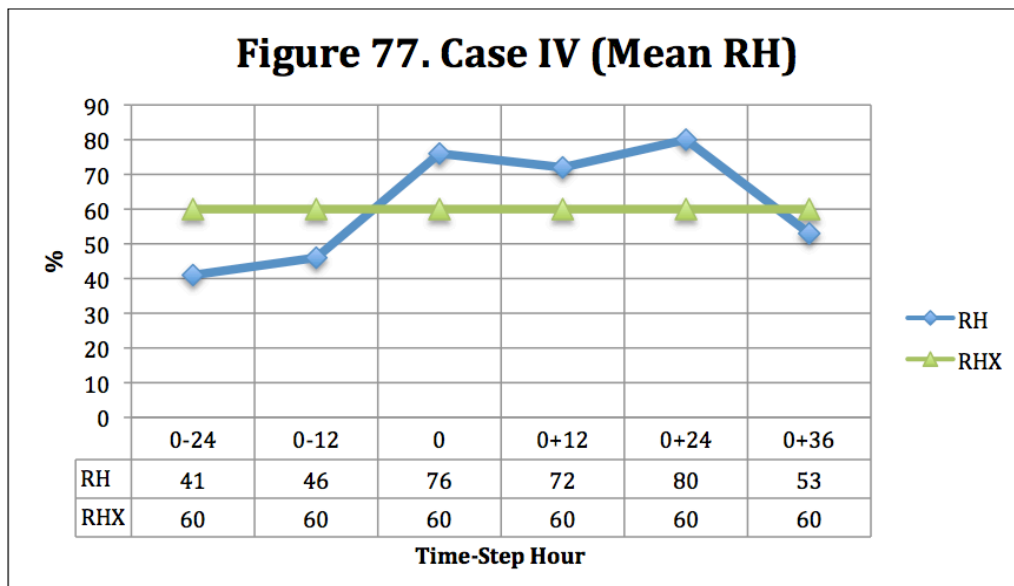
S (Figure 75): S exceeded SX in two time-steps, the 0-12 hour and the 0-hour. During this period, a cold front moved through the area. This shifted wind direction from the southwest to the north. Following the 0-hour, S was below SX in a northerly flow. There was a shift in flow from north-northeast to north-northwest in the final hours of the event, when S increased to 40°.



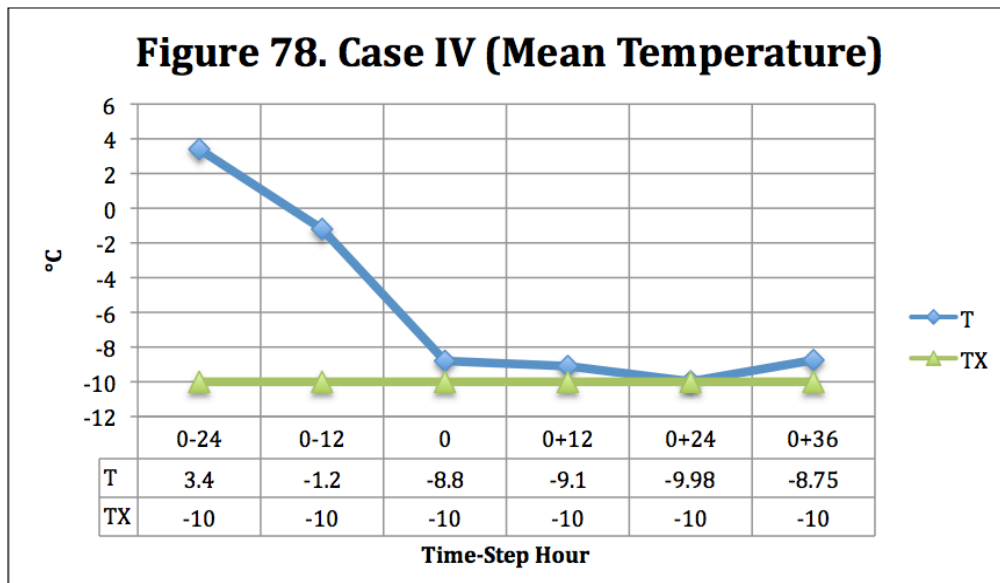
W (Figure 76): W was greater than WX during the early hours of this event and peaked at 16.46 m/s at the 0-24 hour. Following the 0-hour, when it was 8.75 m/s, W increased to 13.38 m/s for the 0+12 and 0+24 hours.



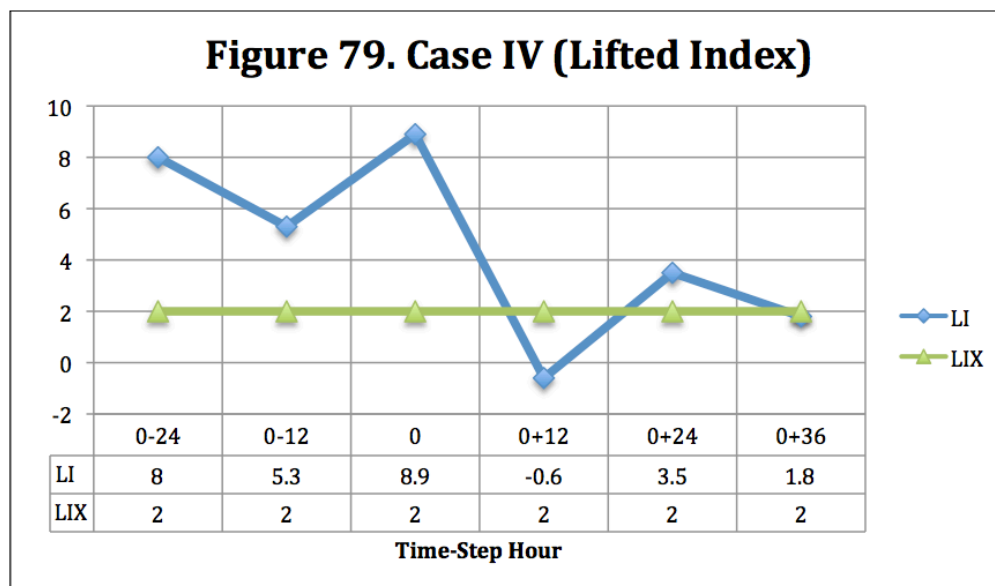
RH (Figure 77): RH was greater than 70% during analyzed time-step hours from the 0-hour through the 0+24 hour. In the final hours of the case, RH fell to 53% at 0+36. It should be noted that the REV sounding was downwind of a Pyramid Lake-effect event during most of this case.



T (Figure 78): T cooled from -8.80 °C at the 0-hour, to a minimum of -9.98 at 0+24 during time-step analysis. This placed the surface-650 hPa layer in the optimum temperature range for snow formation, with 650-hPa level temperatures around -15 °C, and T was close to TX during all time-step hours from the 0-hour through the end of the event.



Instability (Figure 79): From the 0-hour through the end of the event, two time-step hour REV soundings were unstable. The 0+12 hour and 0+24 hour had LI of -0.6 and -3.5 respectively. CAPE was measured at 149 j/kg at the 0+12 hour and 3 j/kg at 0+36. The LES banding with the longest echo structure and highest reflectivity occurred between the 0+12 and 0+24 hours.



Upper Level Support: From the 0-hour through the 0+36 hour, flow was cyclonic and to the right of the 500-hPa trough axis or closed low. This was favorable for upper level divergence and vorticity advection. By the end of the event, as the trough weakened and shifted east, this support was no longer evident by 0+36.

3.4.3 Radar Analysis

LES echoes first appeared in the form of very light activity over the northern half of the lake around 1100 UTC, lingering through the 1200 UTC hour. At 1615 UTC (Figure 80), a convective cell developed with a reflectivity maximum of 35 dBz. The flow was northerly, with a wind direction at the 650-hPa level of 6°. The arrow denotes echo movement.

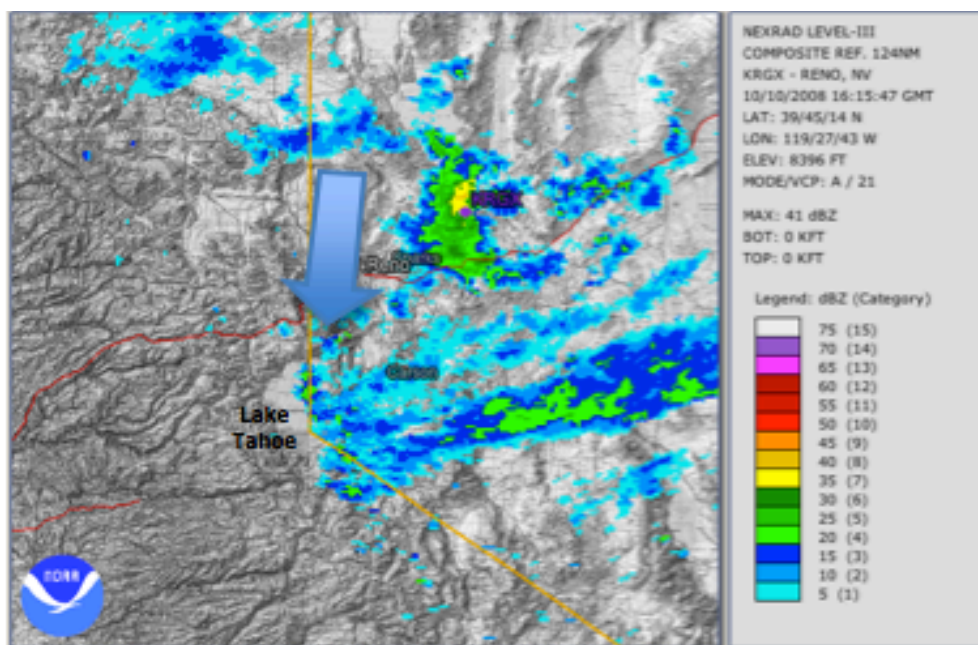


Figure 80. KRGX Composite Reflectivity at 1615 UTC on 10 Oct 2008

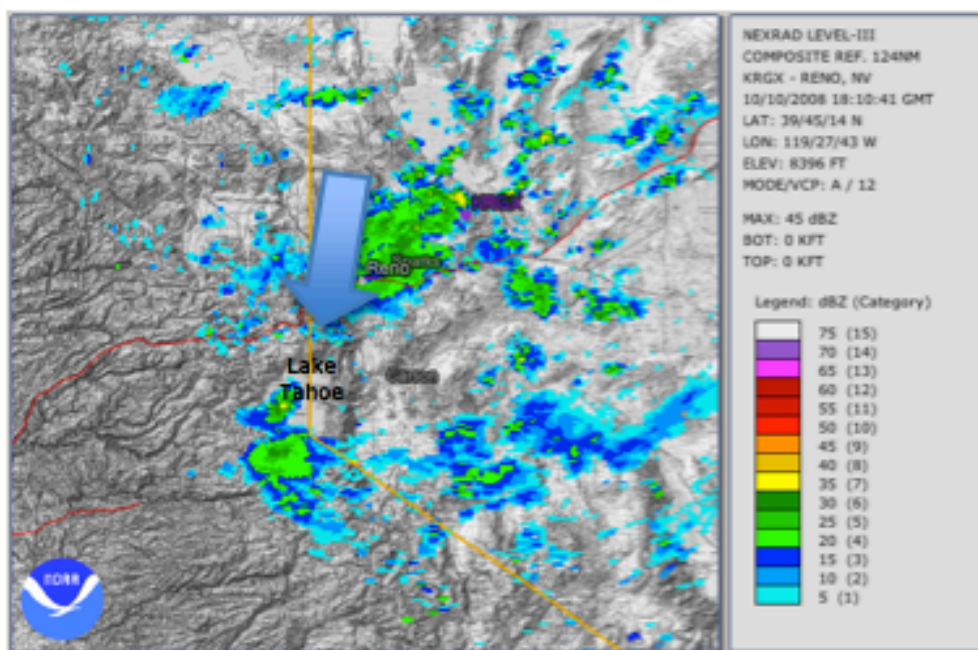


Figure 81. KRGX Composite Reflectivity at 1810 UTC on 10 Oct 2008

By 1810 UTC (Figure 81), cells shifted over the southern half of Lake Tahoe, with one cell over McKinney Bay with a reflectivity maximum of 45 dBz and a developing LES band from South Lake Tahoe west to Emerald Bay over the southwest quadrant of the lake. It should be noted that LES banding associated with Pyramid Lake was pronounced at this hour, affecting the Reno-Sparks area. This activity was continuous from 1200 UTC forward.

Three hours later at 2103 UTC (Figure 82), cells along the south shore dissipated, while the cell in McKinney Bay developed into a well-defined LES band. This band extended from just west of the geographic center of the lake southwest 40 km over Homewood Ski Resort and the Desolation Wilderness. Maximum reflectivity of the band was 40 dBz.

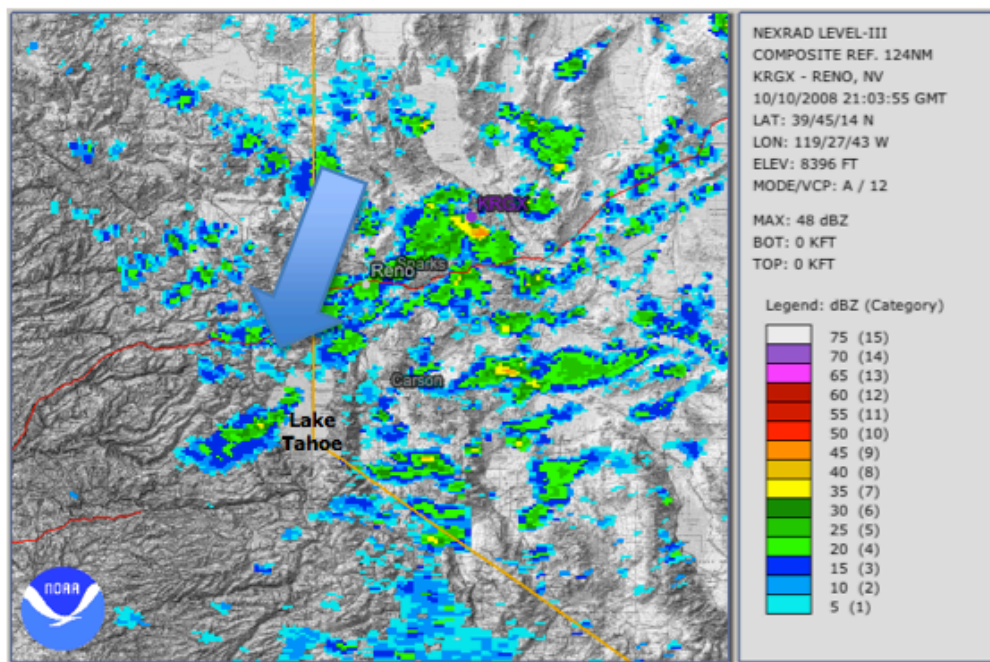


Figure 82. KRGX Composite Reflectivity at 2103 UTC on 10 Oct 2008

By 0000 UTC on 11 October, activity associated with Lake Tahoe shifted south (Figure 83). A LES band extended from just north of the south shore from South Lake Tahoe west to Emerald Bay, southwest 35 km over the Desolation Wilderness. Maximum reflectivity of this band was 35 dBz. It should be noted that the band orientation shifted from the 650-hPa wind direction at the south shore to a more southwesterly to westerly orientation downwind of the lake. It should also be noted that distance from the KRGX radar site was significant with this band, limiting beam angle. Activity also continued downwind of Pyramid Lake at this hour.

By 0036 UTC (Figure 84), while the Desolation Wilderness activity dissipated, snow showers intensified over the southern half of Lake Tahoe. Reflectivity of these echoes ranged from 35 to 45 dBz. This activity dissipated to individual echoes until 0452 UTC (Figure 85), when a new LES band formed over the western half of the lake. This band showed a maximum reflectivity of 40 dBz, and extended southwest from just west of the geographic center of the lake over Rubicon Bay and into the Desolation Wilderness. At its peak, the band stretched 30 km. It dissipated by 0527 UTC (Figure 86). Activity continued downwind of Pyramid Lake through this period.

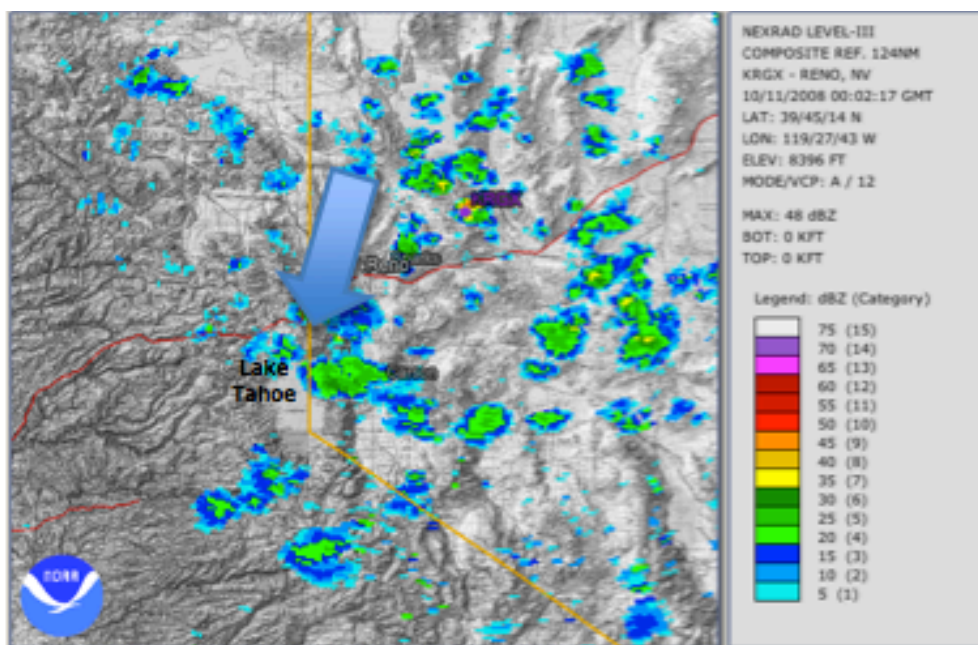


Figure 83. KRGX Composite Reflectivity at 0002 UTC on 11 Oct 2008

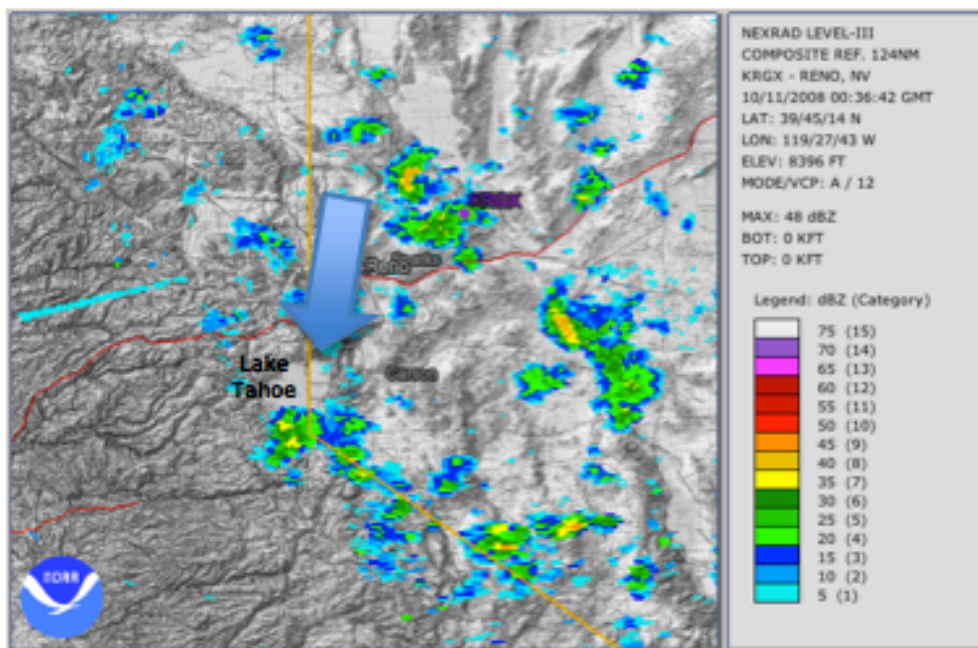


Figure 84. KRGX Composite Reflectivity at 0036 UTC on 11 Oct 2008

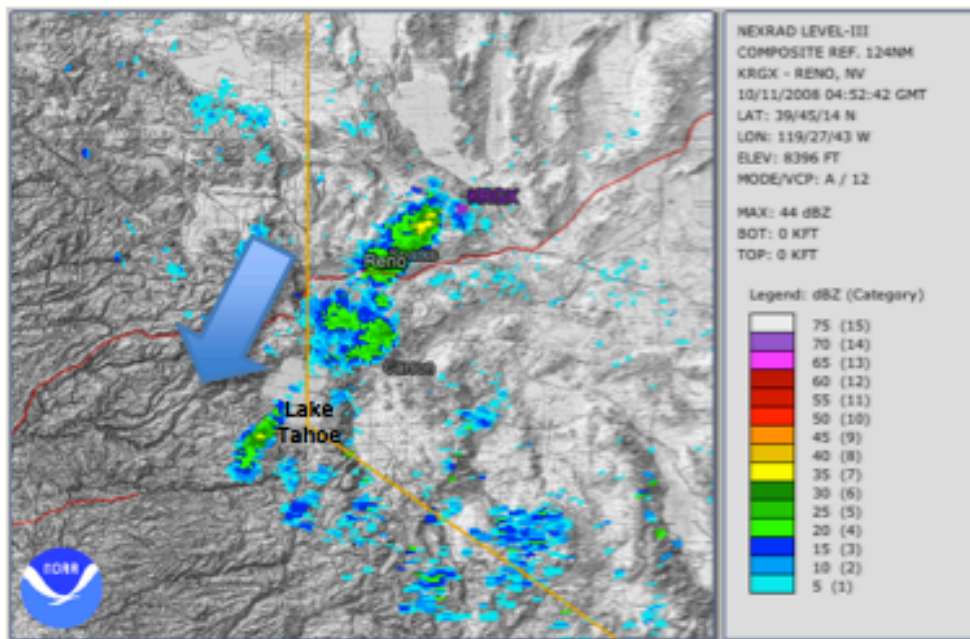


Figure 85. KRGX Composite Reflectivity at 0452 UTC on 11 Oct 2008

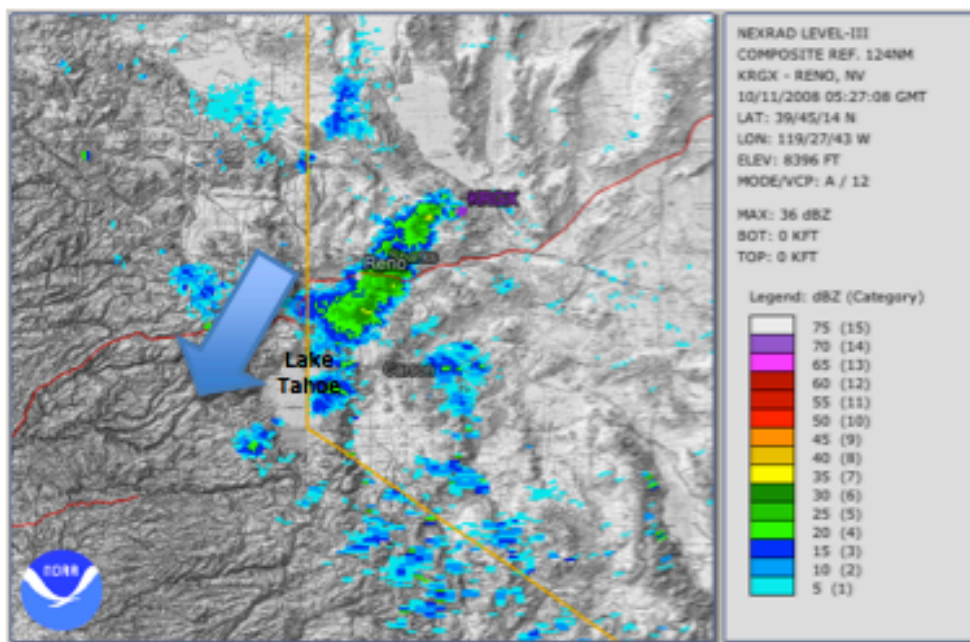


Figure 86. KRGX Composite Reflectivity at 0527 UTC on 11 Oct 2008

Snow showers and weak banding continued to form, dissipate, and reform through 1500 UTC over the southwest quadrant of Lake Tahoe on 11 October. Figure 87 shows the formation of last LES band of the case at 1202 UTC. Figure 88 shows composite reflectivity at 1329 UTC, when the band was at its peak reflectivity of 39 dBz, and extended southwest over Emerald Bay 20 km into the Desolation Wilderness. Figure 89 at 1500 UTC, shows the final LES echoes noted in this case.

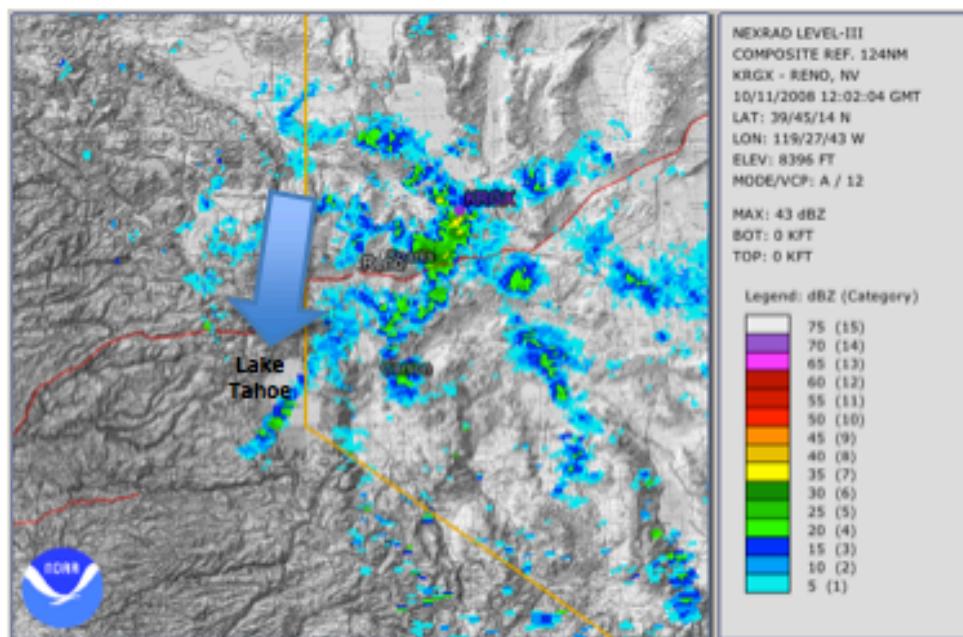


Figure 87. KRGX Composite Reflectivity at 1202 UTC on 11 Oct 2008

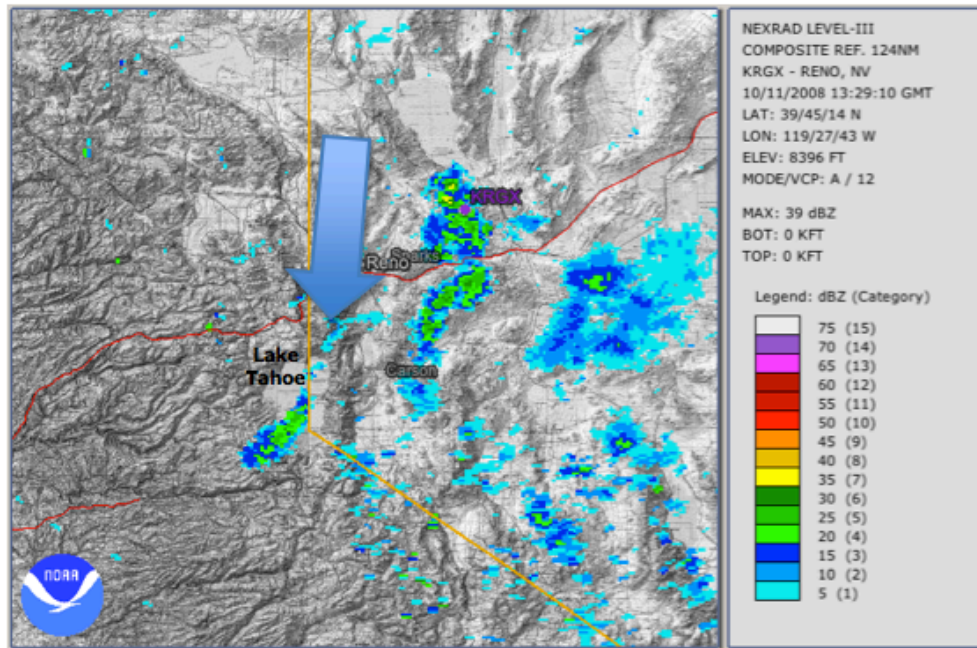


Figure 88. KRGX Composite Reflectivity at 1329 UTC on 11 Oct 2008

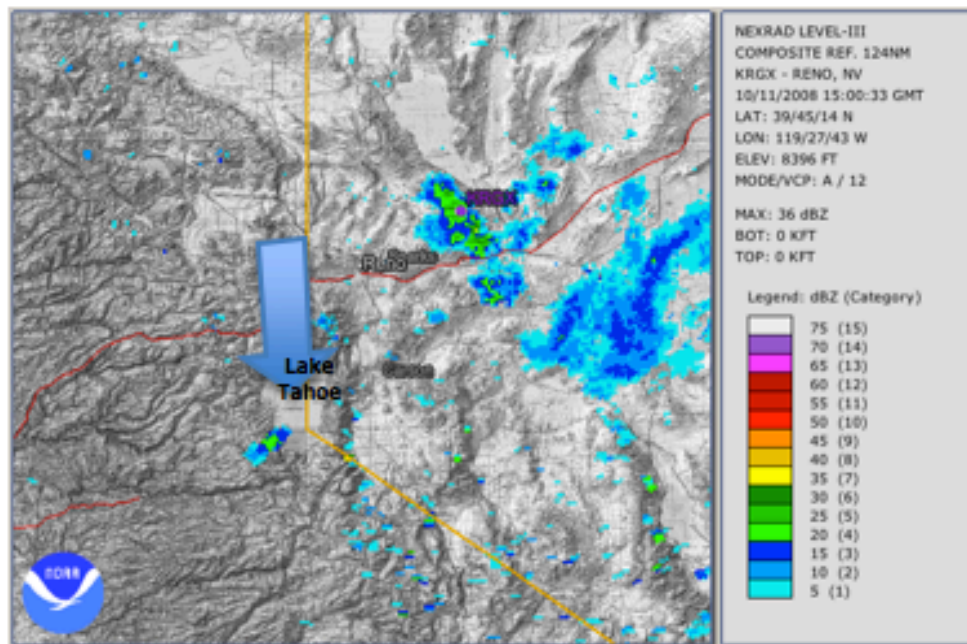


Figure 89. KRGX Composite Reflectivity at 1500 UTC on 11 Oct 2008

3.5 Case V

3.5.1 Event Summary

This early October 2009 LES event occurred in the wake of abnormally cold air advection across Lake Tahoe. Following a week of above average temperatures around the basin, a jet streak of 57+ m/s deepened a low-pressure trough, driving it south into the area. The trough was 2 to 3 standard deviations below average at the 500-hPa level. Lake temperature was near its seasonal peak at 16.15 °C at 0000 UTC on 3 October 2009.

In the hours following 0000 UTC on 4 October, a cold front pushed through the basin. Behind the front by 1200 UTC, Lake Tahoe was to the right of a long-wave low-pressure trough at 200-hPa (Figure 90a, Arrow 1), and under a low-pressure area at the 500-hPa level three to four standard deviations below average (Figure 90b, Arrow 2). As frontal precipitation ended and the boundary moved east into western Nevada, a LES band developed in the cold air advection across the lake. The LES band extended from Tahoe southeast into Douglas County and persisted from 0800 UTC until dissipating into light snow showers around 1400 UTC. A line of orographically enhanced snow showers moved from the west slope of the Sierra Nevada into the Tahoe Basin. As the showers moved over the southern end of the lake, the LES band redeveloped. This band extended into Douglas County for three hours before dissipating.

During this time, the Reno NWSFO issued a lake effect snow advisory for the Tahoe Basin and Carson City and Douglas Counties, which was in effect from 0900 UTC to 1800 UTC.

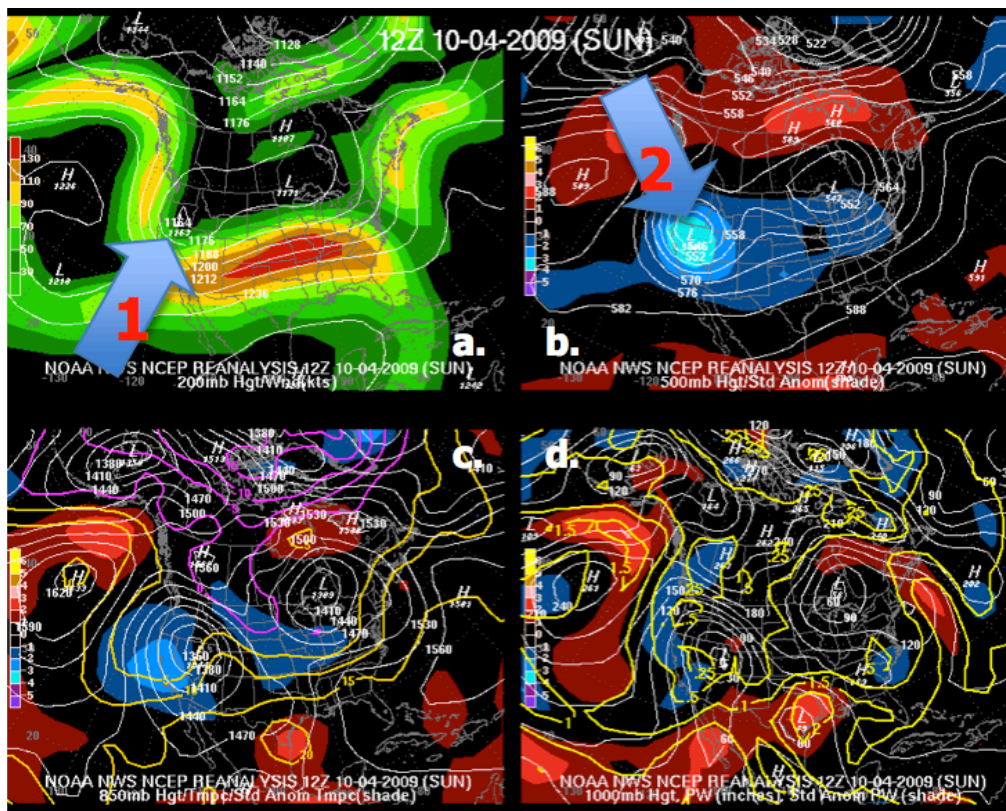
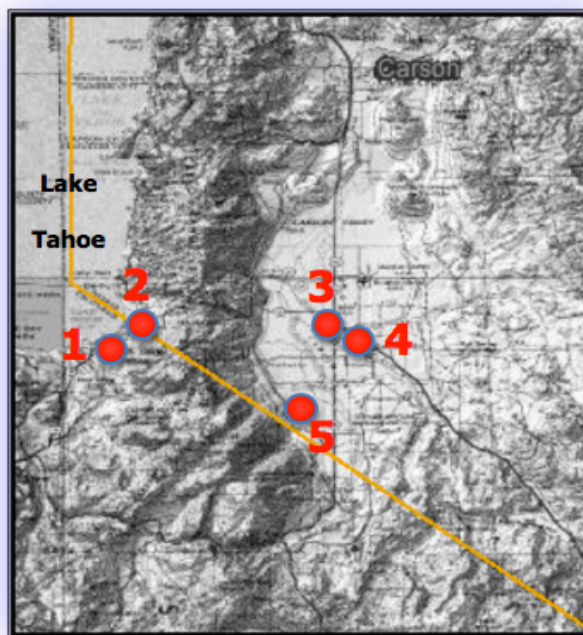


Figure 90. 4 October 2009 1200 UTC: 200, 500, 850, 1000-hPa NOAA Upper Air Analyses

A third band developed with similar orientation in the wake of the passage of another band of convective showers across the lake on the evening of 4 October. This band was short lived, dissipating by 04z on 5 October.

Lake-effect activity degenerated to light showers along the southeast shore of the lake, ending by 1200 UTC.

Figure 91 shows Case V reported snowfall totals. The early October date of this event, along with the warm weather prior to the snowfall, limited accumulation in western Nevada on paved surfaces. With band orientation consistent through the case, occurring in populated areas, a number of significant snow totals were reported.



1. South Lake Tahoe: 12.7 cm
2. Stateline: 10.2 cm
3. Minden: 10.2 cm
4. Gardnerville: 20.3 cm
5. Sheridan Acres: 20.3 cm

Figure 91. Case V Reported Snowfall Totals

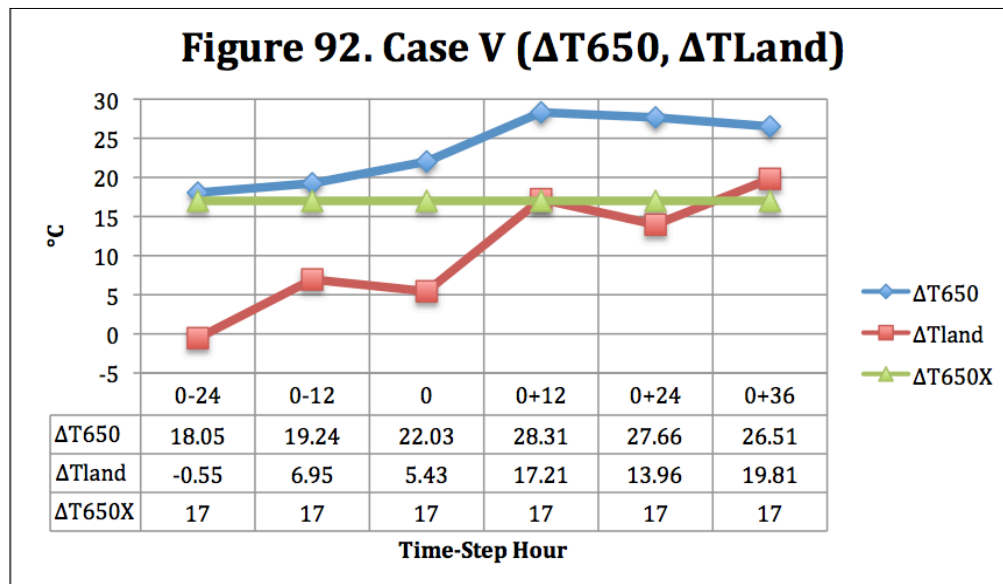
3.5.2 Results of Time-step Analysis

Table 12 is a complete listing of all parameter analysis results during Case V. Figures 92-97 provide time-step analysis of individual LES parameters.

Time-Step Hours:	0-24	0-12	0	0+12	0+24	0+36
ΔT_{650} (°C)	18.05	19.24	22.03	28.31	27.66	26.51
ΔT_{land} (°C)	-0.55	6.95	5.43	17.21	13.96	19.81
Capping Inversion	NO	NO	NO	NO	NO	NO
S (°)	39	25	55	34	55	20
W (m/s)	12.35	12.35	16.46	6.17	8.23	9.26
RH (%)	28	39	33	71	84	80
T (°C)	6.40	2.30	1.02	-7.35	-6.03	-6.48
Instability (LI CAPE) CAPE (J/kg)	1.2 0	7.6 0	-1.4 43	1.4 0	-1.3 147	12.1 0
Upper Level Support	NO	NO	YES	YES	YES	YES

Table 12. Case V Parameter Analysis Results
Blue columns indicate time-step hours when LES occurred
Green columns indicate hours that immediately preceded and followed LES

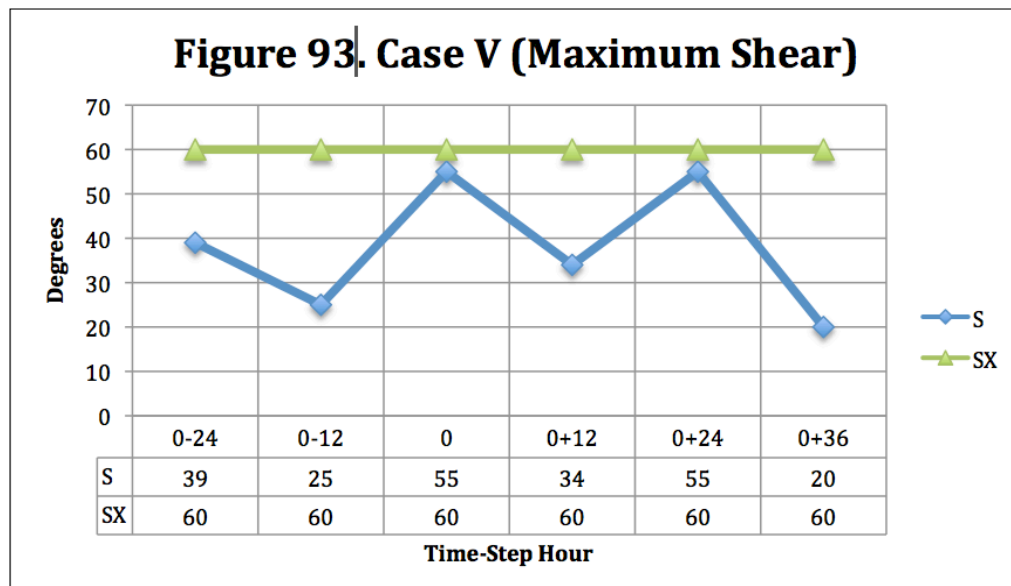
ΔT_{650} (Figure 92): During the time-step hours from the 0-hour through the end of the event, ΔT_{650} ranged from a minimum of 22.03 °C at the 0-hour, to a maximum of 28.31 °C at 0+12. ΔT_{650} was >22 °C during these time-step hours and >27 °C when LES banding was analyzed on the NEXRAD.



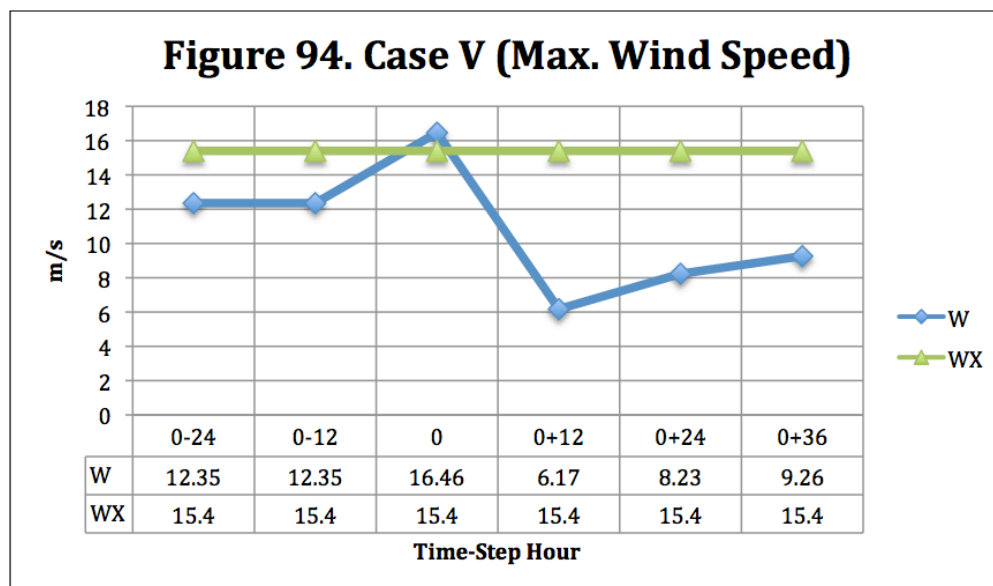
ΔT_{land} (Figure 92): ΔT_{land} was >13 °C during hours when LES banding occurred, peaking during the 1200 UTC hours of 4 October at 17.21 °C and 5 October at 19.81 °C.

Existence of a Capping Inversion: In this case, no capping inversions were observed at or below the 650-hPa level from the 0-hour through the end of the case during time-step analysis. A 646-hPa inversion was evident at 0+36, and this lowered to the 650-hPa level in the following hours.

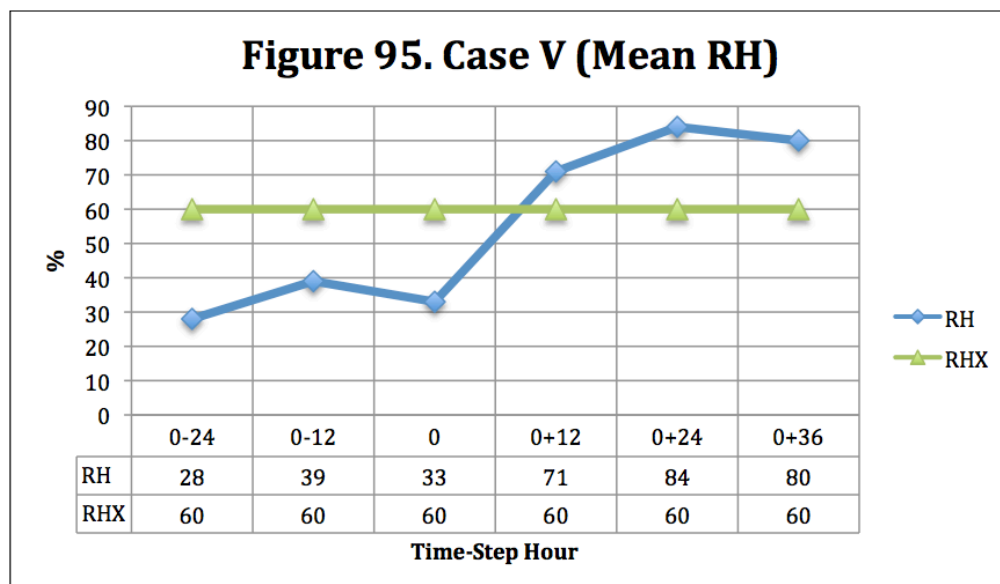
S (Figure 93): S did not exceed SX during time-step hour analysis in this case. S did increase from 34° to 55° between the 0+12 and 0+24 time-step hours. This coincided with a period of reduced LES banding, between 1700 UTC on 4 October and 0200 UTC on 5 October.



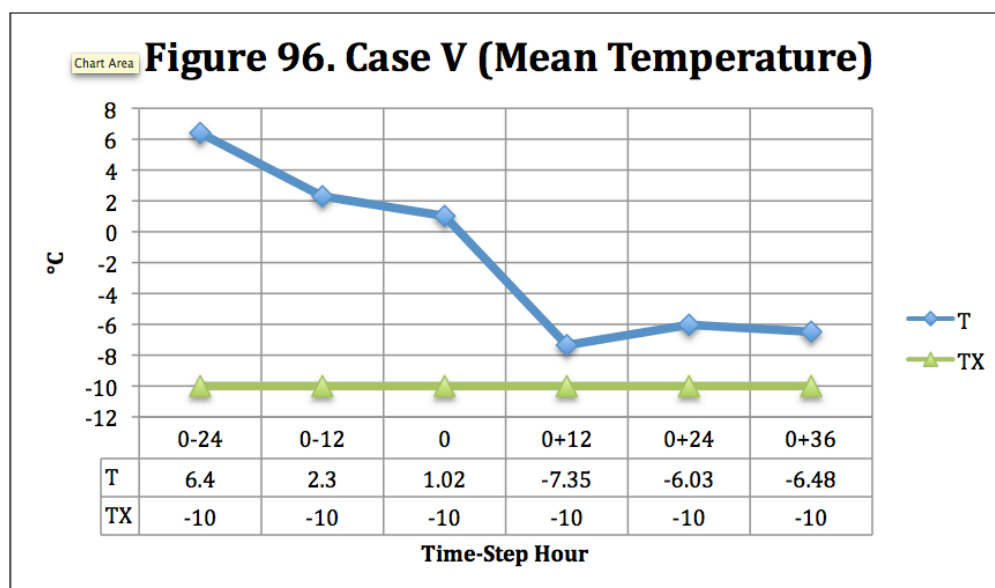
W (Figure 94): W was >WX at the 0-hour and peaked at 16.46 m/s. This was in association with a jet streak dropping southeast and the passage of a cold front. Following the 0-hour, W fell below 10 m/s in all analyzed time-step hours for the duration of the event.



RH (Figure 95): RH was greater than RHX and greater than 70% for all time-step hours from the 0+12 hour through the duration of the case. At the 0-hour, RH was 55% and increasing in a pre-frontal environment. The REV sounding was not downwind of Lake Tahoe during the duration of this event.

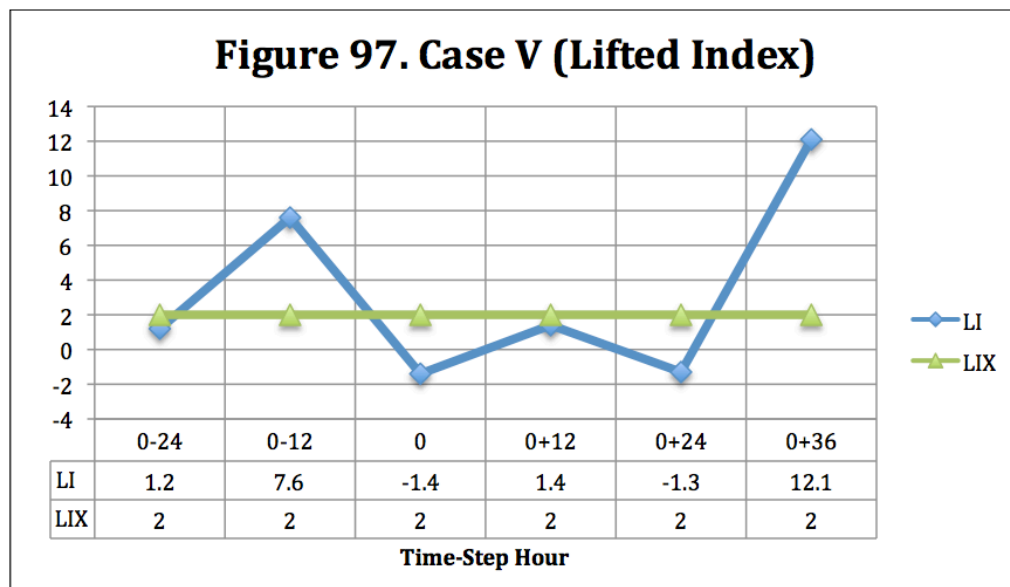


T (Figure 96): T cooled from above freezing at the 0-hour, to a minimum of -7.35 at 0+12. T was > TX in all time-step hours in this case. Temperatures remained within a few degrees of these numbers at 0+24 and 0+36. The 650-hPa level temperature was around -13 °C, making the top of the surface-650-hPa layer optimal for snowfall formation, but temperatures in the lower half of the layer were in the zero to -5 °C range.



Instability (Figure 97): In this case, from the 0-hour through the end of the event, two afternoon REV soundings were unstable. The 0-hour had a LI of -1.4, while the 0+24 sounding showed a LI of -1.3. The 0+12 hour had an LI of 1.4. LI was < LIX during the 0-hour, 0+12, and 0+24. LI showed strong stability at 0+36. CAPE was measured at 43 j/kg at the 0-hour and 147 j/kg at 0+24.

The LES banding with the highest reflectivity and strongest echo definition occurred between 0800 UTC and 1700 UTC on 4 October, when LI was < LIX.



Upper Level Support: From the 0-hour through the 0+36 hour, flow was cyclonic and to the right of the 500-hPa trough axis or closed low. This was favorable for upper level divergence and PVA. During this event, it is important to note that LES banding developed immediately following mesoscale lifting mechanisms, such as the cold frontal passage, and convective snow showers passing over the lake.

3.5.3 Radar Analysis

Rain and snow in association with a cold frontal boundary moved through the Lake Tahoe area on 4 October at 0700 UTC (Figure 98). The arrow denotes echo movement. A rapid change from rain to snow occurred in the basin with falling snow levels in the wake of the cold air advection. By 0800 UTC (Figure 99), the cold front and associated precipitation shifted east and cold air advection intensified across Lake Tahoe. While echoes were dissipating behind the front at this hour, intensification of cells was occurring over the eastern half of the lake. Reflectivity maximums of 35 to 40 dBz were evident in cells that formed from the California-Nevada border east into the Carson Range. A LES band developed in the following hours downwind 40 km into Carson City and Douglas Counties. By 1102 UTC (Figure 100), the band orientation changed as the 650-hPa wind direction shifted from westerly to northwesterly. Cells formed over the geographic center of the lake and just southwest of Crystal bay, and then appeared to intensify into a broad band over the Carson Range. This LES band extended downwind to Minden and Gardnerville. The band had a width of 15 to 25 km, expanding with further enhancement over the Pine Nut Mountains.

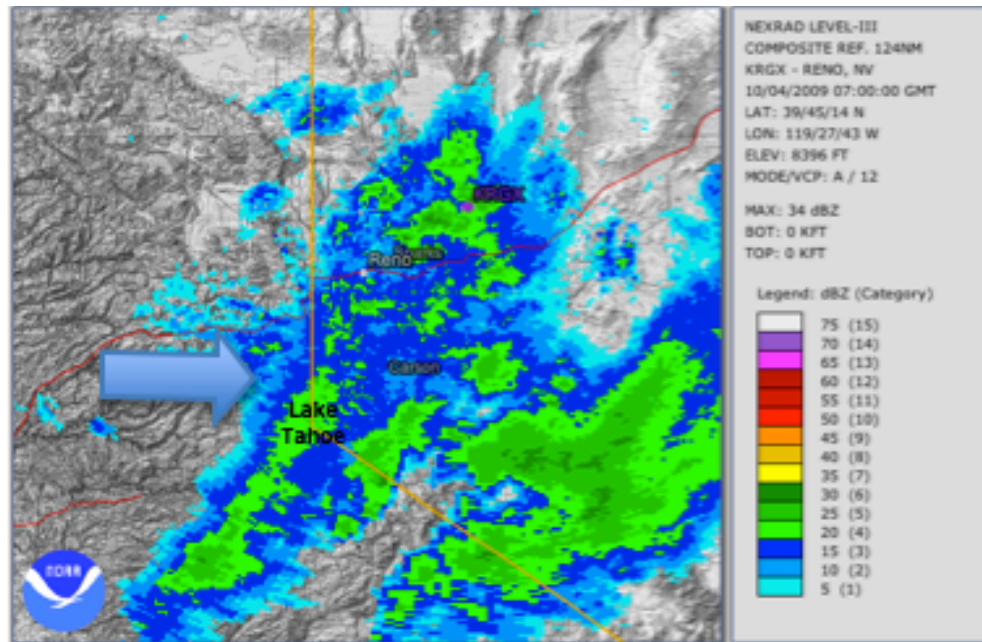


Figure 98. KRGX Composite Reflectivity at 0700 UTC on 4 Oct 2009

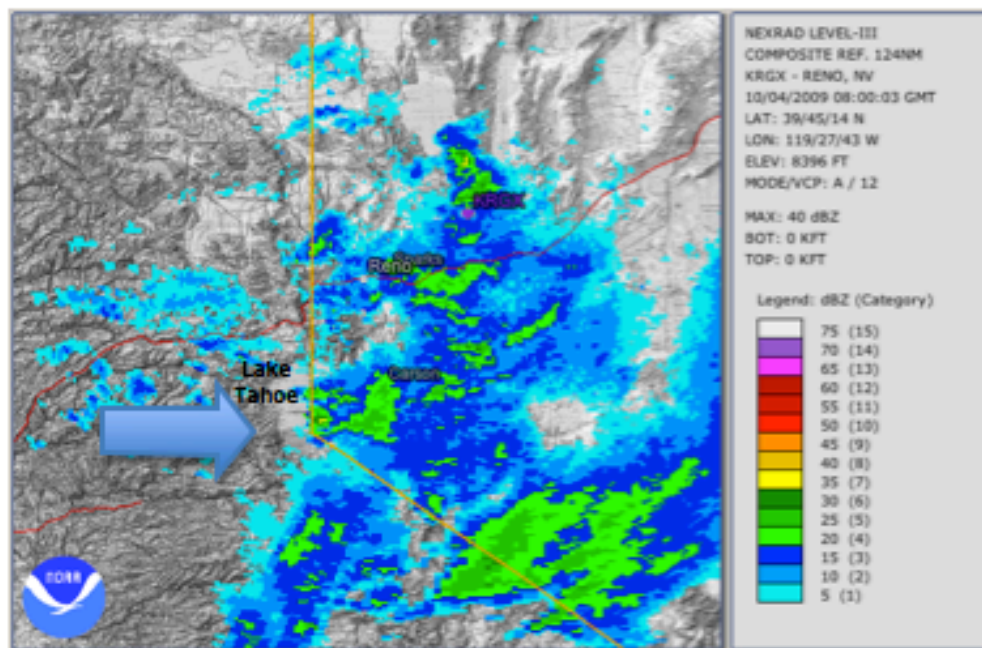


Figure 99. KRGX Composite Reflectivity at 0800 UTC on 4 Oct 2009

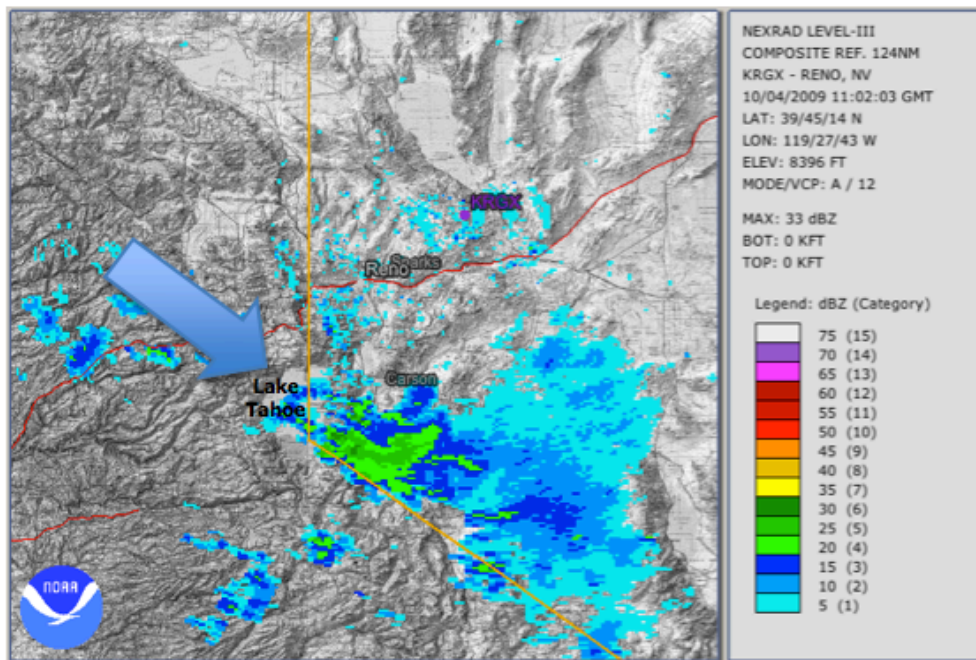


Figure 100. KRGX Composite Reflectivity at 1102 UTC on 4 Oct 2009

By 1403 UTC (Figure 101), the LES band that extended from Lake Tahoe southeast into Douglas County merged with convection enhanced over the terrain of the west slope of the Sierra Nevada. This line of cells over highway 50 moved to the southeast. Several lightning strikes were recorded with this line of cells. The arrow denotes Echo movement. A reflectivity maximum of these showers was 34 dBz, but this was at considerable distance from the RGX radar site. By 1546 UTC (Figure 102), as the convective snow showers moved southeast, a new LES band formed over the southern half of Lake Tahoe. This band showed higher reflectivity, peaking at 44 dBz. The band was only a few km wide, but extended southeast 25 km to Minden.

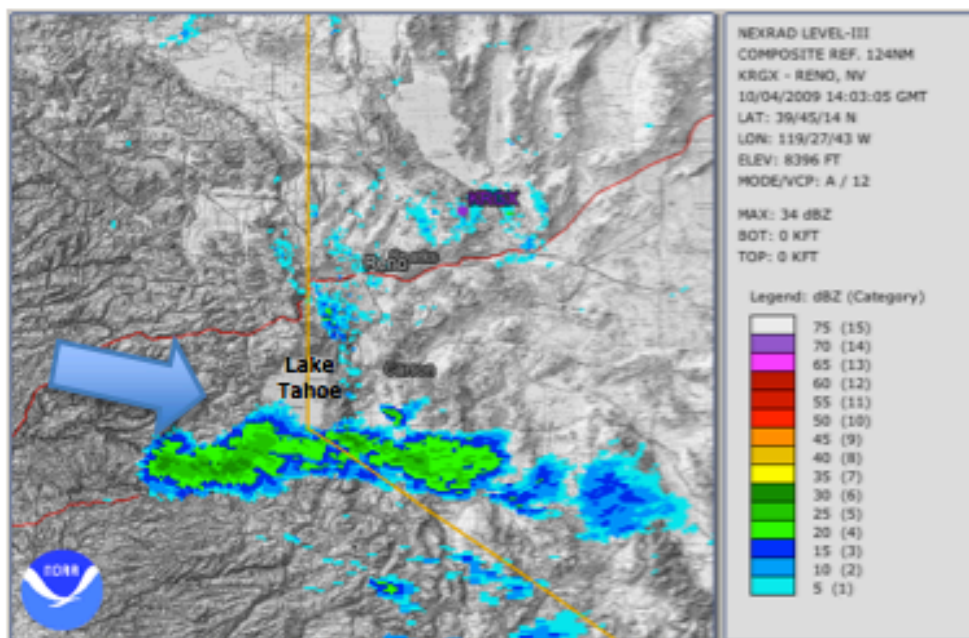


Figure 101. KRGX Composite Reflectivity at 1403 UTC on 4 Oct 2009

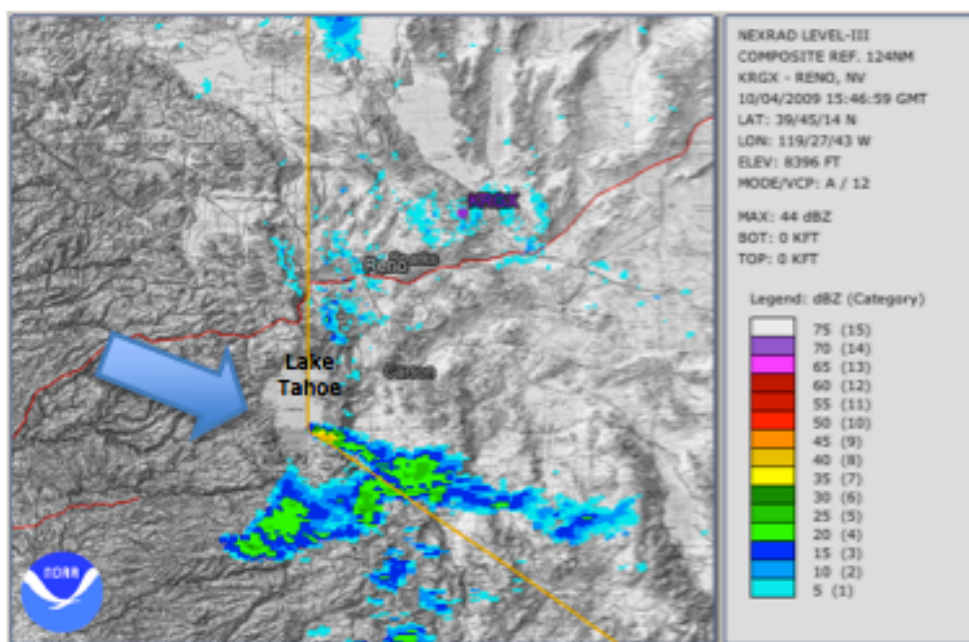


Figure 102. KRGX Composite Reflectivity at 1546 UTC on 4 Oct 2009

Figure 103 shows the LES band holding together through 1700 UTC. Maximum reflectivity decreased to 36 dBz. LES band width increased from less than five km over the lake to more than 15 km in the Carson Valley. The band extended downwind to Minden and Gardnerville. LES band organization disintegrated in the following hours, with only weak echoes forming and dissipating along the southeastern shore.

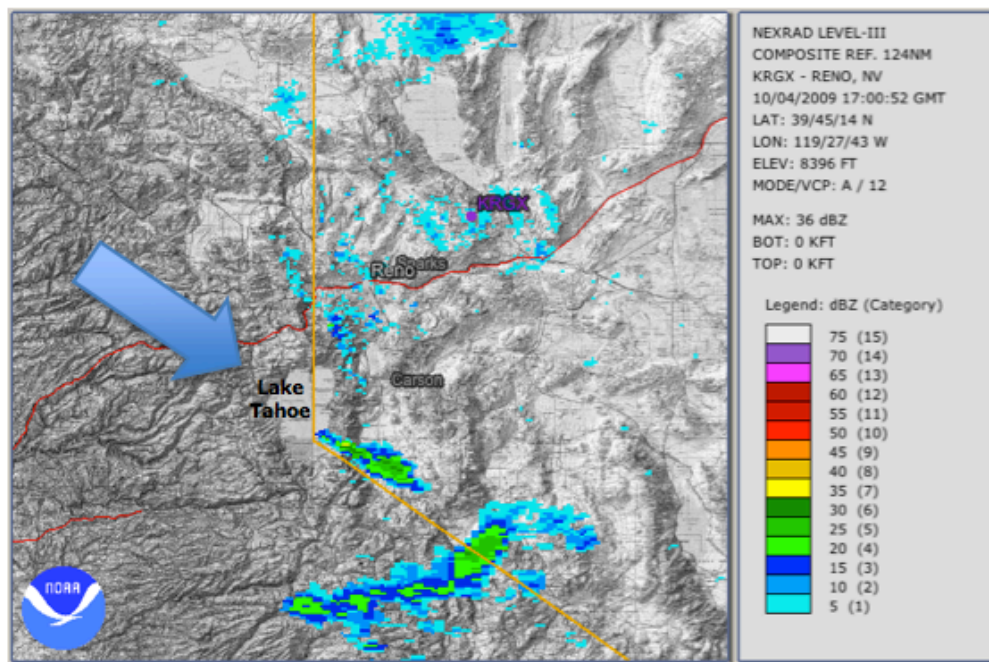


Figure 103. KRGX Composite Reflectivity at 1700 UTC on 4 Oct 2009

LES banding would form once more with this event, in the evening hours of 4 October (5 October, 0200-0400 UTC). A line of echoes, moved from northwest to southeast existed just north of Tahoe (Figure 104). As this line of echoes shifted southward over the lake, lake enhancement occurred. As echoes dissipated west of the lake, intensification of cells occurred over the northern half of Lake Tahoe. By 0401 UTC (Figure 105), an organized LES band extended from cells near the geographic center of the lake with a reflectivity of 37 dBz, downwind to the Pine Nut Mountains, where dBz values fluctuated from 25 to 35. LES band length merged with the earlier line of convective snow showers, extending 40+ km over Spooner Summit to just south of the Carson City area. This band quickly dissipated in the following hours, with light snow showers developing and dissipating along the east shore, ending by 1200 UTC.

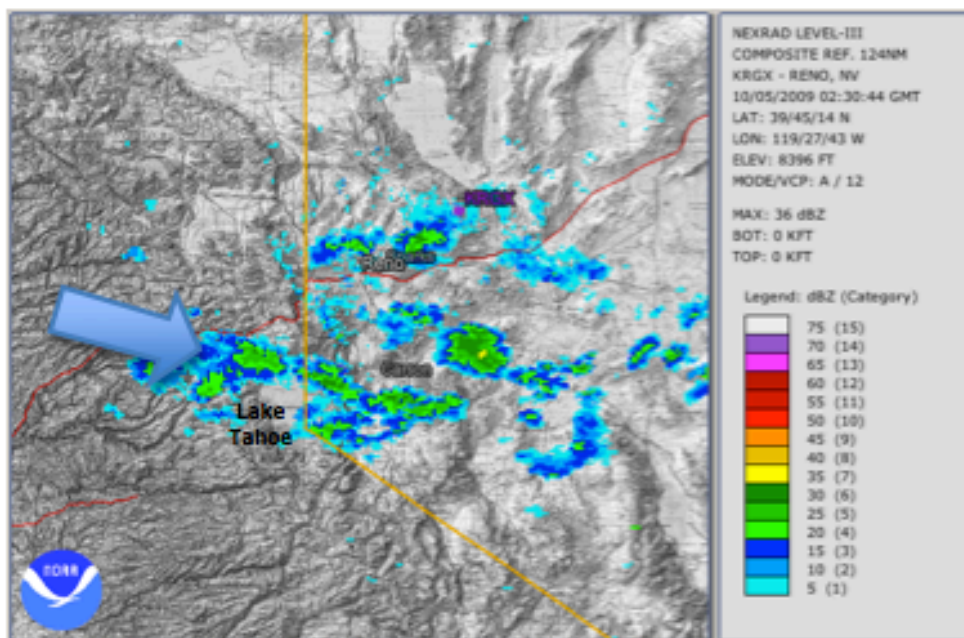


Figure 104. KRGX Composite Reflectivity at 0230 UTC on 5 Oct 2009

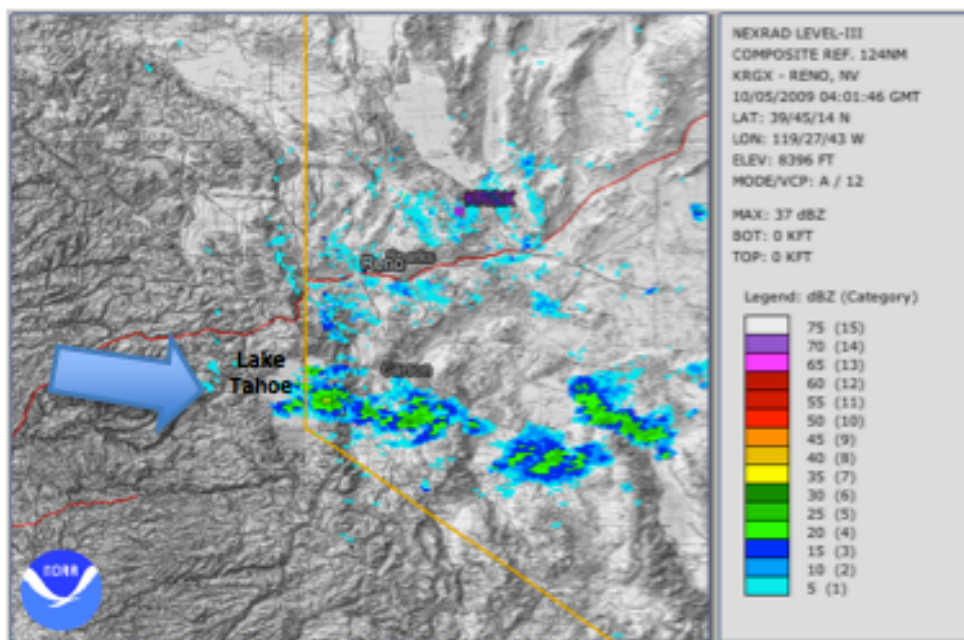


Figure 105. KRGX Composite Reflectivity at 0401 UTC on 5 Oct 2009

4. Summary and Conclusions

4.1 Hypothesis Verification

This study was a quantitative analysis of atmospheric and lake surface parameters that modulate LES at Lake Tahoe. The study provided insight into LES parameter evolution on the lake during specific cases and evaluated established and experimental forecasting thresholds and conditions for the development of LES. The results of the analysis confirm that combinations of these established parameter thresholds were always apparent during these five LES cases on Lake Tahoe.

4.2 Parameter Analysis Summary

1. ΔT_{650} : $\Delta T_{650} > \Delta T_{650X}$ during 100% of the time-step hours when LES occurred. ΔT_{650} was 23 °C or greater during 100% of the time-step hours when LES occurred.
2. ΔT_{land} : ΔT_{land} was 9 °C or greater during 100% of time-step hours when LES occurred.
3. Existence of a Capping Inversion: During periods of LES occurrence, there were no inversions below the 650-hPa level during the case studies.
4. S: S exceeded SX in three of the five cases during time-step hours when LES occurred. S exceeded SX in 33% of the LES time-step hours. When shear exceeded this threshold, LES either occurred when W was less than

5 m/s, or echoes displayed irregular, short lived banding structure that did not extend out of the Tahoe Basin.

5. W: In all five cases, $W < WX$ during 100% of time-step hours when LES occurred. During the strongest banding episodes (spatial extent and temporal longevity), W was greater than 6 m/s, but did not exceed 14 m/s.
6. RH: $RH > RHX$, and exceeded 70%, in 91.7% of time-step hours when LES occurred. The one time-step hour when RH was $< RHX$ was during the Case II. At the 0+24 hour in that case, RH was 44%, as dry air advection occurred at the 750-hPa level, and a lull in radar activity and a wind shift coincided with this drop in moisture.
7. T: During the 12 time-step hours when LES occurred: $T < TX$ 33% of the time, T was between $-7.35\text{ }^{\circ}\text{C}$ and $-13.55\text{ }^{\circ}\text{C}$, KTVL temperature was at or below freezing for all but one period (at the 0+24 hour during Case V, the KTVL temperature was $1\text{ }^{\circ}\text{C}$), Temperatures at the 650-hPa level were between -11 and $-18\text{ }^{\circ}\text{C}$. In the majority of LES time-step hours (67%), T was warmer than the optimal range for dendritic snowfall development. However, it did fall within the zero to $-10\text{ }^{\circ}\text{C}$ range necessary for snowfall crystal growth.
8. Instability: $LI < LIX$ in 67% of time-step hours when LES occurred. CAPE occurred during 34% of time-step hours when LES occurred. This parameter was maximized during afternoon soundings, when surface

heating was also maximized. It is important to note that instability can develop quickly, and was only analyzed during time-step hours when REV sounding data was available.

9. Upper Level Support: During all five cases, upper level support was considered favorable during 100% of time-step hours when LES occurred. This was contrary to Great Lakes research, which often described anticyclonic flow to the west of a departing trough axis.

4.3 Forecasting

The forecasting procedure currently utilized for LES on Lake Tahoe at the Reno NWSFO (Figure 15) handles the parameter analysis findings well in the five cases in this study, with two exceptions and two additions:

1. $\Delta T_{650} > \Delta T_{650X}$ in all five cases in this thesis and the 9-11 November 2000 event (Cairns et al., 2001; Huggins et al., 2001). This value did not fall below 23 °C during hours (time-step analysis hours) of LES. When the value did fall below 20 during the final 12 hours of the January 2008 case, LES rapidly dissipated. Looking at lesser and null events would be the next logical step in investigation of this parameter.
2. S exceeded SX during LES time-step hours, but when this occurred, W was < 5 m/s, banding became less characteristic, or activity ended altogether. SX was applicable in these cases for organized banding, but LES echoes persisted locally even in highly sheared environments. The

Reno NWSFO procedure calls for little or no shear, which does not quantify a threshold, but nullifies several of these events.

3. The five cases investigated in this study showed favorable upper-level support, with cyclonic flow aloft and location to the right or at the base of a trough axis. Close proximity to low-pressure areas extending from the 500-hPa level down to the surface was also noted in two of the cases. This is not currently a LES forecasting parameter for Tahoe, but it was a factor the five case studies in this thesis.

Based on this investigation, a modified forecast procedure for Tahoe LES is shown in Figure 106. This is by no means a challenge to current forecasting procedure, but rather insight based on the specific cases in this research. For structured banding that affects areas outside of the Tahoe Basin, the four parameter thresholds are numbered. The Reno NWSFO forecasting procedure did not mention existence of a capping inversion, however based on the importance of this parameter in other regions and the findings in this study, it was included as conditional. Also, Figure 107 shows parameters beneficial to higher snowfall rates, but not conditional on LES band development. This procedure was developed based on significant LES events. Many more cases, including null and lesser magnitude events are needed to advance existing procedure. RH and upper level support are parameters that need to be investigated further in future studies, when more data becomes available.

Figure 106. Modified Lake Tahoe LES Forecast Procedure

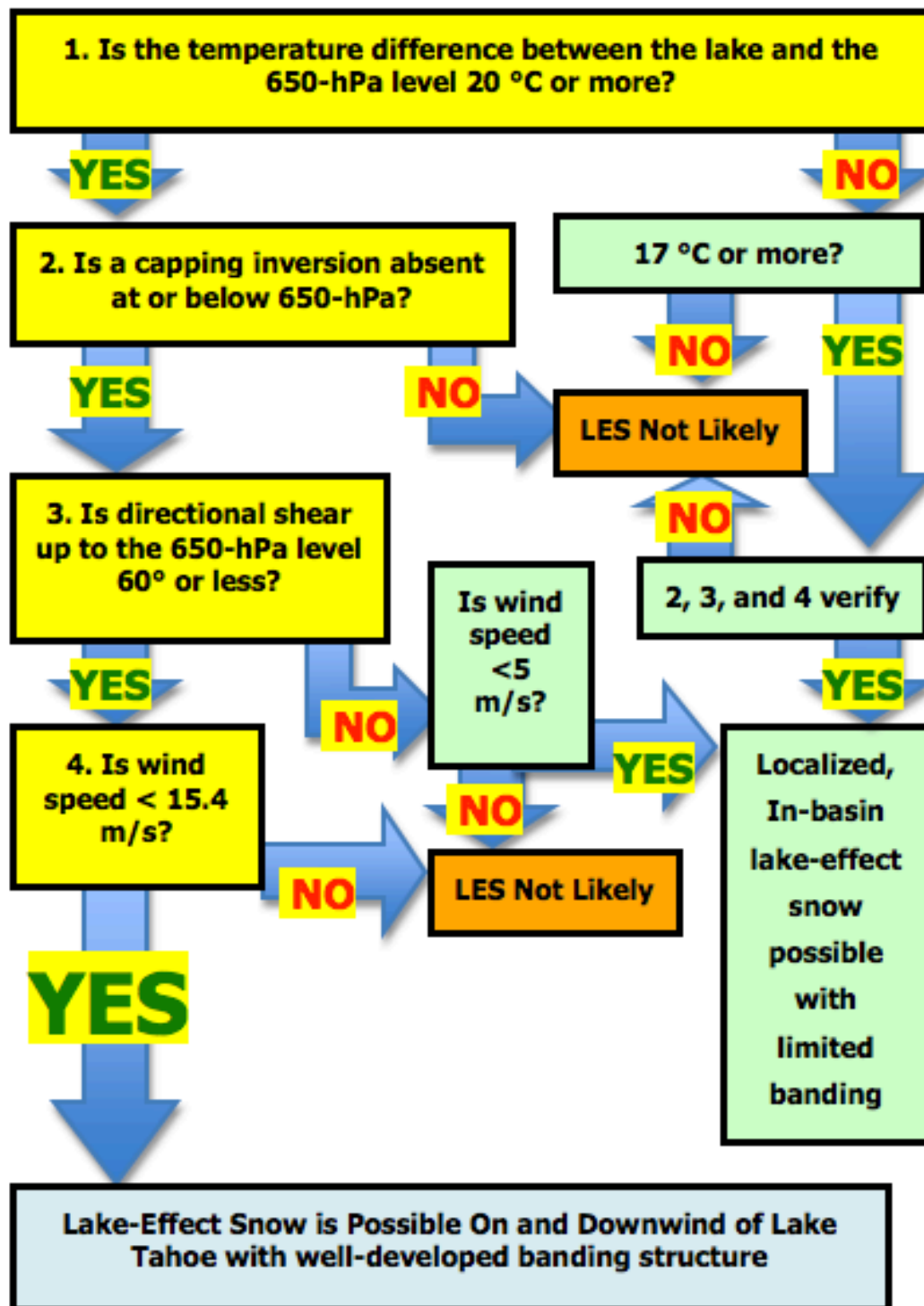
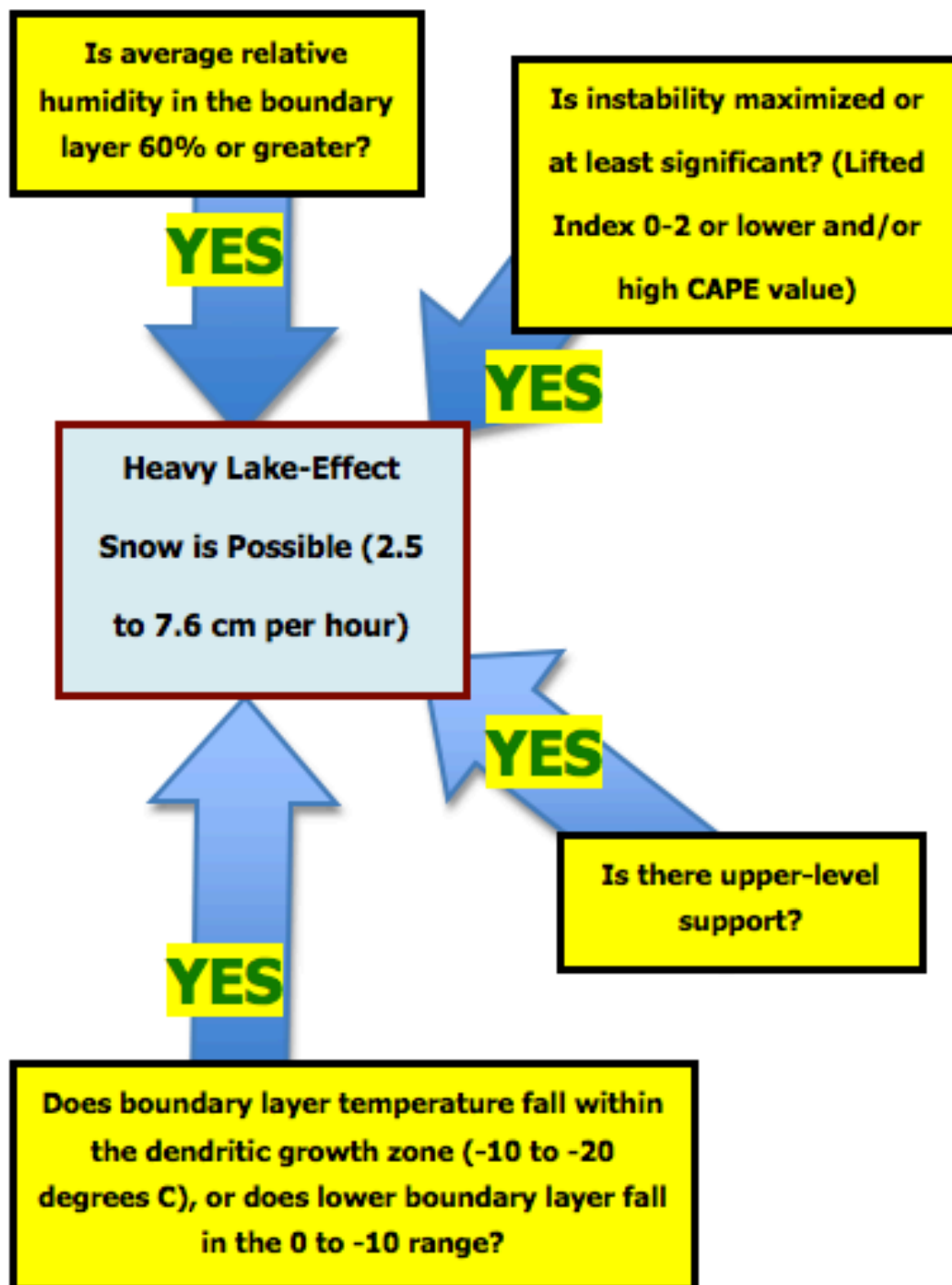


Figure 107. Parameters for Heavy LES



The findings of this research advance the understanding of Tahoe LES and improved knowledge of Tahoe LES parameters. This study was one more step in furthering our understanding of LES on Lake Tahoe and other smaller water bodies in the United States.

References

- Ahrens, C.D., 2003: *Meteorology today*. Brooks/Cole, Thomson Learning, Inc., 544 p.
- Brong, B., 10/17/2009: Personal communication. National Weather Service Forecast Office, Reno, Nevada.
- Burnett, J.L., C.R. Goldman, and J. Court, 1968: *Geology of the Lake Tahoe Basin- Geologic studies in the Lake Tahoe Area, California and Nevada. Annual Field Trip Guidebook of the Geological Society of Sacramento, 1968*, J.R.Evans, and R.A. Matthews, Editors, p 1-13, p 60.
- Cairns, M.M., R. Collins, T. Cyclke, M. Deutschendorf, and D. Mercer, 2001: A lake effect snowfall in Western Nevada- Part I: Synoptic setting and observations. Preprints, *18th Conference on Weather Analysis and Forecasting*, Boston, MA: American Meteorological Society, 329-332.
- Carpenter, D.M., 1993: The lake effect of the Great Salt Lake: Overview and forecast problems. *Weather and Forecasting*, Vol. 8, 181-193.
- Dockus, D.A., 1985: Lake-effect snow forecasting in the computer age. *National Weather Digest*, Vol. 10, 5-19.
- Dole, R.M., 1925: Snow squalls of the lake region. *Monthly Weather Review*, Vol. 56, No. 12, 512-513.
- Ellis, A.W., and D.J. Leathers, 1996: A synoptic climatological approach to the analysis of lake-effect snowfall: potential forecasting applications. *Weather and Forecasting*, Vol. 11, 216-229.
- Glickman, T.S., 2000: *Glossary of Meteorology: Second Edition*. American Meteorological Society, 855 p.
- Graham, R., 3/16/2010: Personal communication. National Weather Service Forecast Office, Salt Lake City, Utah.
- Heggli, M.F., and D.W. Reynolds, 1985: Radiometric observations of supercooled liquid water within a split front over the Sierra Nevada. *Journal of Climate and Applied Meteorology*, Vol. 24, 1258-1261.
- Hill, J.D., 1971: *Snow Squalls in the Lee of Lakes Erie and Ontario*. NOAA Tech. Memo, NWS ER-43.

Hjelmfelt, M.R., and R.R. Braham, 1983: Numerical-simulation of the air-flow over Lake-Michigan for a major lake-effect snow event. *Monthly Weather Review*, Vol. 111, Issue 1, 205-219.

_____, 1990: Numerical study of the influence of environmental-conditions on lake-effect snowstorms over Lake-Michigan. *Monthly Weather Review*, Vol. 118, Issue 1, 138-150.

_____, 1992: Orographic effects in simulated lake-effect snowstorms over Lake-Michigan. *Monthly Weather Review*, Vol. 120, Issue 2, 373-377.

Holroyd, E.W., 1971: Lake-effect cloud bands as seen from weather satellites. *Journal of the atmospheric sciences*, Vol. 28, Issue 7, 1165-1170.

Huggins, A.W., D. Kingsmill, and M.M. Cairns, 2001: A lake effect snowfall in Western Nevada- Part II: Radar characteristics and quantitative precipitation estimates. Preprints, *18th Conference on Weather Analysis and Forecasting*, Boston, MA: American Meteorological Society.

Justo, J.E., and M.L. Kaplan, 1972: Snowfall from lake effect storms. *Monthly Weather Review*, Vol. 100, No. 1, 62-66.

Kelly, R.D, 1982: A single Doppler radar study of horizontal-roll convection in a lake-effect snow storm. *Journal of the Atmospheric Sciences*, Vol. 39, Issue 7, 1521-1531.

_____, 1986: Mesoscale frequencies and seasonal snowfalls for different types of Lake-Michigan snow storms. *Journal of Climate and Applied Meteorology*, Vol. 25, Issue 3, 308-312.

Kristovich, D.A.R., and N.F. Laird, 1998: Observations of widespread lake-effect cloudiness: Influences of lake surface temperature and upwind conditions. *Weather and Forecasting*, Vol. 13, 811-821.

_____, G.S. Young, J. Verlinde, et al., 2000: The lake-induced convection experiment and the snowband dynamics project. *Bulletin of the American Meteorological Society*, Vol. 81, Issue 3, 519-542.

_____, N.F. Laird, and M.R. Hjelmfelt, 2003: Convective evolution across Lake Michigan during a widespread lake-effect snow event. *Monthly Weather Review*, Vol. 131, Issue 4, 643-655.

Lackmann, G.M., 2001: Analysis of a surprise Western New York snowstorm. *Weather and Forecasting*, Vol. 16, 99-116.

Laird, N.F., J. Desrochers, and M. Payer, 2009: Climatology of lake-effect precipitation events over Lake Champlain. *Journal of Applied Meteorology and Climatology*, Vol. 48, 232-250.

Lavoie, R.L., 1972: A mesoscale model of lake effect snowstorms. *Journal of Atmospheric Science*, Vol. 29, 1025-1040.

Lee, T.F., 1987: Seasonal and interannual trends of Sierra Nevada clouds and precipitation. *Journal of Climate and Applied Meteorology*, Vol. 26, 1270-1276.

Maher, N.M., 2000: *Satellite-Topographic Relief Map of Lake Tahoe, California/Nevada*. Wall map published by Tahoe Maps, single sheet, 24"x36".

McLaughlin, S., 1/25/2010: Personal communication. National Weather Service Forecast Office, Buffalo, New York.

Mote, T.L., D.W. Gamble, S.J. Underwood, and M.L. Bentley, 1997: Synoptic-scale features common to heavy snowstorms in the southeast United States. *Weather and Forecasting*, Vol. 12, 5-23.

National Centers for Environmental Prediction, 2010: <http://www.hpc.ncep.noaa.gov/ncepreanal/> last accessed on April 12, 2010.

National Climatic Data Center, 2010: <http://www.ncdc.noaa.gov/nexradinv/> last accessed on April 24, 2010.

National Weather Service Forecast Office, Reno, NV, 2010: <http://www.wrh.noaa.gov/rev/> last accessed on March 23, 2010.

Niziol, T.A., 1987: Operational forecasting of lake effect snowfall in Western and Central New York. *Weather and Forecasting*, Vol. 2, 310-321.

_____, W.R. Snyder, and J.S. Waldstreicher, 1995: Winter weather forecasting throughout the Eastern United States. Part IV: Lake effect snow. *Weather and Forecasting*, Vol. 10, 61-77.

O'Hara, B.F., G.E. Barbato, J.W. James, H.A. Angeloff, and T. Cylke, 2007: *Weather and Climate of the Reno-Carson City-Lake Tahoe Region*. Nevada Bureau of Mines and Geology, Special Publication 34, University of Nevada, Reno, 82 p.

_____, M.L. Kaplan, and S.J. Underwood, 2007: Synoptic climatological analysis of extreme snowfalls in the Sierra Nevada. *Weather and Forecasting*, Vol. 24, 1610-1624.

_____, 3/12/2010: Personal communication. National Weather Service Forecast Office, Reno, Nevada.

Onton, D.J., and W.J. Steenburgh, 2001: Diagnostic and sensitivity studies of the 7 December 1998 Great Salt Lake-effect snowstorm. *Monthly Weather Review*, Vol. 129, 1318-1338.

Peace, R.L. Jr., and R.B. Sykes Jr., 1966: Mesoscale study of a lake effect snow storm. *Monthly Weather Review*, Vol. 94, No. 8, 495-507.

Petterssen, S., 1956: *Weather analysis and forecasting: Volume II. Weather and Weather Systems*. McGraw-Hill, 266 p.

_____, and P.A. Calabrese, 1959: On some weather influences due to warming of the air by the Great Lakes in winter. *Journal of Meteorology*, Vol. 16, No. 6, 646-652.

RAOB, The Universal Rawinsonde Observation Program, 2010: Environmental Research Services, LLC.

Reinking, R.F., R. Caiazza, R.A. Kropfli, et al., 1993: The Lake-Ontario winter storms (LWS) project. *Bulletin of the American Meteorological Society*, Vol. 74, Issue 10, 1828-1849.

Rothrock, H.J., 1969: *An Aid in Forecasting Significant Lake Snows*. Kansas City, MO, Weather Bureau Central Region Technical Memorandum WBTM CR-30, 12 p.

Saulesleja, A., 1986: *Great Lakes Climatological Reference*. Environment Canada, Ottawa, 145 p.

Schladow, G., 2009: *Tahoe State of the Lake Report*. U.C. Davis Tahoe Environmental Research Center, <http://terc.ucdavis.edu/stateofthelake/index.html>, 12 p.

Steenburgh, W.J., S.F. Halvorson, and D.J. Onton, 2000: Climatology of lake-effect snowstorms of the Great Salt Lake. *Monthly Weather Review*, Vol. 128, 709-727.

_____, and D.J. Onton, 2001: Multiscale analysis of the 7 December 1998 Great Salt Lake-effect snowstorm. *Monthly Weather Review*, Vol. 129, 1296-1317.

_____, 2003: One hundred inches in one hundred hours: Evolution of a Wasatch Mountain winter storm cycle. *Weather and Forecasting*, Vol. 18, 1018-1036.

University of California, Davis, Remote, 2010: http://remote.ucdavis.edu/tahoe_location.asp last accessed on April 7, 2010.

University of Wyoming, 2010: <http://uwyo.edu/upperair/naconf.html> last accessed on April 15, 2010.

Wiggin, B.L., 1950: Great snows of the Great Lakes. *Weatherwise*, Vol. 3, No. 6, 123-126.